THESIS

ANALYSIS AND REFINEMENT OF METHANE NUMBER TEST PROCEDURE FOR GASEOUS FUELS

Submitted by

Dawson Baucke

Department of Mechanical Engineering

In partial fulfillment of the requirements

For the Degree of Master of Science

Colorado State University

Fort Collins, Colorado

Spring 2024

Master's Committee:

Advisor: Daniel B. Olsen

Daniel M. Wise
Jeremy S. Daily

ABSTRACT

ANALYSIS AND REFINEMENT OF METHANE NUMBER TEST PROCEDURE FOR GASEOUS FUELS

Methane Number (MN) is an experimentally determined parameter for quantifying the resistance of gaseous fuels to End Gas Auto Ignition (EGAI). Originating from Leiker et al. in Graz, Austria, MN was introduced as an alternative to traditional gasoline rating techniques due to limitations on maximum obtainable values without extrapolative methods. Through funding provided to AVL, Leiker, et al. explored the impact of gas composition on fuel reactivity, although the specific details of their testing method remain unpublished. Subsequently, refinements to Leiker's proposed analytical method were made by AVL and MWM including digitizing of the AVL experimental data and the use of a computer program. The American Society of Testing Materials (ASTM) developed a standard for calculating a methane number (MN_C)based on the gaseous fuel composition using the latest MWM methodology and experimental data. Amidst growing interest in renewable and hydrogen-blended natural gas, uncertainties within the experimental data used in the MN_C method have spurred re-evaluation of the MN testing method.

The purpose of this research is to create a repeatable method for determining the knock resistance of gaseous fuels analogous to the methods used for gasoline utilizing reference fuel blends of methane, hydrogen, and carbon dioxide.

While Leiker, et al. did not disclose details of their MN quantification testing method, numerous research groups have developed their own methods, often without divulging test specifics or operating conditions. Presently, there is no standardized method for experimentally determining the MN of a gaseous fuel. This study aims to establish and share a repeatable method for MN determination using a modified Cooperative Fuel Research Engine (CFR). The investigation includes justification of allowable environmental parameters and operating variation limits, as well as exploring potential adaptations to the original proposed method.

A pivotal aspect of the MN method involves identifying and quantifying a Knock Index (KI) parameter during engine operation, a challenge tackled through various approaches. CFR engines, originally designed for gasoline EGAI testing, come equipped with their own knock detection measurement systems. CSU has devised its method for determining a KI, and a comparison between the two systems was conducted to facilitate the publication of a standardized MN testing protocol.

ACKNOWLEDGMENTS

I would like to recognize the people who supported during the work presented in this Thesis. My advisor, Dr. Daniel B. Olsen, for his support throughout my undergraduate and graduate studies and allowing me the opportunity to work within his research group. Dr. Daniel Wise, Dr. Christian Puttlitz, Dr. Jeremy Daily for their interest in this work, for the time they invested on my behalf, and for the guidance they provided me throughout this process. I would also like to thank Robin Bremmer for guidance regarding ASTM requirements and input regarding the MN_C calculation program. Mark and Andy Malet with Mark's Knock Engine Service for their support of this project regarding the well-established CFR knock detection equipment. The powerhouse staff – Mark, Kirk, and James, who guided me through the additions/repairs to the CFR system. I would also like to thank many others who assisted me, Reece Churchill, Cole Cooper. My father Kent Baucke for accompanying me during late night testing and asking for no compensation. Finally, my friends and family, who supported me throughout every step of the way while listening to me speak about my research and offer guidance whenever possible.

TABLE OF CONTENTS

LIST OF TABLES

LIST OF FIGURES

CHAPTER 1: INTRODUCTION

1-1 Background and Motivation

With the challenge of climate change on the horizon, the need for cleaner and more efficient power generation technologies has never been more pressing. The development and optimization of high-efficiency natural gas engines have been at the forefront in a push for a carbon neutral, sustainable, energy future. Natural gas engines have demonstrated their potential across the energy sector as a viable power generation source due to their high Hydrogen/Carbon ratio compared to conventional fuels like gasoline and diesel. Natural gas, a blend of flammable gaseous hydrocarbons, is generally accepted to be a cleaner alternative to traditional fossil fuels.

Internal Combustion Engines (ICE) operate on the principle of converting chemical energy into mechanical work to power a vehicle or convert the work into electricity. At the heart of this investigation is the complex combustion chemical reaction within the cylinders of the engine involving a cause-and-effect relationship between many parameters. However, harnessing the available energy efficiently requires a balancing act to maximize power delivery and engine operating life while minimizing emissions and fuel consumption. One of the challenges in optimizing ICE lies in managing End Gas Auto Ignition (EGAI). EGAI is a phenomenon characterized by a second abnormal combustion event caused by unburned gases spontaneously combusting due to elevated temperatures and pressures found within the cylinder [1]. Depending on the severity, EGAI can have profound effects on engine efficiency and emissions. Understanding and controlling this process is essential for achieving high efficiency and low emissions in natural gas engines. When considering other forms of ICEs, one method of reducing the level of EGAI without reducing engine power is utilizing a fuel with lower reactivity.

Despite the growing interest in natural gas engines, there is a notable lack of an industry-wide metric for quantifying natural gas knock resistance. This gap in standardized measurement poses a challenge for researchers, industry professionals, and consumers. Not having consistent benchmarks for autoignition resistance generates a situation where the performance of engines across the industry is reduced to account for the worst-case-scenario fuel composition.

In conclusion, this research aims to contribute to the understanding of natural gas combustion by exploring the cause-and-effect relationships between environmental and testing variables. Simultaneously, it seeks to address the lack of an industry-wide method for experimentally determining the metric used to quantify gaseous fuel autoignition resistance, laying the groundwork for more informed and efficient advancements in the field. Through this research, we aspire to make a meaningful contribution to the ongoing efforts to transition towards cleaner and sustainable energy solutions.

1-2 Literature Review

Natural Gas

Natural Gas is a naturally occurring mixture of hydrocarbon and nonhydrocarbon gases found in porous geologic formations beneath the earth's surface, often found in association with petroleum [2]. Natural Gas is a nonrenewable fossil fuel primarily consisting of methane, CH_4 (75 – 98 vol%), ethane, C_2H_6 (0.5 – 13 vol%), and propane, C_3H_8 (0 – 2.6 vol%) along with varying proportions of other hydrocarbons, nitrogen, carbon dioxide, and trace elements. Following extraction from the earth and separation from petroleum, Natural Gas undergoes purification to remove impurities like sulfur compounds and water. The fuel is then compressed

up to 24821 kPa in the gaseous state and piped into pipelines for distribution as Natural Gas and may be used as fuel for internal combustion engines. Renewable Natural Gas (RNG) is pipeline-quality gas that is all or in part from renewable sources and is fully interchangeable with nonrenewable natural gas [2]. RNG can be obtained from sources including landfills, wastewater treatment facilities, and livestock farms expanding its role in sustainable energy practices [3].

Natural Gas blending with hydrogen ranging from < 1% to 30% mole fraction depending on the application and is gaining traction as a viable method for reducing carbon emissions as it further increases the hydrogen/carbon ratio of the natural gas. Natural Gas has a wide range of applications, serving as a crucial energy source for residential heating, electricity generation, industrial processes, and transportation. The relatively clean combustion, lower carbon emissions, and versatility make Natural Gas an essential component of the global energy landscape.

End Gas Auto Ignition:

End Gas Auto Ignition (EGAI) refers to the spontaneous combustion of unburned fuel molecules in an engine combustion chamber. This phenomenon (depicted in **Figure *1***) occurs after the initial spark induced ignition event, exposing the yet-to-burn mixture to a higher energy environment during the propagation of the flame front throughout the cylinder [4]. If the temperature is sufficient, and the required energy to propagate is low enough, a secondary ignition site is formed, leading to a secondary flame front and subsequent pressure wave advancing outward in the yet-to-burn mixture. When the primary and secondary pressure waves meet, they cause a disturbance which results in pressure fluctuations that produce the distinctive "knock" or "ringing" associated with auto-ignition events [5]. The term "knock" is used to

describe both the noise and high-frequency vibrations resulting from EGAI. However, the term is commonly employed as a simplified reference for the overall phenomenon.

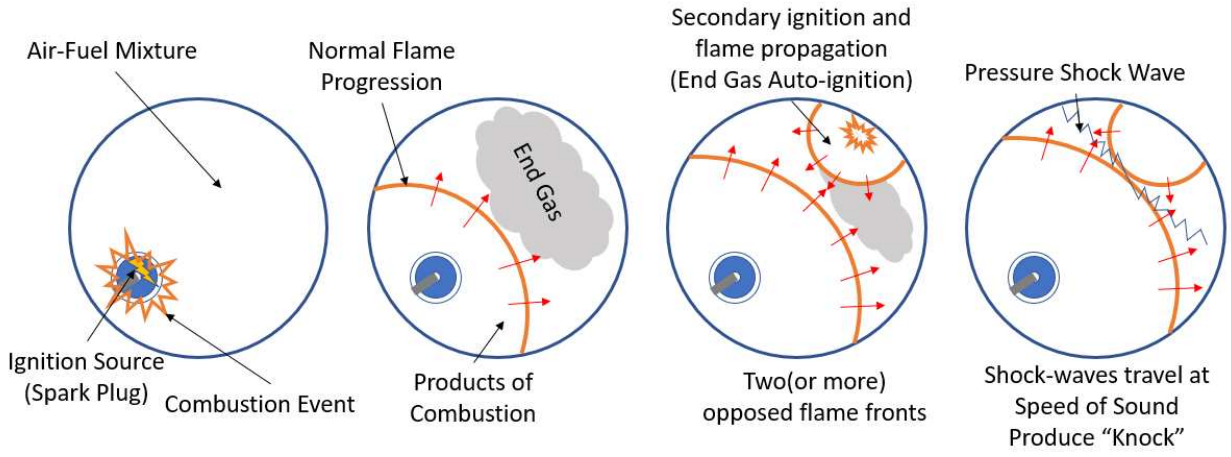

Figure 1: Top view of End Gas Auto Ignition Progression

EGAI is an encompassing term and has many different classifications describing the nature of the event as well as the origin location. Heywood categorized many different situations and terms regarding EGAI in a textbook published in 1988 (depicted in Figure 2). The figure was digitized by Wise in his PhD dissertation [6] and was published with permission.

When changing the compression ratio (CR), intake pressure, or intake manifold temperature of an engine without proper precautions, the propensity for EGAI increases. The primary ignition timing, typically controlled by the Engine Control Module (ECM), is another metric influencing autoignition. To mitigate EGAI without altering fuel composition, options include advancing ignition timing, reducing intake manifold pressure (IMP), decreasing CR, or lowering intake air temperature. Each option poses varying difficulties and often results in performance penalties. Advances in engine monitoring technology allow for the detection of knock and subsequent reduction in ignition timing to prevent engine damage.

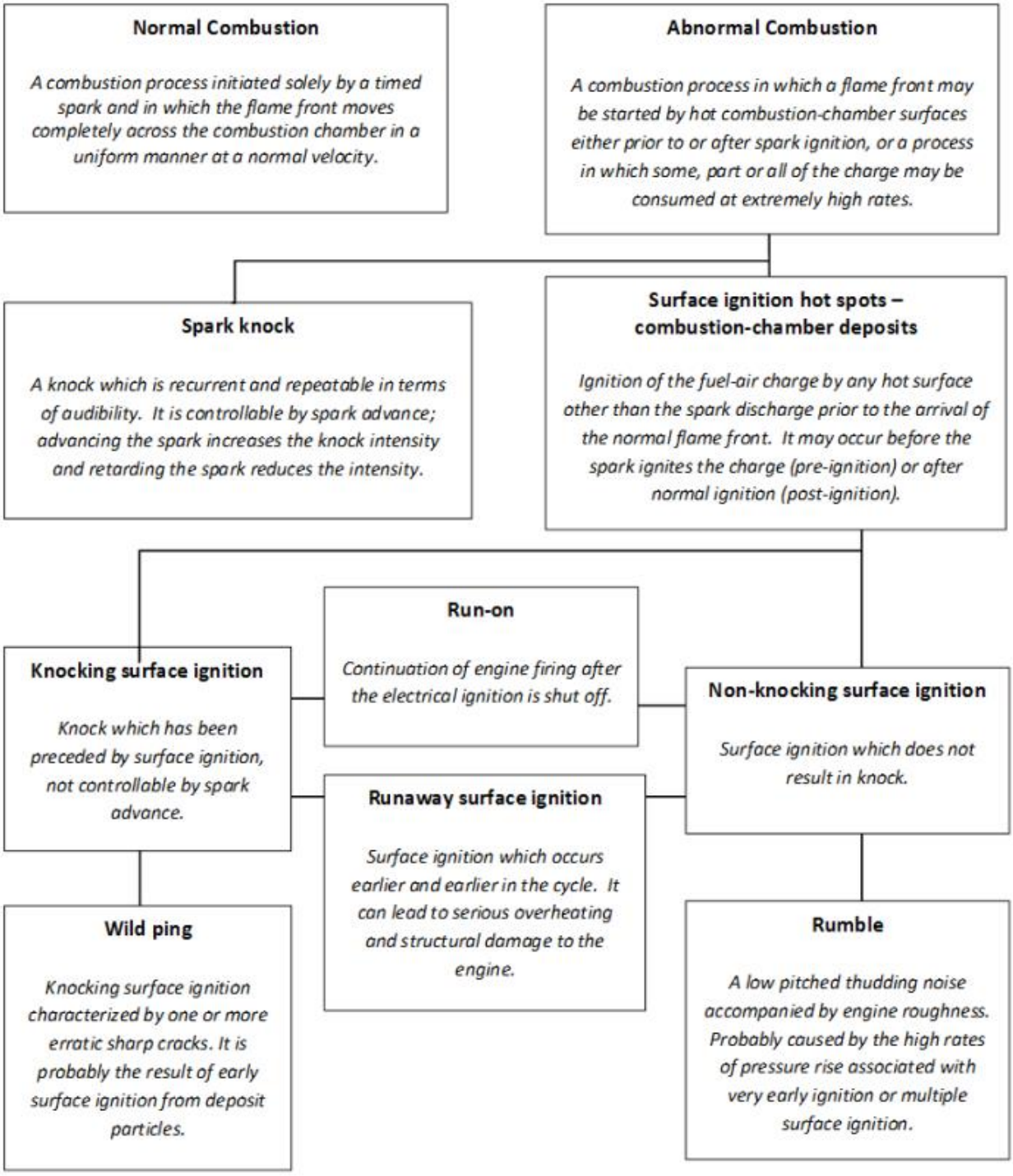

Figure 2: Combustion Phenomena Definition for Spark-Ignited Engines *[1]*

Autoignition events often occur at the combustion chamber boundary, leading to the combustion of the protective quench layer, and through repeated exposure to the high heat of

combustion, the cylinder can be damaged [4]. Prolonged EGAI contributes to increased combustion chamber wear, uneven heating, and piston distortion. Using fuel with sufficient EGAI resistance is crucial to eliminate engine knock while promoting increased service life, enhanced power output, and reduced emissions.

Rating Fuel for EGAI Resistance

Predicting EGAI resistance with combustion modeling software with 21st century computational resources would be a challenging endeavor. During the development of internal combustion engines in the late 19th and early 20th century, performing these calculations with any degree of accuracy without computing resources was impossible. Without such means of direct measurement, researchers adopted an indirect method of determining and quantifying EGAI resistance using reference fuel blends. The standardized metric used for liquid fuels was called the Octane Number (ON) and allowed for a common ground for comparisons across various fuels, engines, and testing conditions.

Gasoline consists of various hydrocarbons, additives, and blending agents and is assessed using ON, a comparative scale utilizing reference fuels for EGAI resistance quantification. ASTM outlines standard testing methods for Research Octane Number (RON) [7] and Motor Octane Number (MON) [8], both utilizing the Cooperative Fuel Research (CFR) Engine. In both methods, isooctane (C_8H_{18}), normal heptane (n-C_7H_{16}), and toluene ($C_6H_5CH_3$) serve as the components of the reference blends used to match the knock behavior of the tested fuel. The ON represents the average of the RON [7] and MON [8], tests and serves as the EGAI resistance of the fuel. The intention behind having two independent methods rating fuels are that they test the engine under different operating conditions with RON [7] emulating low severity (600 rpm, 49^{o}C

air temperature) compared to MON [8] with more severe conditions (900 rpm 149ºC air temperature). Tetraethyl lead (TEL) a known knock suppressant, may be added to the reference blends to allow for octane numbers exceeding 100. During WWII, TEL was added to aviation fuels in such quantities that reached ON ratings of 150 but this posed a significant risk to the environment and service members. The EPA has since placed a limit on the allowable addition of TEL up to an ON of 120.34. Fuels exceeding an ON of 120.34 lack a generally accepted method for knock rating without utilizing a method of extrapolation that introduces a significant degree of error. [6]

Testing gaseous fuels with the RON [7] and MON [8] test methods is possible and for fuels such as Propane (LPG) where the ON of the fuel is between 105-115. Problems arise when there is a high concentration of CH_4, CO, or CO_2, which places the fuel above the 120.34 ON limit. With its high concentration of CH_4, Natural Gas requires a different scale for rating its resistance to autoignition.

Methane Number (MN) is the gaseous fuel equivalent of the ON and is a rating system used to quantify the resistance to autoignition. Introduced in 1972 by Leiker [9] and associates at the Institute for Internal Combustion Engines (Anstalt für Verbrennungskraftmaschinen List) AVL in Graz, Austria, the methane number is a resistance-to-knock quantification method for gaseous fuels [9]. The Methane Number is like octane number, which uses isooctane and n-heptane as reference fuels, the methane number method employs a mixture of methane (CH_4) as the Primary Reference Fuel (PRF) and hydrogen (H_2) or carbon dioxide (CO_2) as a Secondary Reference Fuel (SRF). In this method, the knock characteristics of a test fuel are compared to a mixture of methane and hydrogen. The mixture includes 100% methane (assigned a methane number of 100), 100% hydrogen (assigned a methane number of 0). For example, a mixture of

80% methane to 20% hydrogen would correspond to a methane number of 80. To assign methane numbers greater than 100, the SRF is substituted for carbon dioxide (CO_2) which acts as a knock inhibiter along with methane, allowing for methane numbers equaling 100 plus the percentage of carbon dioxide added to the blend. For example, a fuel blend consisting of 75% CH_4 and 25% CO_2 would correspond to a MN of 125. Fuel composition significantly influences natural gas auto-ignition characteristics, with higher methane numbers indicating lower susceptibility to auto-ignition. This study investigated a typical natural gas fuel blend with a methane number of 85, resembling the typical blend available to consumers from the utility provider. Fuels with lower methane numbers exhibit reduced ignition delays and faster flame speeds, fostering conditions for low-temperature combustion chemistry and auto-ignition initiation. Unlike the Octane Number, ASTM does not have a standard defining a testing procedure for determining the MN of fuels and thus, there have been multiple groups of researchers and manufacturers that utilize their own methods.

Leiker, et al. [9] Laboratory Work

The information for this study was obtained from a paper written by Leiker, Christoph, Rankl, Cartellieri, and Pfeifer brought it their findings be presented at the Diesel and Gas Engine Power Conference & Exhibit in 1972 [9]. Along with the introduction of MN, Leiker, et al. documented the effects of gas composition on EGAI resistance. For the bulk of testing, researchers utilized a standard CFR engine (3.25” bore x 4.5” stroke), but they also utilized two different engines to determine the effects of different bore and stroke combinations on the measured MN [9]. Validity engine I was a 2-cylinder engine (4.92” bore x 5.71” stroke) with a variable CR utilizing piston crown inserts to change the cylinder volume. Validity engine II was

a single-cylinder engine (12.6” bore x 18.9” stroke) with a variable CR utilizing intermediate plates in the connecting rod to change the position of the piston at a given crank shaft position. For their determination of KI, they developed a KI-meter that considers the different combustion behaviors of gaseous fuels. This need for a new KI meter was determined in preliminary testing where different knock patterns were observed depending on the fuel that was being utilized. The KI meter utilized a technique where the positive peak of the second derivative of pressure with respect to time (“pressure acceleration”) marks the onset of knock and the peak pressure marks the end. The amplitude of the steep-fronted pressure rise (“knock jump”) is the difference in pressure between the onset of knock and peak pressure and serve as the KI for an individual cycle. The amplitude for each cycle is summed over a number of preselected working cycles. In Table 1, Leiker, et al. published MN results of the single gas tests [9]. Leiker analyzed the effects of binary and ternary mixtures on MN using the same operating conditions and testing methods and published those results.

Table 1: Leiker, et al. Methane Number Results [9]

Gas	MN
Methane, CH_4	100
Ethane, C_2H_6	44
Propane, C_3H_8	34
n-Butane, n-C_4H_{10}	10
Butane, C_4H_{10}	15
Ethylene, C_2H_4	15
Propylene, C_3H_6	19
Hydrogen, H_2	0

Over a period of 10 months, Leiker, et al. [9] documented variations of ambient conditions resulting in a change of peak cylinder pressure of +/- 50 kPa (7.2 psi). Throughout the testing period Leiker, et al. determined an average testing error of +/- 1.5 MN.

Calculated Methane Number (MN_C)

Following the research conducted by Leiker, et al. [9] and the improvements made by MWM, ASTM adopted a numerical method for predicting the Calculated Methane Number (MN_C) and standardized it in ASTM D8221 [10]. The MN_C method utilizes the gaseous fuel sample component values from a gas chromatograph converted to volume faction as input. Then, after simplifying the component data and selecting the appropriate ternary mixtures to use in the calculation, a methane number is calculated for each selected partial-ternary mixture. An iterative process is used to minimize the differences in methane number for each of the selected partial-ternary mixtures. The methane number is determined from a weighted average of the methane number of the partial ternary methane numbers. Finally, the methane number of the gaseous fuel sample is calculated by correcting the methane number of the simplified mixture to allow for the presence of any inert gases found in the sample. [11] The methane numbers for the ternary mixture data used by the method were determined experimentally by Leiker, et al. [9] and digitized by MWM. The ternary mixtures have many regions of low MN resolution and hence, possible uncertainty in the methane number values may exist.

1-3 Overview & Specific Aims

Internal Combustion Engines (ICEs) have been an inexpensive means of converting chemical energy to usable work for many applications ranging in size and operating conditions. Fossil fuels are decreasing in abundance and their utilization in ICEs is a large greenhouse gas contributor. Increasing ICE efficiency can be accomplished, but doing so can lead to a phenomenon known as end gas autoignition or knock. Engine knock can be reduced by using

fuel with a higher ability to withstand compression and elevated temperatures without detonating. When using liquid fuels, one can address EGAI by selecting a fuel with a higher Octane-Number; however, for gaseous fuels like natural gas, there is no equivalent advertised metric available. Research beginning in the mid-20th century explored implementing a similar metric to the Octane Number, named the Methane Number. Unfortunately, the laboratory responsible for developing the MN did not publish detailed step-by-step instructions for the tests they carried out. Without the method used to determine the MN, manufacturers used confidential internal methods for rating fuels leading to an industry without a universally accepted standard. Cooperative Fuel Research Engines (CFR) are manufactured with the intention of testing liquid fuels for their resistance to knock. The intention of this research is to provide a repeatable method for testing the knock resistance of gaseous fuels, based on a mixture of methane and hydrogen using a CFR engine.

Goal #1: Document required modifications to CFR engine for use in Methane Number testing. Generating a document of required adaptations is necessary to allow for continued testing at other institutions and the creation of an ASTM Standard.

Goal #2: Vary methods while testing MN to determine a repeatable and accurate procedure for testing the resistance of gaseous fuels to auto-ignition and generate a Methane Number.

Goal #3: Introduce small fluctuations in environmental variables such as relative humidity, intake air pressure, etc. and document the change in test results. Approximate associated test uncertainty and place a limit on testing condition variations.

The absence of an ASTM method for assessing the knock resistance of gaseous fuels creates a void in the American market, hindering the comparison of fuel qualities. The establishment of a recognized method, if achieved, would empower both internal combustion engine manufacturers and consumers to confidently evaluate the knock resistance of a fuel using the MN before utilization.

CHAPTER 2: MATERIALS AND METHODS

2-1 Experimental Setup

CFR Engine Specifications

Cooperative Fuel Research (CFR) engines are indispensable tools in petroleum refining and fuel research, serving a diverse range of applications. These engines are engineered to withstand extended periods of strenuous operation, enduring elevated cylinder pressures, temperatures, and vibrations beyond “typical” levels. Widely employed by petroleum refineries, CFR engines aid in the comprehensive testing of fuel formulations to ensure compliance with quality standards. State laboratories utilize these engines to assess fuel quality, conducting thousands of tests annually to protect the consumer and verify fuel quality. Beyond refining processes and regulatory entities, CFR engines are instrumental in alternative fuel research endeavors exploring the impact of new fuel sources have on EGAI resistance.

The author and colleagues visited the Colorado Division of Oil and Public Safety Petroleum Laboratory. We toured the facilities and observed the procedures employed by the state of Colorado for testing the RON [7] and MON [8] of gasoline samples from fuel stations around the state. In the petroleum laboratory, two CFR F-2 engines operated concurrently, one following RON test parameters and the other adhering to MON criteria. Through this experience, insights into the typical operating conditions of a CFR engine were gained, suggesting the implementation of a natural gas testing standard in a similar laboratory. Through the research conducted, the proposed MN method technical specifications and practices could be used for an ASTM procedure.

Initially the CFR engine was crafted by the Waukesha Motor Company in 1928 at the request of the Co-operative Fuel Research committee, remaining virtually unchanged in design nearly a century later. With minor adjustments to the electrical system, CFR engines available today closely resemble their original counterparts. Table 2 presents CFR standard specifications [4]. Included in Table 3, are 14 adjustable ranges of operating conditions used for testing on the CFR. And finally, in Table 4, there are non-critical operation ranges having weak to no impact on the registered EGAI.

Table 2: CFR Engine Physical Dimensions and Specifications

Item	Parameters
Cylinders	1
Valves per Cylinder	2
Bore	3.250 in (8.255 cm)
Stroke	4.500 in (11.430 cm)
Displacement	37.331 in^3 (611.744 cm^3)
Valve Lift	0.238 in (0.605 cm)
Intake Valve Open	10^o +/- 2.5^o aTDC
Intake Valve Close	34^o +/- 2.5^o aBDC
Exhaust Valve Open	40^o +/- 2.5^o bBDC
Exhaust Valve Close	15^o +/- 2.5^o aTDC

Table 3: CFR Engine Operation Parameter Ranges

Item	Parameters SI (Imperial)
Compression Ratio	4-18
Intake Manifold Pressure (IMP)	60 – 250 kPa (8.7 – 36.26 psia)
(EMP)	Atmospheric – 2.5 bar (12.32 – 36.26 psia)
Intake Air Temperature (IAT)	10^{o} – 37^{o} C (50^{o} – 100^{o}F)
Intake Manifold Temperature (IMT)	25^{o} – 175^{o} C (77^{o} - 347^{o}F)
Crankshaft rotation speed RPM (ω)	600 – 900 (62.83 – 94.28 rad/s)
Fuel Mixture (λ)	0.75 – 2.00
Fuel Rail Pressure	100 – 500 kPa (14.5 – 72.5 psig)
Ignition timing	0^{o} - 40^{o}bTDC

Table 4: CFR Non-Critical Instrumentation and Operation Ranges

Item	Parameters SI (Imperial)
Cylinder Jacket Coolant Temperature	100^{o} +/- 1.5^{o} C (212^{o} +/- 2^{o}F)
Engine Crankcase Lubricant Temperature	57^{o} +/- 8^{o}C (135^{o} +/- 10^{o}F)
Engine Crankcase Lubricant Pressure	172 – 207 kPa (25 – 30 psig)
Exhaust Gas Temperature (EGT)	350^{o} – 550^{o}C (662^{o} – 932^{o}F)
Exhaust Manifold Back Pressure	Atmospheric +/- 2.5 kPa (+/- 0.36 psig)
Crankshaft Internal Pressure	Atmospheric – 1.5 kPa (- 0.21 psig)

One of the key attributes of the CFR engine is that the CR can be changed in real-time without changing other operating parameters. This is facilitated by the design of the cylinder head and cylinder sleeve enabling it to move relative to the piston, rotating assembly and lower casing. The "upper" and "lower" sections can move relative to each other a total of 1.235" allowing for the range of CRs of 4-18 [6].

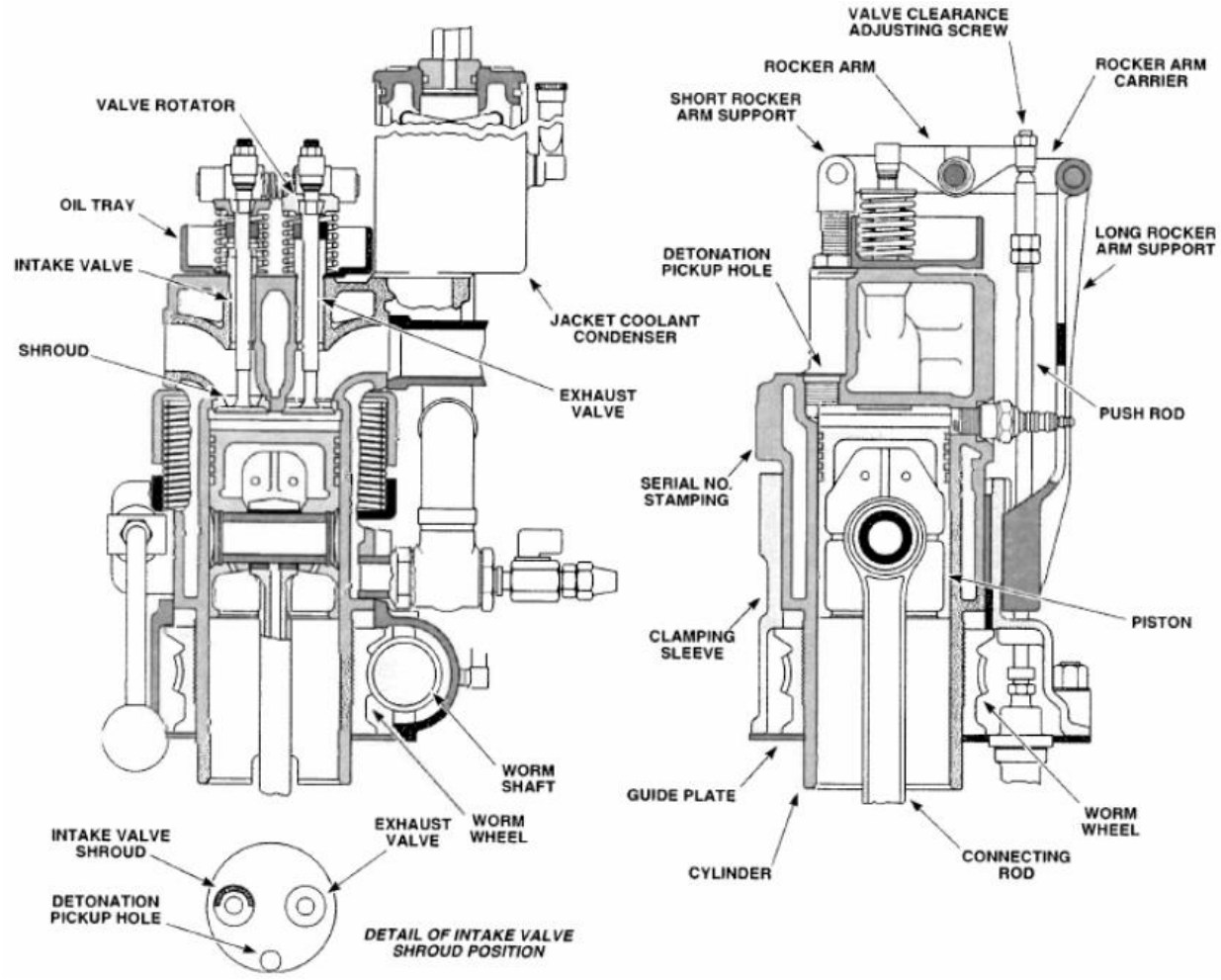

Figure 3: Waukesha CFR F-1/F-2 Clamping Sleeve Schematic [7] [12].

The CFR F-2 engine, SN: 9651 was manufactured in 1957 and is currently utilized at the Colorado State University Powerhouse Energy Campus. The engine has undergone numerous modifications to its auxiliary systems to align with the specific research objectives pursued at

CSU. The modified knock measurement system uses a water-cooled, piezoelectric pressure transducer (Kistler 6061A) [6] in the cylinder detonation port, replacing the CFR Type D-1 pickup. High-speed Kistler piezo-resistive (Type 4007D) pressure transducers were installed in the intake and exhaust manifolds [4]. The system also includes optical engine encoder (BEI L25) which is rated with 0.1° rotation resolution (3600 data points per engine revolution) to allow for the data from pressure traces to be aligned with crank position [6]. Ignition timing control is facilitated using the Woodward Large Engine Control Module (LECM). For more details on the LECM and setup and capabilities see Scott Bayliff's thesis [4]. CFR engines are equipped with a 5hp synchronous motor-generator with the required gearing to produce AC power when under operation. The original motor control unit was replaced with a Yaskawa regenerative Variable Frequency Drive (VFD), enabling precise adjustment of the engine rotational speed within +/- 0.2 rpm of the desired setting and testing at both 600 and 900 for the RON [7] and MON [8] respectively [4].

Accurately measuring the air/fuel mixture is a very important element of the MN test procedure. There is a direct correlation with EGAI and mixture ratio therefore having a repeatable method of measuring the air/fuel mixture is essential for the CFR engine. The instrument tasked was a Motorsports Technology (MoTeC) Professional Lambda Meter (PLM) system [13], the O2 sensor location is referenced in Figure 4 and Figure 5. According to the user manual, the PLM can sense lambda ranges of 0.7-32 and has an accuracy of +/- 1.5% [13].

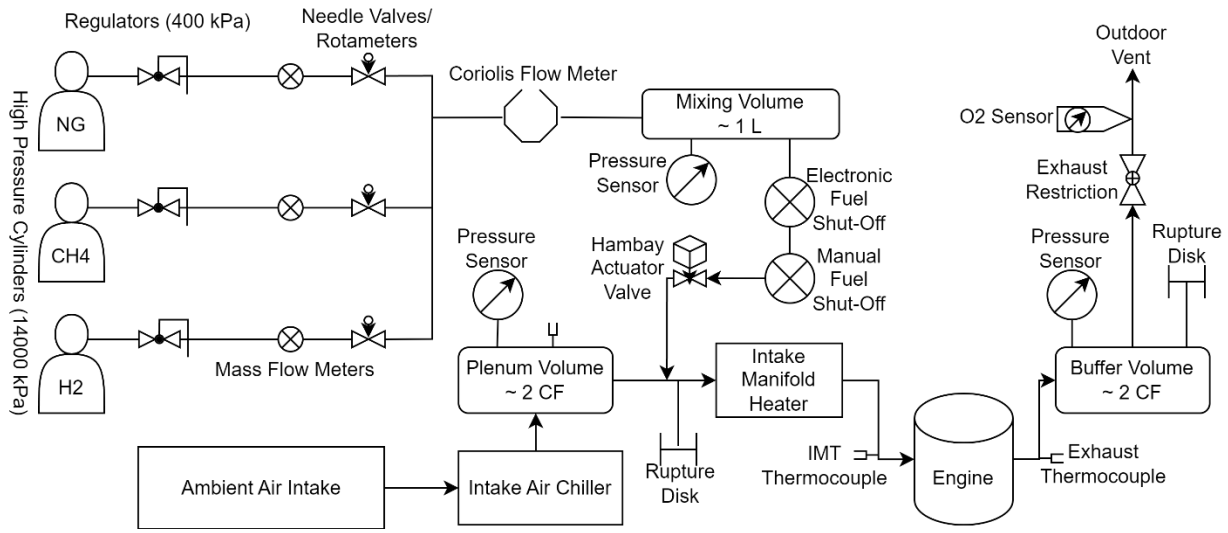

Figure 4: Engine fuel and intake system for ambient operations

The conditioning of incoming air to meet certain environmental parameters is an important task that is required to achieve consistent results. For altering IAT or reduce incoming water vapor, a 5000 BTU/hr. residential air conditioning unit was installed, and its location can be referenced in Figure 4. When operating at elevated intake air pressure conditions, the CFR intake system was connected to the building compressed air system. In Figure 5, A butterfly valve controlled by a Proportional Integral-Derivative (PID) control loop was used for air pressure control. An Omega Air Flow Meter is responsible for managing IAP and is responsible for a total pressure fluctuation of +/- 5 kPa. A manual restriction valve was installed in the exhaust to control engine back pressure with a 2-ft^3 buffer volume [6] [4].

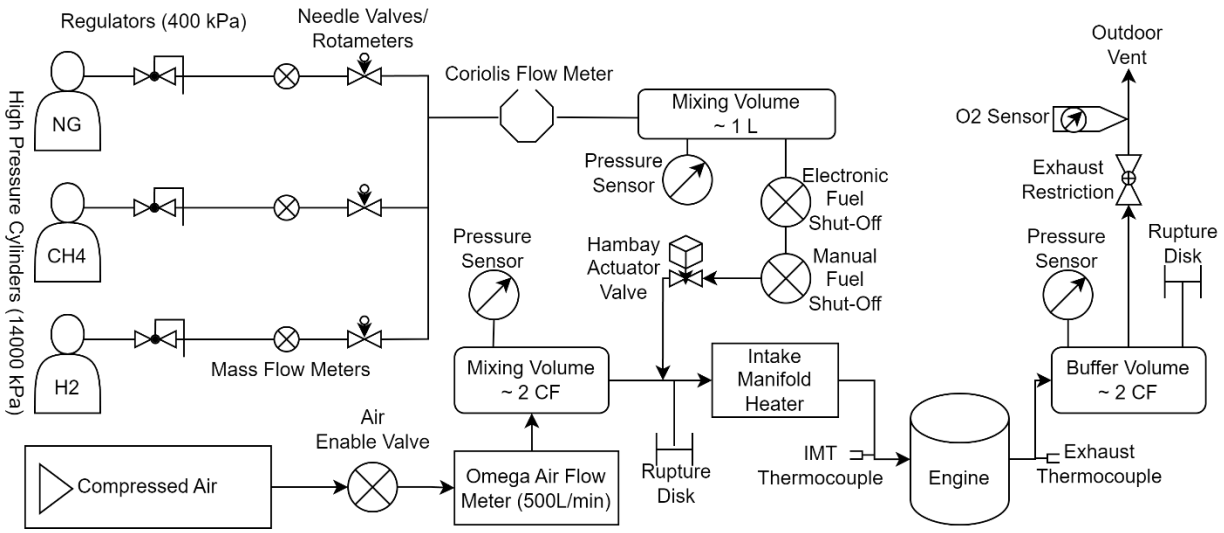

Figure 5: Engine schematic including compressed air system.

Fuel Management

Designed by Waukesha and now distributed through CFR Engines Inc., the original carburetor features a gravity feed system with multiple fuel bowls, each intended for different mixtures of fuel. Each fuel bowl is adjustable in height via a mounted screw, impacting the supplied fuel mixture. CFR carburetors are now equipped with a secondary port to facilitate the use of gaseous fuels to achieve stable operating conditions. This design enables engine operation for long durations without the addition of liquid fuel.

Unfortunately, the carburetor on the CSU CFR was not equipped with a secondary fuel port, requiring another solution for fuel delivery. The solution devised was to introduce fuel to a plenum volume preceding the carburetor. The fuel begins in pressurized fuel bottles ranging from 10-140 bar when it travels through fuel pressure regulators, which reduces pressure to 4 bar. The regulated fuel then passes through Omega FMA-1700 mass flow meters, which precisely measures the mass flow rate of each type of fuel. The fuel flows through a needle

valve, allowing for fine flow rate control before entering the common fuel rail, where multiple fuel components are blended. The fuel mixture then passes through a Coriolis flow meter, which measures the mass flow rate with high accuracy. The fuel then enters a mixing chamber, where it is given adequate volume for mixing and serves to reduce fluctuations in fuel pressure. An electronic fuel shutoff solenoid allows it to be shut off instantly if needed. Fuel flowrate is managed by a Hanbay MCM-050AB actuator valve, with fine adjustment control facilitated by a Swagelok SS-4MG 1/4-inch Stainless Steel metering valve. To accommodate both liquid and gaseous fuels, the liquid carburetor is retained for testing purposes. The fuel is directed to a 2 ft^3 plenum volume to dampen pressure pulsations upstream of the intake manifold.

Required Safety Additions

When operating an internal combustion engine (ICE) indoors, safety measures are paramount to protect operators and prevent environmental damage. Exhaust gases are vented outdoors to safeguard against carbon monoxide buildup, with a detector installed to warn of any leaks. An explosive gas detector is also in place to alert of potential fuel leaks. Smoke and oxygen depletion alarms were also installed as a precaution in case of a fire or large leak of nonflammable gas. Burst disks are utilized in the intake and exhaust manifolds to relieve pressure in the event of ignition or valve closure. Additionally, a safety isolation switch in the LabVIEW Virtual Instrumentation (VI) and an emergency shutdown button on the CFR provide immediate response capability in case of accidents.

2-2 Knock Quantification Methods

This section describes knock quantification process methods utilized in industry and academic settings. The common idea between the methodologies lies in the necessity of a robust metric to quantify knock amplitude. Given the diverse landscape of industry and academia, a standardized approach is imperative to ensure consistency across varying environmental conditions. The methods used for knock quantification within the scope of this project are the Fast Fourier Transform of Bandpass Signal and the Original CFR Knock Measurement System. The other methods of knock quantification employed by others are described by Bayliff [4].

Fast Fourier Transform of Bandpass Signal:

The method involves a Fast Fourier Transform (FFT) analysis of cylinder pressure readings to assess pressure trace dynamics in the frequency domain, aligning with methodologies by Brunt [14] and Elmqvist [15]. It quantifies auto-ignition events by correlating pre-detonation points with cylinder geometry, factoring in the time for a pressure wave to travel twice the cylinder diameter at the local speed of sound. Key equations are provided for speed of sound in Equation (1), event period in Equation (2), and anticipated knock frequency in Equation (4).

$$\boldsymbol{c = \sqrt{\gamma R T}} \qquad \text{Equation (1)}$$

Where:

c = Speed of Sound

γ = (ratio of specific heats): 1.3

R = ideal gas constant: $\boldsymbol{287 \frac{J}{kg*K}}$

T = Estimated Air Temp: 2500 K

$Bore$ = Diameter of CFR cylinder = 0.08255 m = 3.250 in

Using the equation for speed of sound in $\boldsymbol{c = \sqrt{\gamma RT}}$

Equation (*1*), the predicted period of knock can be approximated by using the distance the wave travels from one side of the cylinder to the other then divided by the speed of the wave which results in Equation (2).

$$\boldsymbol{\tau = 2 * Bore/c} \qquad \text{Equation (2)}$$

Converting the anticipated period to a frequency is done with Equation (3).

$$\boldsymbol{f = 1/\tau} \qquad \text{Equation (3)}$$

Combining Equations 1, 2, and 3 results in Equation (4).

$$\boldsymbol{f = \sqrt{\gamma RT}/(2 * Bore)} \qquad \text{Equation (4)}$$

The anticipated frequency, calculated for representative parameter values, is 5850 Hz. LabVIEW, used for the combustion logger program, employs a FFT Power Spectrum function to analyze real-time cylinder pressure signals. A bandpass filter eliminates operating frequency, revealing pressure distortions indicative of knocking. The CFR-F2 engine operates at 900 rpm (15 Hz). Figure 6 depicts a light and heavy engine knock conditions, with multiple oscillations in pressure occurring after the peak pressure and subsequent peak on the FFT plot with a frequency near 6 kHz corresponding to the anticipated value.

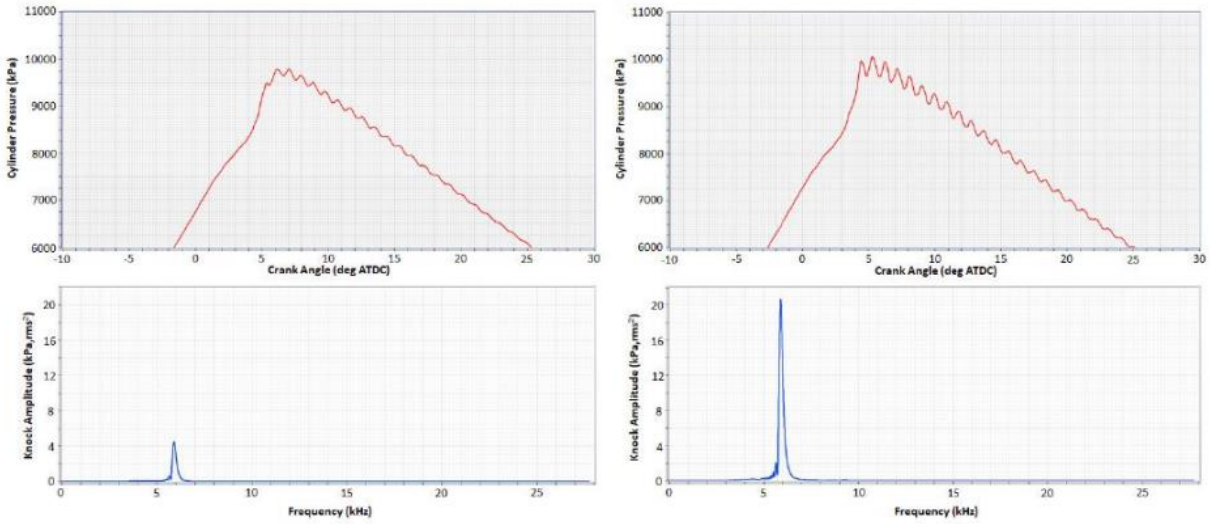

Figure 6: Pressure Trace and FFT Plots of Light & Heavy Knock Intensities [6]

The upper plots in Figure 6 display the in-cylinder pressure [kPa] trace plotted relative to crank angle [aTDC] and in the plot below the FFT result, amplitude [kPa·rms^2] versus frequency [Hz]. The data represents two conditions of engine knock with the left pressure trace demonstrating a light knock intensity, and the right pressure exhibiting heavy knock intensity. The FFT plots exhibit a prominent spike at the frequency of the knock event, approximately 6 kHz, with spike magnitude correlating to knock intensity. The bandpass filter removes low and high frequency noise, tailored to the CFR engine geometric dimensions. Knock Intensity is the measure of the amplitude of the FFT of an individual pressure trace. The Knock Integral represents the sum of maximum FFT spike magnitudes over successive combustion cycles. The equation for the Knock Integral is given in Equation (5).

$$\boldsymbol{KI = Area_{bounded}} = \sum_{\boldsymbol{i=1}}^{\boldsymbol{n}}\{(\boldsymbol{i+1}) - \boldsymbol{i}\}\{\boldsymbol{KL(i+1) + KL(i)}\}/\boldsymbol{2} \qquad \text{Equation (5)}$$

In Figure 7, FFT magnitude variations over 1400 cycles at different knock levels are plotted demonstrating the typical variation over the course of 3 minutes of operation at 900 rpm. Knock Integral is used because it quantifies knock severity and persistence and is displayed to

the operator as a rolling 200 cycle value. This was done to allow the operator to better match knock intensities between samples and allow for a greater difference between similar knocking conditions.

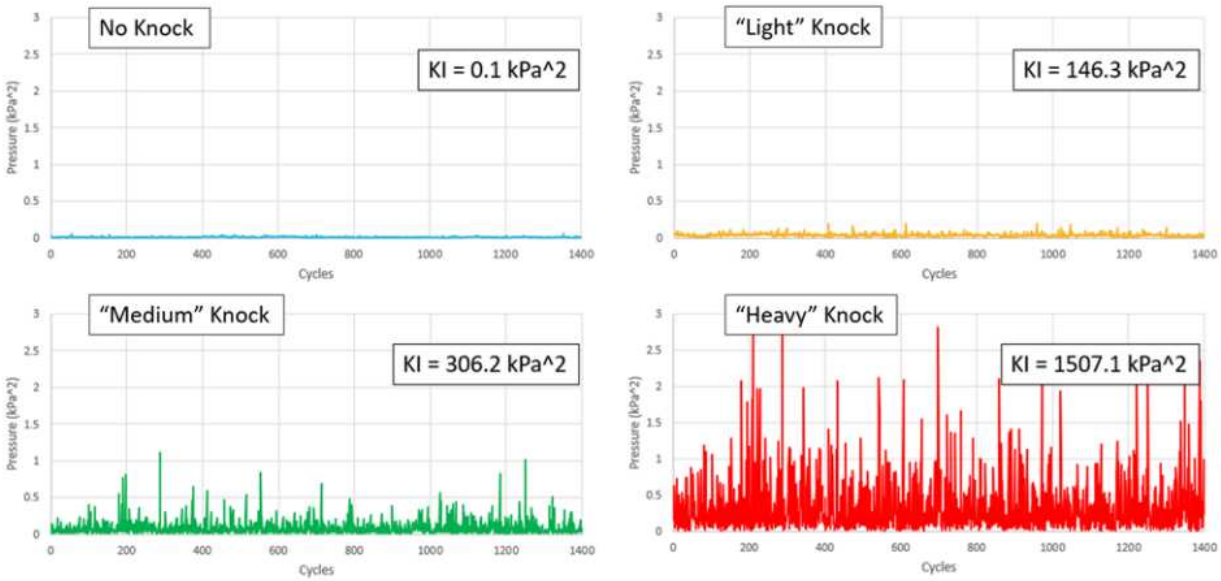

Figure 7: Variation of Cyclic FFT Magnitudes [4]

When analyzing EGAI characteristics in post-processing, the Knock Intensity values are averaged over the course of the test and referred to as Average KI. The Knock Integral is used during the test by the operator and is not considered in post-processing.

CFR Knock Measurement System

The CFR Knock Measurement System serves as an analog method for gauging the intensity of engine knocking during operation. When conducting tests with the CFR, this system provides a means to measure the knock intensity, allowing operators to fine-tune various settings impacting the recorded data. In this section, the intricacies of the CFR Detonation Meter are

reviewed including its functionality, adjustments, and the impact of these variables on the quantification of engine knock intensity.

The original CFR engine knock measurement system comprises a power supply, detonation meter, detonation pickup, and knock meter face. The pickup sensor, mounted through the cylinder head, utilizes a flexible diaphragm exposed to combustion chamber pressure changes. The diaphragm reaction induces a voltage in a coil wound around a magneto-restrictive alloy, directly proportional to the rate of cylinder pressure change. Depicted in Figure 8, there is a labeled simplified drawing of a detonation pickup. The analog detonation meter isolates relative knock amplitude through signal averaging and filtering, transmitting it to the knock meter, which displays the relative intensity on a comparative scale. An optional analog strip chart recorder was also available to provide a permanent record of the data set. An electrical block diagram is provided in Figure 9 as an overview of what processes are involved to convert the voltage signal from the detonation pickup to the knock intensity reading on the dial.

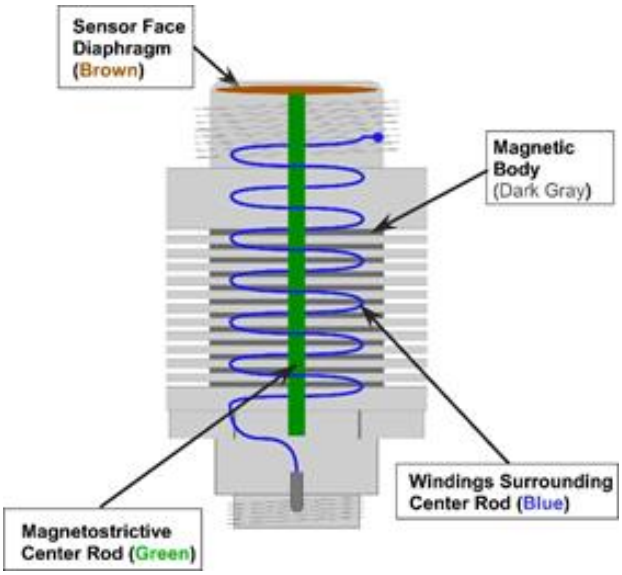

Figure 8: CFR Detonation Pickup Internal Schematic *[16]*

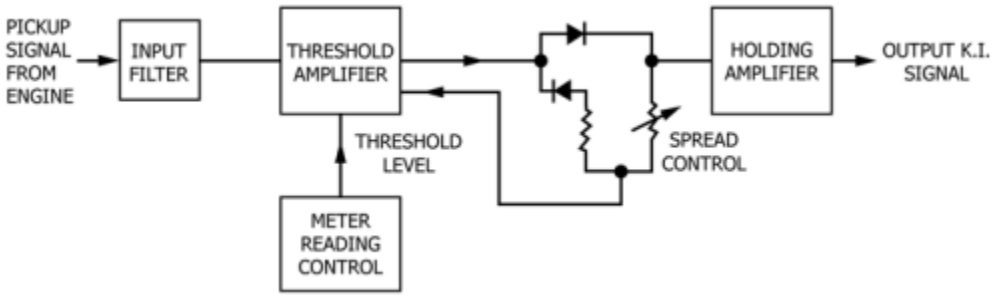

Figure 9: Block Diagram of Detonation Meter *[7] [8]*

Table 5: CFR Knock Measurement System Adjustment Methods

Name	Location	Purpose	Adjustment
Meter Reading	Left Dial Detonation Meter Face	An offset for the Knock meter reading	Coarse & Fine Adjustment Increase – Larger Offset
Spread	Right Dial Detonation Meter face	The Sensitivity expressed in knock meter divisions per octane number	Coarse & Fine Adjustment Increase – Greater Resolution
Meter	Left side Detonation Meter Face with tethered cover cap	Another offset for the Knock meter reading	To be used in conjunction with Meter Reading
Operate / Zero	Toggle Switch on Left Panel	Returns meter to zero	Needs to be in Operate position
Time Constant	Center Dial Detonation Meter Face	Reactivity of Knock Meter reading	Increase – Less reactive
Knock Meter Tension Screw	Bronze Screw Knock Meter Face	Influences resistance of needle movement	Should be positioned to allow for needle to return to zero

The original knock measurement system requires the operator to audibly detect knock onset, then adjust the METER READING and SPREAD dial settings, and select a time constant. Table 5 outlines each dial/switch purpose and location with a picture used for reference. Choosing each of these settings while initializing the knock measurement system is subjective process but through documented procedures is acceptable for rating the autoignition resistance of fuels. This system does not have the required data resolution and time response for maintaining the necessary objectivity required for a nuanced analysis of knocking in a research environment.

Operational Parameter Monitoring/Management

The project test cell monitoring and control system, developed by Colorado State University Engines and Energy Conversion Laboratory using LabVIEW© software, integrates input from various sensors to control fuel injector PWM duty cycles, intake air pressure, and flow rate, as well as calculate desired exhaust backpressure. The software displays engine operating status and allows for monitoring and control of various parameters including intake air pressure and temperature, fuel mixture, air-fuel ratio, exhaust temperature and pressure, coolant temperature, and power generation level. Data from engine operating conditions such as RPM, fuel flow, and temperatures are saved at user-defined frequencies. Additionally, the system includes a separate VI for collecting and processing signals from pressure transducers and position sensors, which are then analyzed to determine cycle metrics such as KI, MFB, and BMEP [4].

Flow Meter Calibration

The Omega FMA-1700 mass flow meter utilizes a direct method of measurement that involves the thermal properties of gases. The flow meter uses a heated tube to heat transfer to measure the molecular gas flow rate allowing for an accuracy of +/- 1.5 % of full scale and remains linear between 15º and 25ºC. The sensor also advertises a repeatability of +/- 0.5% of full scale making this sensor a great option for testing the MN of fuels.

The calibration of flow meters is a crucial step in the testing process and is a necessary investment of time early in the testing timeline. The process taken for this research involved a Positive Displacement Gas Flow Meter (PDGFM) that was installed in series with the calibration flow meter following the Calibration procedure in Figure 10, The PDGFM was a certified unit with 1 ft^3 volumetric deviations which allowed for adequate resolution for calibration purposes.

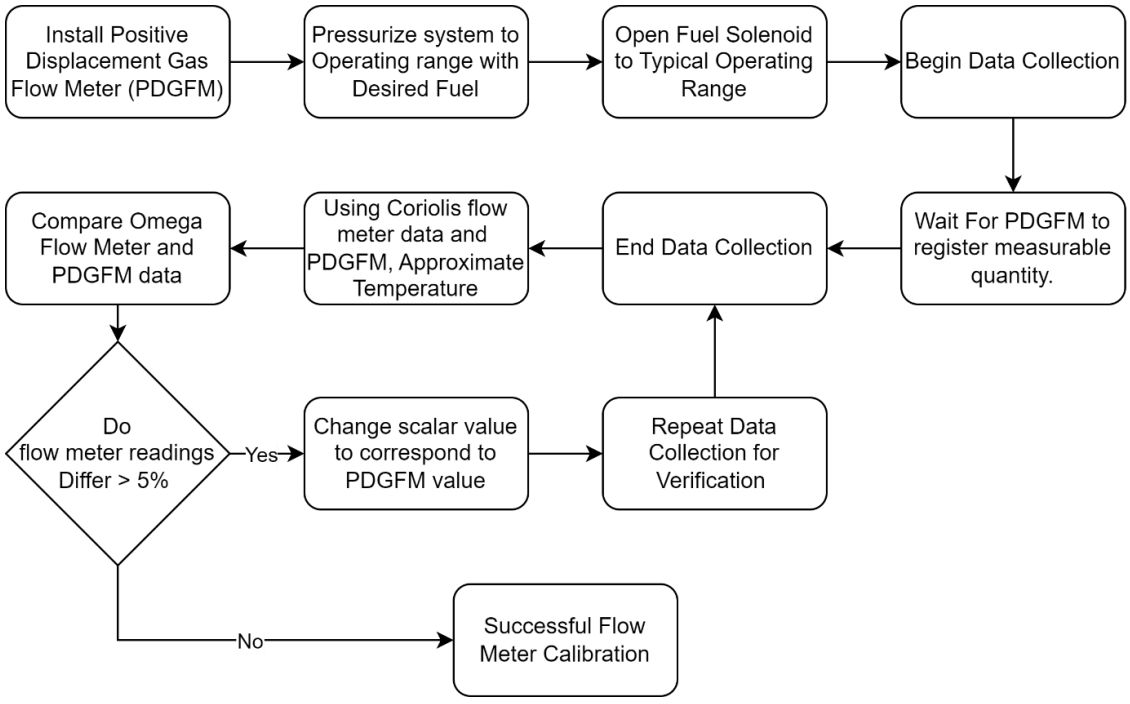

Figure 10: Omega Flow Meter Calibration Procedure

Flow meters for methane and hydrogen were calibrated multiple times using the ideal gas law, with approximations for gas temperature and isentropic process conditions. Calibration involved three methods: Omega FMA-1700, Coriolis mass flow meter, and PDGFM. The Coriolis meter revealed a ~5°C temperature difference in the methane measurement due to the Joule-Thompson effect, with coefficients of is $4.6285\frac{K}{MPa}$ for Methane and $-0.285\frac{K}{MPa}$ for hydrogen [17]. The Joule-Thompson effect dictates the change in temperature of a substance based on the change in pressure with constant enthalpy (isenthalpic) [18]. Methane decreased while hydrogen increased in temperature due to their differing coefficients. Heat transfer into the gas due to line distance and diameter mitigated a larger predicted temperature difference. hydrogen was assumed to be at ambient temperature, while methane was assumed to be 5°C lower during calibration.

2-4 MN Testing Method: Matching KI Value

Originally pioneered by Leiker [9], and used by Wise [6] for the testing of Methane Number, the procedure relies on the matching of knock intensity between the test sample and a reference fuel blend. Using this method requires finite control of fuel dilutant ratio and the means of accurately measuring fuel flow rates determination of MN. A flow chart outlining the testing procedure for the determination of MN is displayed in Figure 11.

Calculating MN from methane and hydrogen flow data meters requires converting from a mass flow ($\frac{g}{min}$) to molar flow ($\frac{mol}{min}$). This requires the average molecular weight for methane ($16.04\frac{g}{mol}$), hydrogen ($2.016\frac{g}{mol}$) and carbon dioxide ($44.01\frac{g}{mol}$). Finally, to convert from molar flow to MN, the average flow rate of methane for the test is divided by the total number of mols

(mol H_2 + mol CH4) and multiplying by 100. In the case of tests with a fuel that has a higher resistance to EGAI than pure methane, carbon dioxide is added, and the MN is calculated by taking the average molar flow of CO_2 dividing it by the total flow rate, adding 1 and multiplying by 100.

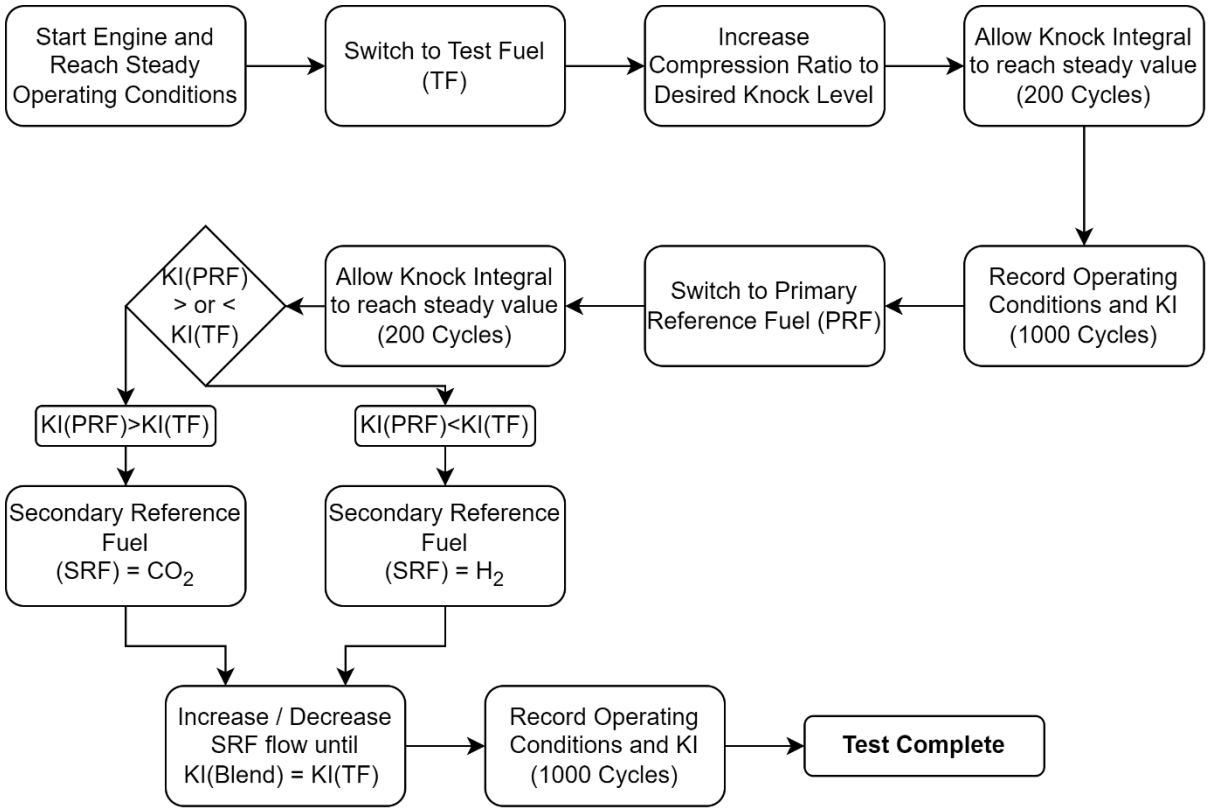

Figure 11: Methane Number Test Procedure Flow Chart

Beginning with the original method implemented by Leiker [9] and utilized by Wise [6], for the determination of MN, there were questions raised regarding the sensitivity of the method to environment conditions and testing variables. In the following chapters, the effects of these parameters are investigated as well as possible adaptations to the method addressing shortfalls that were identified throughout the testing process.

CHAPTER 3: IMPACT OF CONTROL PARAMETER VARIATION

3-1 Environment Parameter Variation

The testing environment is an important consideration when measuring the knock resistance of a fuel. There are multiple parameters that have varying levels of impact on the knock tendencies and repeatability of a MN test. When analyzing the testing environment, there are many conditions of the air that have a direct link to the knock tendencies of a fuel. The air humidity and pressure have direct impacts on the severity of engine knock and are not able to be changed without additional equipment. Such equipment introduces its own variation and requirement for calibration.

Humidity

Humidity is a crucial factor in fuel knock resistance testing that is typically overlooked and affects the ability to resist knock. Water vapor is a known EGAI inhibitor with larger presence of water accounting for a lower flame temperature following the combustion event and lower overall knock intensity. While the work of Leiker, et al. [9] overlooks the impact of humidity, Essen's research provides insight into its significance in lean burn natural gas applications [19]. Given water has a direct influence on engine EGAI characteristics, measuring and establishing a desired humidity range for testing becomes imperative.

While the method used by Leiker, et al. [9] does not mention incoming air water content, liquid fuel testing methods prescribe an acceptable range of absolute humidity, typically between 0.00356 kg to 0.00712 kg of water per kg of dry air. Analyzing the work of Essen et al. [19],

they concluded that the water content in the air had a substantial effect on the knock characteristics while all other parameters remain constant. Testing they conducted showed that the measured MN of a fuel was changed by 5 because of transitioning from 0.0043 kg to 0.011 kg of water. These results underscore the necessity of defining acceptable absolute humidity ranges for accurate test outcomes and ensuring consistent variance throughout a test.

Barometric Pressure

Barometric pressure is influenced by altitude and weather conditions. The change due to elevation is approximately 1.2 kPa (0.174 psig) per 100 m (328 ft). Variations in temperature affect air density and, consequently, barometric pressure. This pressure can fluctuate significantly within a 24-hour period, as observed at the Colorado State University Atmospheric Science Fort Collins Weather Station [20]. For instance, on December 14th, 2023, atmospheric pressure ranged from 854 to 842 millibar, equivalent to a 1.2 kPa change or a shift in altitude of 100 m.

Changes in barometric pressure directly impact engine operation, influencing both IMP and Exhaust Manifold Pressure (EMP). Changes in these values impact fuel consumption, power output, emissions and EGAI. Modern engines utilize mass air flow sensors to account for variations and employ turbochargers/superchargers to modulate IMP.

Considering the MON method, CR is altered so that the KI will match that of an engine at standard barometric pressure. For conditions with lower ambient air pressures, the CR and thus KI is increased. The MON method lists correction factors to apply to the dial/digital reading based on measured barometric pressure. Considering the RON method, the cylinder height has a similar correction factor based on barometric pressure, but included in the correction factor is a

correlation between barometric pressure and intake air temperature. The RON [7] method also mentions an acceptable value for EMP; the static pressure should be as low as possible but shall not create a vacuum nor exceed 255 mm (10 in.) of water differential in excess of atmospheric pressure [8].

In the work by Leiker, et al. ambient conditions were not referenced, but a change in peak cylinder pressure of +/- 50 kPa (7.2 psi) was included and attributed to the +/- 1.5 MN uncertainty [9]. The CFR engine used by Leiker, et al. [9] was naturally aspirated, and located in Graz, Austria with an altitude of 350 m (1148 ft). This correlates to an approximate barometric pressure of 96 kPa without the effect of weather variations.

3-2 Testing Conditions

This section focuses on parameters that possess inherent variability but can be adjusted by the operator. When assessing the CFR for repeatability, considering the engine operating conditions is crucial, which influences its performance. Intake Air Temperature (IAT), coolant water temperature/level, engine lubricant oil temperature, and engine operating speed are all parameters that will be introduced in this section. These parameters play a significant role in fuel knock characteristics and must be maintained within specified ranges for accurate testing. To reduce the effects of environmental conditions, MN sensitivity analysis results will only be compared to tests conducted on the same day. Additionally, the engine was given sufficient time to stabilize before testing commenced, mitigating any potential impact from transient thermal effects.

Test Cell / Intake Air Temperature

When testing the MN, the IAT is a parameter that must remain consistent, but the acceptable range of this value was not published. The intake air temperature is a metric that directly impacts compression temperatures and the total heat capacity of the charge (trapped mass). When the air is combined with fuel and compressed to high pressures yields an environment capable of triggering an ignition event without a spark. When consulting the resources available for the RON [7] and MON [8] tests, ambient air temperature and humidity are treated as independent. But when using a chiller to reduce the humidity of incoming air, setting IAT is a possibility but would need to be exceedingly low to reach saturation with the required humidity.

The IAT requirements between RON [7] and MON [8] test methods are different. The RON [7] method specifies an IAT value but overlooks Intake Mixture Temperature (IMT) mentioned in the MON [8] method, suggesting the RON [7] IAT aligns better with IMT for consistency. In contrast, the MON [8] test necessitates a fixed IAT of 38°C ± 2.8°C (100°F ± 5°F) regardless of barometric conditions. Considering the paper by Leiker [9], charge Air Temperature of 20ºC (68ºF) was used, which measures the temperature of the mixture before the combustion chamber. The document did not mention ambient air temperature, but it could be assumed to be the temperature of the test cell. Leiker [9] concluded knock tendency was influenced by intake temperature with lower MN exhibit a larger change in knock intensity with when compared to higher temperatures.

Cooling Water Temperature

The CFR engine is equipped with an ebullient cooling system. Engine coolant, a mixture of water with glycol antifreeze, circulates through channels in the cylinder head and sleeve, absorbing heat from the engine and evaporating to carry away excess heat of combustion. The vaporized coolant then circulates to a heat exchanger where it condenses back into liquid form, releasing the absorbed heat into a coolant circuit consisting of non-potable water before being recirculated back into the engine. In this system the non-potable water and glycol mixture remain separate to prevent calcium buildup in the engine or heater core. Higher coolant temperatures lead to increased KI in a fuel, assuming all other conditions remain constant. Glycol is added to counter the impact of decrease in atmospheric pressure with altitude on boiling temperature.

The RON [7] and MON [8] test methods specify cylinder jacket coolant temperature should remain at 100° +/- 1.5 °C (212° +/- 3 °F) when operating. These standards require the temperature to remain constant within +/- 0.5°C (1°F) when CR or KI results used for octane determination on each fuel are recorded [8]. The liquid fuel standards also require a specific level of coolant, requiring the level in the condenser sight glass shall be within +/- 1 cm (+/- 0.4 in.) of the LEVEL HOT mark on the coolant condenser. The coolant water temperature used by Leiker, et al. [9] differs from the RON [7] and MON [8] standard, and is referenced to be 80ºC with no reference to an acceptable range or variation. Leiker, et al. does mention a direct correlation between coolant temperature and KI like intake air temperature. The work did not mention a required coolant level in reference to the LEVEL HOT mark. For this research, glycol was added to increase the coolant boiling temperature to 100ºC according to the MON [8] method.

Engine Lubricating Oil Temperature

The CFR engine is equipped with an electric resistance oil heater to increase the oil temperature to a user-specified value. The oil heater has three power settings and lacks a thermal shutoff, requiring the operator to remain vigilant about the engine oil temperature during operation. The CFR engine is not equipped with an oil cooler but easily stays within the specified temperature range outlined in the MON [8] and RON [7] methods on warm days, and it may even require the oil heater to remain on during cold days, Both methods stipulate the requirement for oil temperature to be 57°C +/- 8°C (135°F +/- 15°F). Leiker [9], does not mention the engine oil temperature for the CFR engine, but it can be assumed to align with the specifications outlined in the RON [7] and MON [8] methods. A target range of 57°C +/- 3°C (135°F +/- 5°F) is used for this research to remain well within the required tolerance outlined by the liquid fuel testing.

Engine Operating Speed (RPM)

The engine operating speed is directly tied to the frequency of ignition events, which is influenced by the flame speed of the fuel. Speed requirements vary depending on the method and the type of engine used. In the MON [8] standard for liquid fuels, the engine operates at 900 rpm with a maximum variation of +/- 9 rpm during a rating, and a maximum difference of 3 rpm between motoring and firing conditions. In contrast, the RON [7] method specifies a slower speed of 600 rpm with a variation of +/- 6 rpm during a rating and requires no more than a 3rpm difference between motoring and firing conditions.

Analyzing the work of Leiker et al. [9], researchers primarily used a CFR engine operating at the same speed as the MON test. Although Leiker et al. did not publish the range of RPMs experienced with their testing, it is assumed to align with MON standards. Leiker [9] also tested the validity of the MN test results using larger engines and by running the CFR engine at a slower speed, finding appreciable differences in MN. The comparison showed a drop in knock rating with decreasing methane number, influenced by the engine speed difference. Knock depends on pressure, temperature, and time. MN comparisons between engines with different speeds showed a maximum difference of 15-20 units, decreasing to 10 units when the CFR engine matched the slower engine speeds (375 rpm). Before VFD implementation for finer speed control, the system Wise used operated at 940 +/- 5 rpm without mention of its effect on measured MN [6].

In this study, the engine RPM mirrored the work of Leiker [9], with the VFD set to 900 +/- 1 rpm, aligning with the MON [8] method. However, the intention behind the smaller allowable variation between motoring and firing conditions in the MON [8] and RON [7] methods remain unclear. Operating speed is crucial, as it affects the flame speed of the fuels tested. While natural gas, rich in methane, aligns with the reference fuel, hydrogen has a significantly higher flame speed which is sensitive to piston speed variations. This challenge is exacerbated with fuels like ethane, propane, and butane, each with distinct flame speeds. A standardized approach would streamline MN referencing regardless of engine speed.

3-3 Intake Manifold Temperature

The objective of this section is to explore the impact of Intake Manifold Temperature (IMT) on the MN test procedure. The investigation of IMT is split into three different studies. **KI**

Variability: IMT, investigates the relationship between increasing CR and KI at different IMT setpoints. **IMT Parameter sensitivity** analyzes the direct correlation between KI and temperature fluctuations to establish an acceptable variation**. IMT Effect on MN** examines the effect different IMT setpoints have on MN results.

KI Variability: IMT

When analyzing the effects of IMT on MN, the first step is determining the relationship of CR and IMT on KI. The two independent variables in this study are CR and IMT. The objective of this study is to better understand the effect these two independent variables have on the onset and intensity of knock. For this study there were two days of testing conducted with the same NG sample and ignition timing utilized. Figure 12 and Figure 13 are the results from the two days of testing. On each plot there are exponential trend lines with equations and R^2 values.

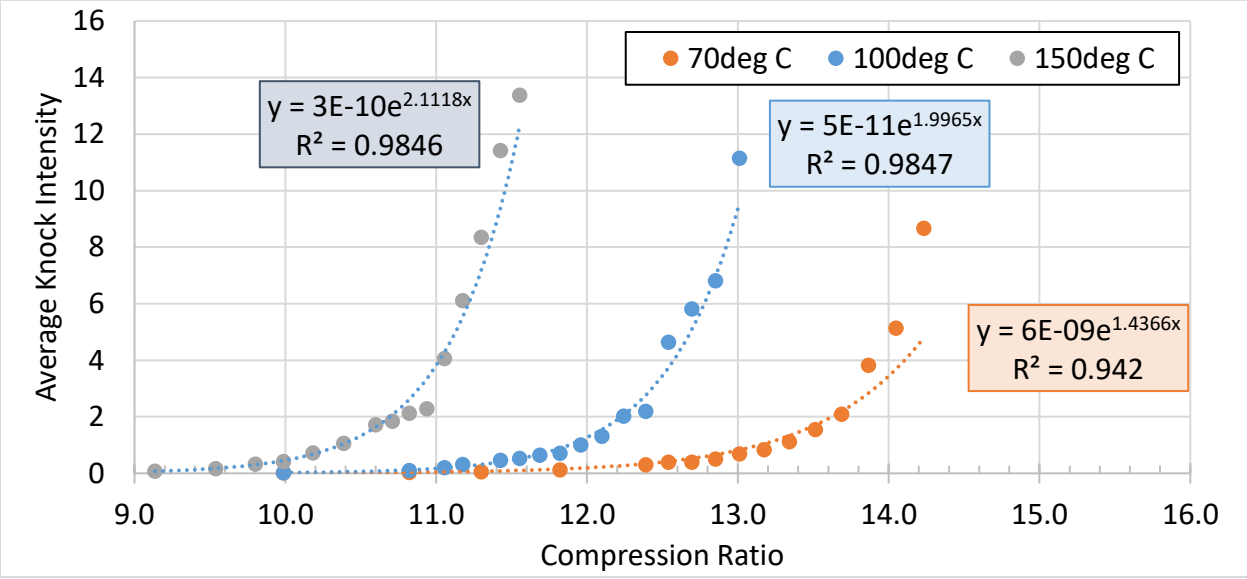

Figure 12: Results of Fuel Variability: IMT/CR Variation (11/28/23)

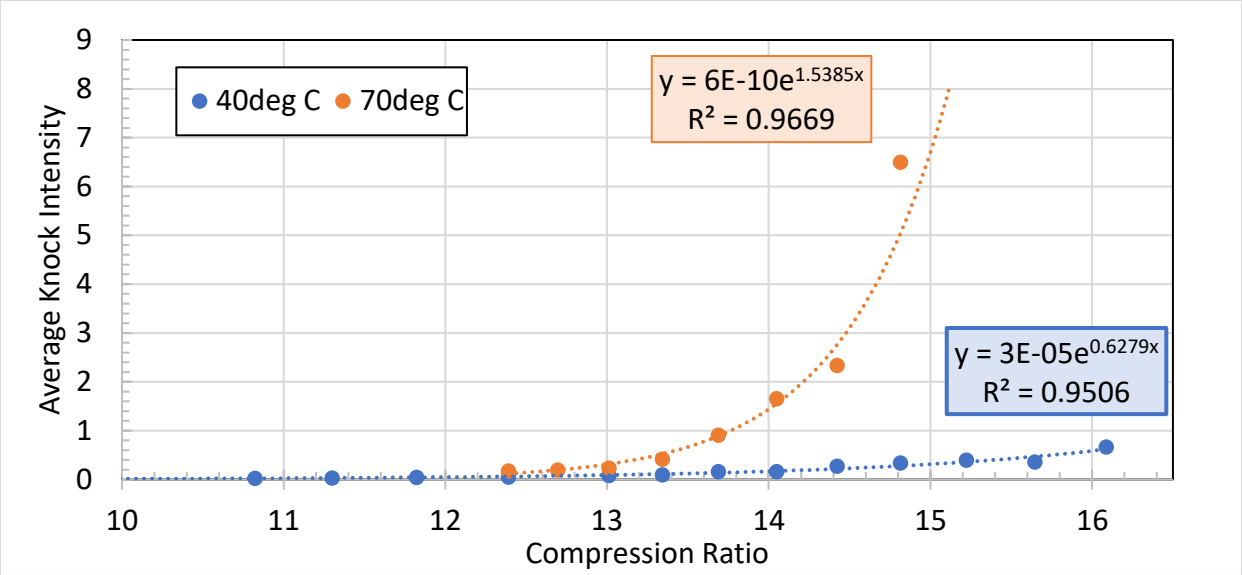

Figure 13: Results of Fuel Variability: IMT/CR Variation (12/5/23)

Figure 12 and Figure 13 show a high correlation between the exponential trend lines and the experimental data with the lowest coefficient of determination being 0.942. The common 70°C tests between the two days of testing at have similar trends, R^2 values, and trend line exponents, which impacts KI sensitivity. For higher IMTs, the KI increases at a greater rate indicating knock is more sensitive at similar knock values. This is further demonstrated by evaluating the slope at a given knock intensity for each of the trend lines and comparing them. In **Table 6** the relationship between the slope of the KI trendline line and IMT are presented.

Table 6: IMT Variability Study Calculations

IMT	Trendline $KI(CR) = a * e^{b*CR}$	$\frac{dkI}{dCR}$ @ $KI = 4 \rightarrow \text{CR} = \frac{\ln\left(\frac{KI}{a}\right)}{b}$	$\left.\frac{d(KI)}{d(CR)}\right\|_{CR}$
70	$6 * 10^{-9} * e^{1.4366*CR}$	14.1	5.75
100	$5 * 10^{-11} * e^{1.9965*CR}$	12.6	7.97
150	$3 * 10^{-10} * e^{2.1118*CR}$	11.0	8.45

The IMT sensitivity study results indicate a greater increase in KI for a given increase in CR for higher temperatures. Comparing the results between the two days of testing for similar IMT, there is enough of a difference between the trend lines to support the decision that KI values taken on different days cannot be compared directly.

IMT Sensitivity

The next stage of the IMT investigation is determining the magnitude of effect small variations in IMT play in the KI experienced by the CFR engine. The Knock Measurement system used for this section was the CSU in cylinder pressure transducer utilizing the FFT method. This was done to ensure consistent KI values without influence from the operator and the objective onset of knock. Throughout this section, there were no changes made to the in-cylinder pressure transducer, signal processing, or the method used for knock quantification. To isolate IMT as the independent variable, the engine was operated with as little variation as possible in other systems including fuel composition, ignition timing, mixture, air pressure, oil and coolant temperature. The engine was allowed ample time to reach steady state before testing began to reduce any possible effects of thermal conditions outside the intake manifold. In selecting the set point for the IMT fluctuation tests, 70°C was chosen. At this temperature range, the current supplied to the mixture heater could be accurately measured, while reducing the risk of backfires in the intake manifold. Figure 14 depicts a flow chart for measuring the effect small variations in IMT have on the KI for the CFR engine.

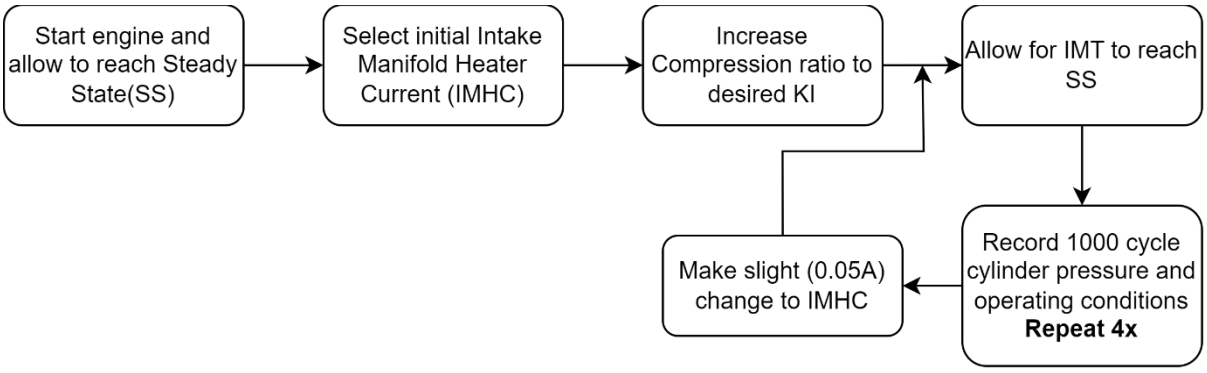

Figure 14: Test Strategy for Intake Manifold Temperature Fluctuations

In practice, with an IMT of 70°C, ignition timing of 15° bTDC, 85 kPa atmospheric pressure, and a constant CR of 14:1, the CFR engine was able to maintain very consistent knock intensities. The test included 5 Intake Manifold Heater Current (IMHC) levels ranging from 1.2 to 1.4 amps, which correlated with a variation in IMT of ~ 4°C. Over the small temperature range of 4°C, there was a significant change in KI. The result of the Intake Manifold Temperature Fluctuation study is plotted Figure 15.

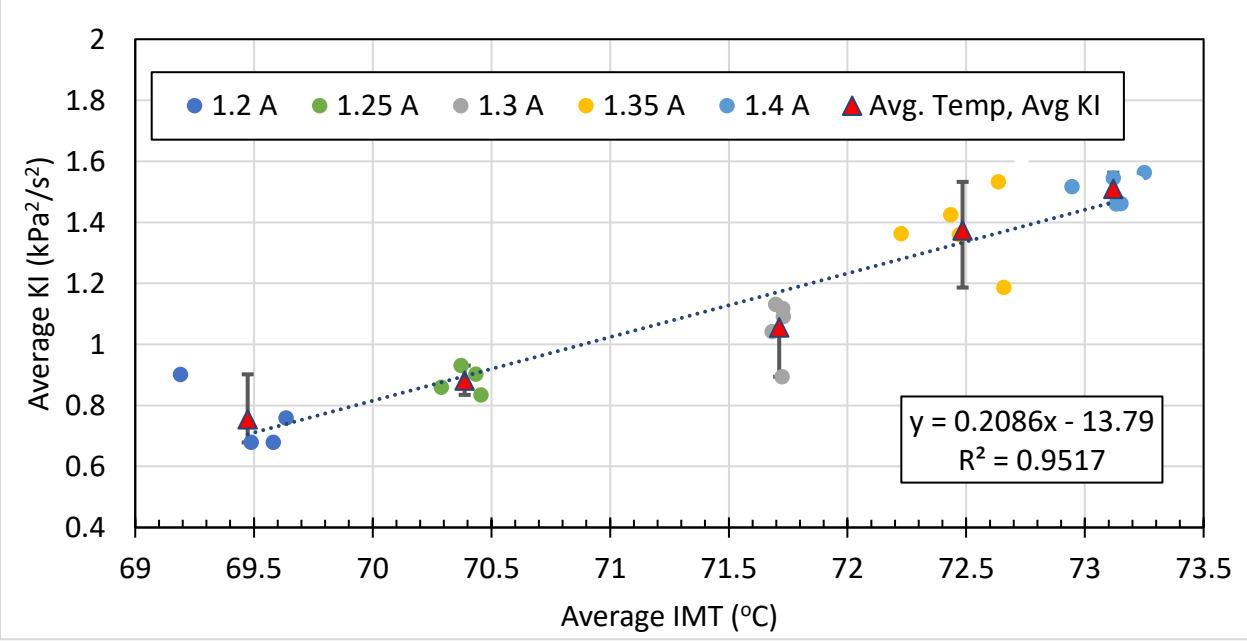

Figure 15: Intake Manifold Temperature vs. Knock Intensity

In Figure 15, the average temperature for the 1000 cycle tests serves as the independent variable plotted on the x-axis while the test average KI is plotted on the y-axis. The red triangles represent the average temperature and KI values for the five IMHC settings, with error bars indicating knock intensity variation for each average temperature. The plot includes a linear curve fit slope with an R^2 value of 0.9517, indicating a strong correlation. Each point from the linear curve fit intersects with the error bars, further reinforcing the correlation. The linear curve fit slope predicts KI change per temperature change. In the 1.35A data two high-temperature points show notable KI variation (0.346) with minimal temperature difference (0.023ºC). Figure 16, shows the IMT over these two tests demonstrating the minimal differences therefore should produce similar KI results.

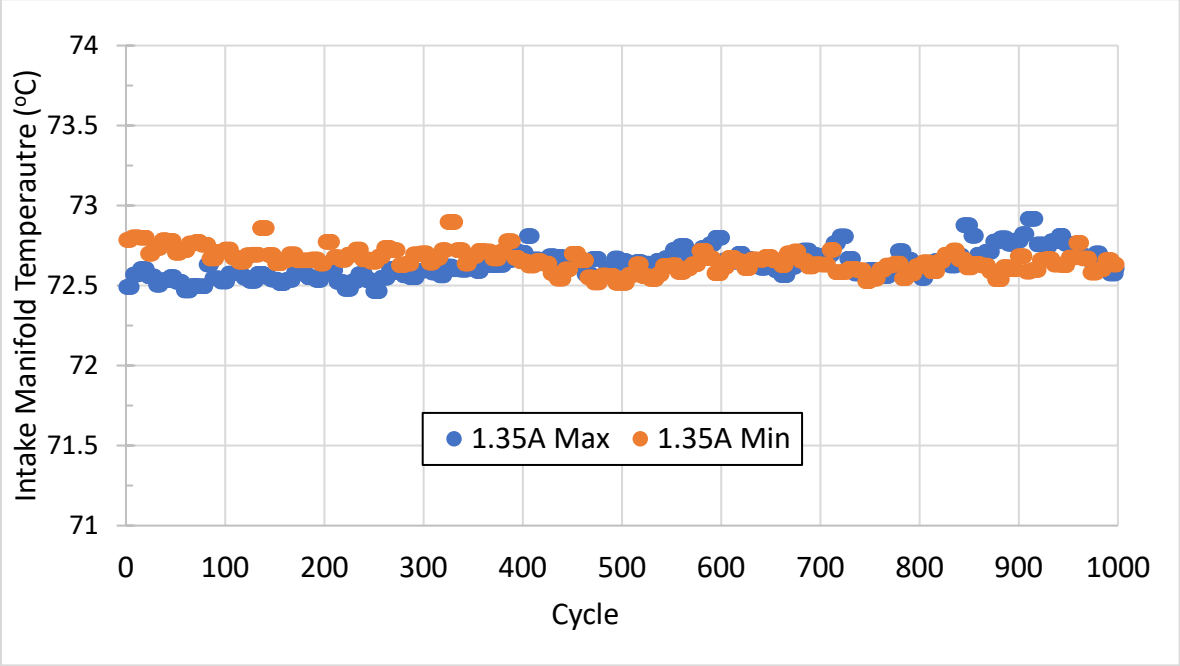

Figure 16: Temperature fluctuation Between 2-1000 Cycle Tests

The temperature fluctuation during each test, excluding outliers, was restricted to 0.25ºC, despite a notable KI change. To establish an acceptable IMT variation that prevents a significant

KI shift surpassing the observed difference between similar temperature results, the following relationship was used:

$$\frac{0.346\frac{kPa^2}{s^2}}{0.2086 * \frac{\frac{kPa^2}{s^2}}{1^oC}} = 1.66^oC$$

Effect of IMT Set Point

The second part of this section was to determine the effect varying IMT has on MN results. Several different IMTs were considered for this evaluation spanning the typical temperatures seen in the RON [7] and MON [8] methods. When operating using low IMT values (< 30°C), even with the use of a chiller (or very low ambient air temperature), heat from the engine transferred through the intake manifold and subsequently raised the IMT. Conversely, when using high IMT such as the MON [8] method where temperatures are to reach 149°C (300°F), there is a very real possibility of ignition in the intake manifold (backfire). Such an event is very possible when utilizing reference fuel blends with high concentrations of hydrogen.

To reduce the effects of uncontrolled variables such as ambient temperature, MN test results are only compared within tests conducted on the same day. Additionally, the engine was given sufficient time to stabilize before testing commenced, mitigating any potential impact from transient thermal effects. The method for determining MN was described in Section 2-4 MN Testing Method: Matching KI Value. Figure 17 shows results spanning 2 different days of testing with the maximum variation occurring on one day of +/- 1.5 MN. For each day of testing, there was a linear trendline fit to the data in order to investigate the relationship between IMT setpoint and MN.

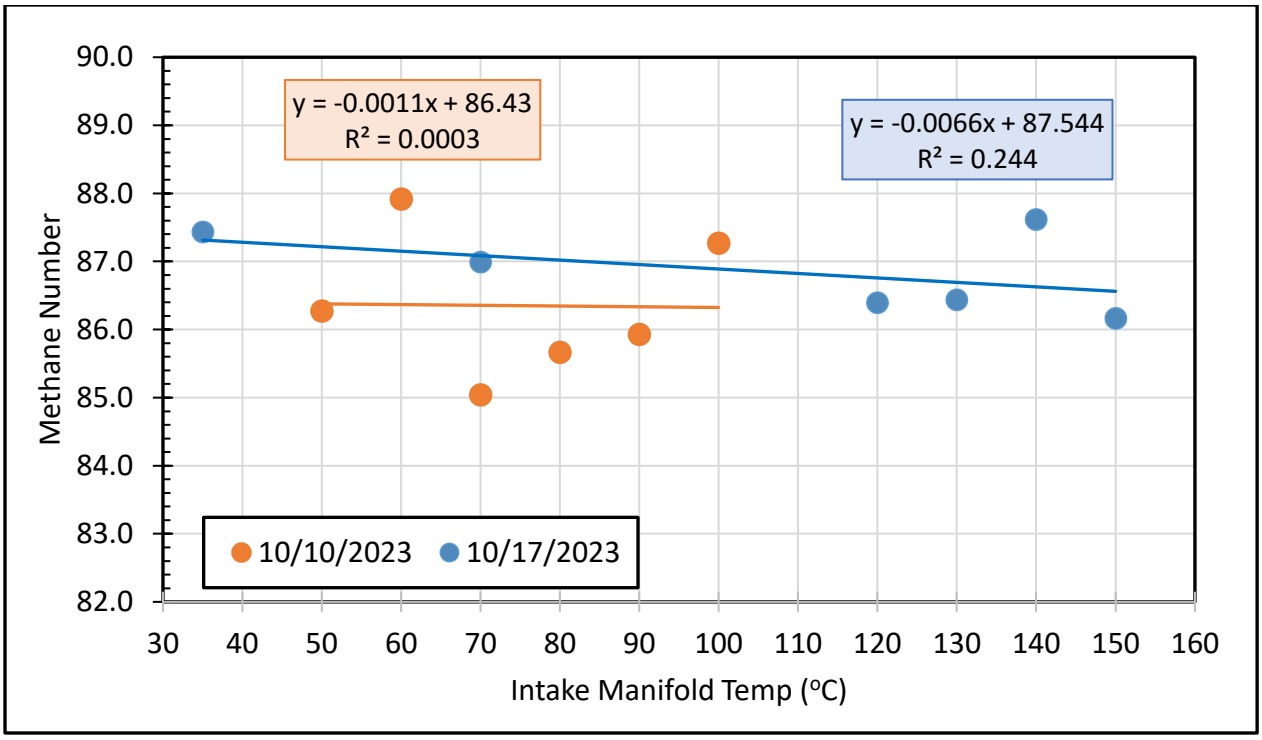

Figure 17: Methane Number vs. IMT Setpoint

On 10/10/2023, the data showed a maximum variation of 1.5 MN from the median value when considering the trendline between the data points. Within the bounds of the test, it was observed that the Intake Air Temperature (IAT) had a minimal effect on the MN. A second test was conducted on 10/17/2023 with wider bounds to span the range covered by the RON [7] and MON [8] test methods. The results of the test on 10/17/2023 concluded with low R^2 value the effect of IMT on MN:

$$-\frac{0.0066\ (MN\ units)}{1^oC\ (IMT)}$$

Discussion

IMT has a strong role in the propagation of EGAI for a fuel sample with higher temperatures leading to an increase in both KI and sensitivity to CR. In this section the effect of

slight variations in IMT play on the KI experienced by the engine. This was complicated by the unpredictable nature of EGAI and the ability for different knock levels to vary with consistent engine operating conditions. When operating an engine as in any control system, constraining testing variables unnecessarily adds complications and inherent expenses, thus the objective with the IMT Variation study was to set the largest bound on IMT while not exceeding an expected change in KI between two tests with similar temperature. Based on the data from this natural gas sample, the maximum allowable IMT variation over the course of a test is +/- 1.7°C (3.0°F).

The studies conducted for the IMT setpoint had low correlation between IMT and MN over a wide temperature range. This is because control variables are inherently normalized in the MN test method since the same values are used for test and reference fuels. Consequently, the ability to control the parameter at a consistent value is more important than the specific value selected. The evidence in the study indicates IMT can be selected by the operator such that reduces the required equipment and variation while also allowing for an adequate resolution in KI.

3-4 Ignition Timing

The objective of this study is to explore the effect varying ignition timing has on the MN of a given test. Autoignition is affected by ignition timing and generally the earlier the initiation of spark, the greater KI will be registered. MON utilizes a technique where depending on the CR, the ignition timing is varied. At higher CRs, spark is retarded to reduce the knock tendency effectively increasing the resolution that can be achieved by only adjusting CR. The ignition timing range utilized by the MON method is between 14°-26° bTDC. The RON [7] method utilizes a constant 13° bTDC ignition timing value. Leiker et al. [9] employed a consistent 15°

bTDC ignition timing, with no mention of alternative values in their MN test results, thus leaving the effect on MN unpublished. The ignition timing study is divided into two sections. The first study **KI Variability: Ignition Timing** determines the effect varied ignition timing has on KI, while the second **Effect of Ignition timing on MN** investigates the correlation between ignition timing values and MN results.

KI Variability: Ignition Timing

Studying the variability of fuel with ignition timing required increasing CR until the onset of knock and then advancing ignition timing and measuring the effect on KI. The data in from a single day of testing with consistent fuel composition, IMT (+/- 0.25°C), stoichiometric mixture ratio (λ = 1 +/- 0.005), barometric IMP and EMP, along with other steady state operating parameters. There were two different CR values tested to determine the correlation in KI.

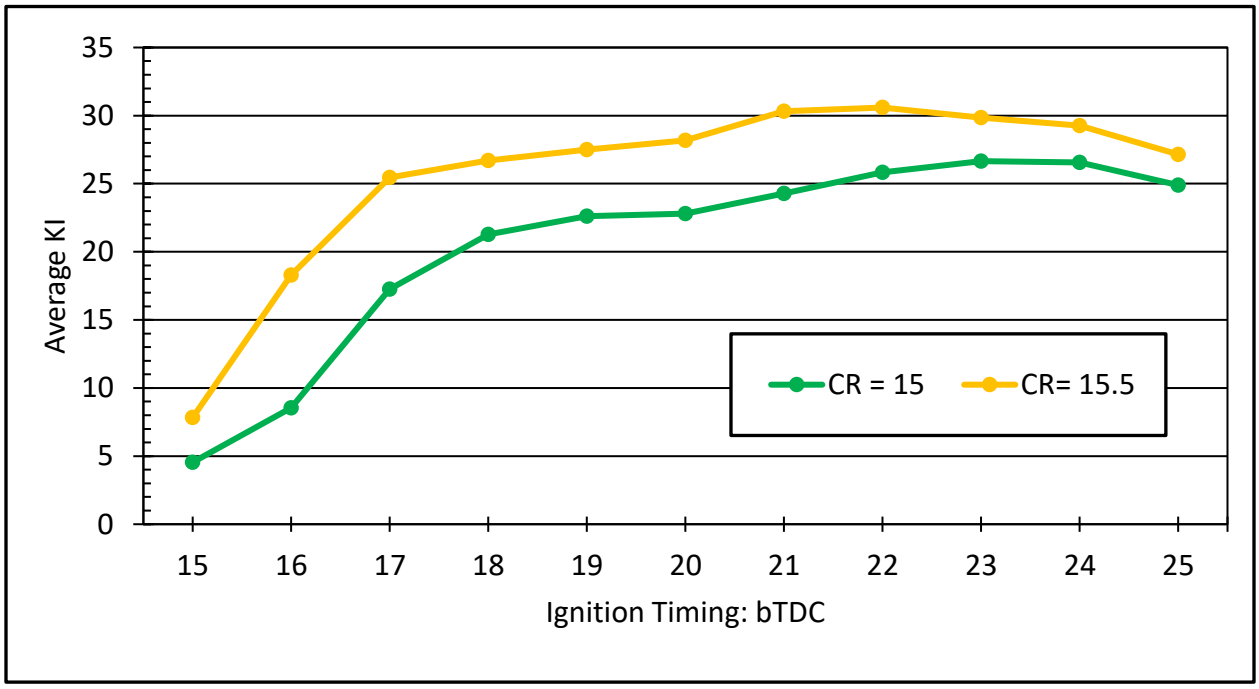

Figure 18: KI Variability: Ignition Timing vs. CR Results

The fuel reactivity study consisted of two cases utilizing 70ºC IMT and ignition timing set for 15ºbTDC while differing only in compression ratio. Figure 18 shows the results plotted with ignition timing on the x-axis and average KI on the y-axis. Between the two cases, there was a nearly linear relationship between KI for timing values 15º - 20º, and then decreased a following 23º bTDC. Comparing the two test results, the KI metrics closely matched throughout the duration of ignition timing values tested.

Effect of Ignition Timing on MN

The second study investigates the effect varying ignition timing has on MN results. The procedure involves testing the MN of a NG sample using ignition timing ranging from 12º to 21º bTDC. Figure 19 presents results for the 5 MN tests using different ignition timing.

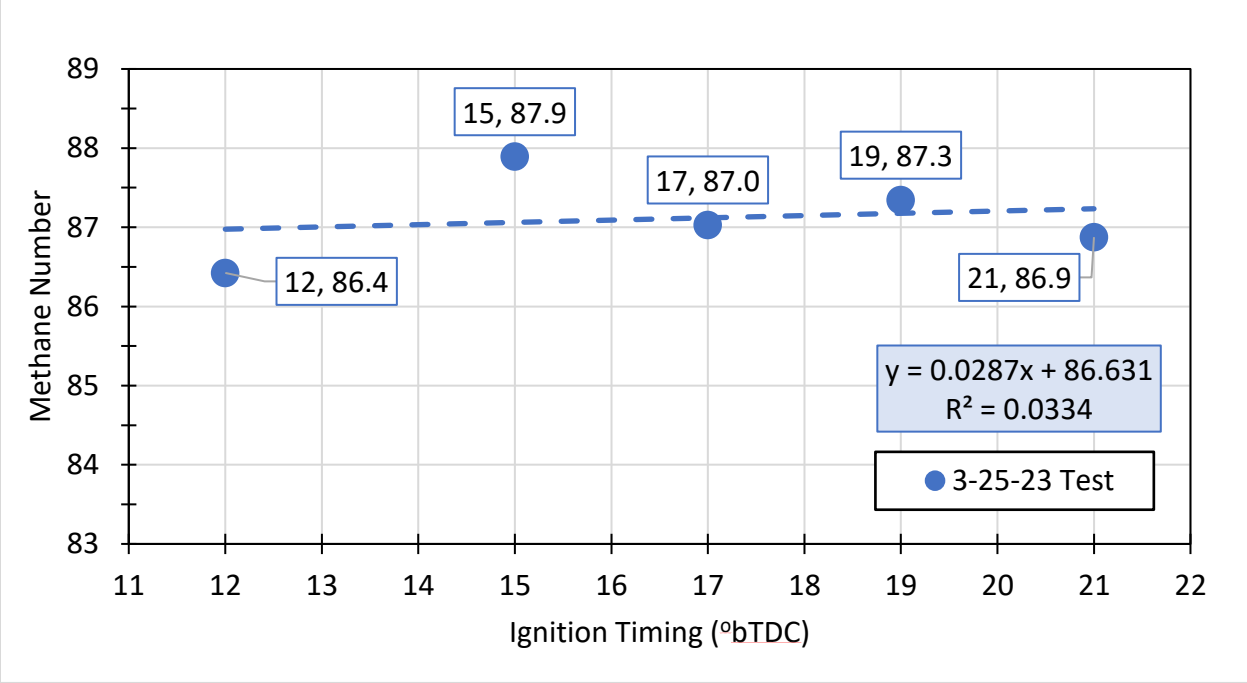

Figure 19: Methane Number Ignition Timing Study Results

The very low slope of the linear regression and R^2 indicates the MN is not greatly affected by ignition timing utilized. The other point of significance is that the tolerance of +/- 1 MN sustained with multiple tests occurring with similar operating parameters. Using the slope of the linear regression, a relationship between MN and Ignition timing can be formed:

$$\frac{dMN}{d(IgnitionTime)} = 0.03 \frac{MN\ units}{\Delta 1^o bTDC}$$

Discussion

Ignition timing is a value that is set and does not vary over the operation of the engine, making for a variable that can be easily forgotten, the test of investigation of ignition timing vs MN revealed a very low correlation, indicating the value can be left to the user as long as it remains constant between the reference blend and test fuel. An interesting phenomenon occurred comparing 12° bTDC and 17° bTDC case, hydrogen addition had a greater impact on knock intensity for lower (closer to TDC) ignition timings, indicating greater EGAI sensitivity to fuels with a lower knock resistance.

3-5 Intake Manifold Pressure

The objective of this section is to explore the effect IMP has on the measured MN of a test gas. For this study IMP is regulated via the compressed air system, while EMP is raised using a manual exhaust restriction valve. However, lowering EMP beyond ambient conditions is not feasible. The CFR engine at the CSU powerhouse can simulate elevated pressure conditions but introduces fluctuations in the intake pressure system of +/- 5 kPa. These variations, occurring every few seconds, allow for the average KI value to encompass variations after 1000 cycles

such that IMP remains constant. Analyzing the feasibility of the MN method, Fort Collins, Colorado which lies at ~ 5000 ft above sea level will serve as the lowest possible IMP encompassing most NG testing facilities in the country (excluding facilities in southern Wyoming). This study is split into 3 sections. **KI Variability: IMP**, investigates the relationship between increasing CR and KI at different pressure setpoints. **IMP Parameter Sensitivity** analyzes the direct correlation between KI and pressure fluctuations to establish an acceptable variation. **IMP Effect on MN** examines the effect different pressure values have on MN results.

KI Variability: Intake Manifold Pressure

When analyzing the effects of IMP, the first step is determining the relationship of CR and IMP on KI. The two independent variables in this study are CR and IMP. For this study the same NG sample, IMT, and ignition timing values were utilized. In Figure 20, the results of the KI Variability study with trend lines using exponential regression and R^2 values.

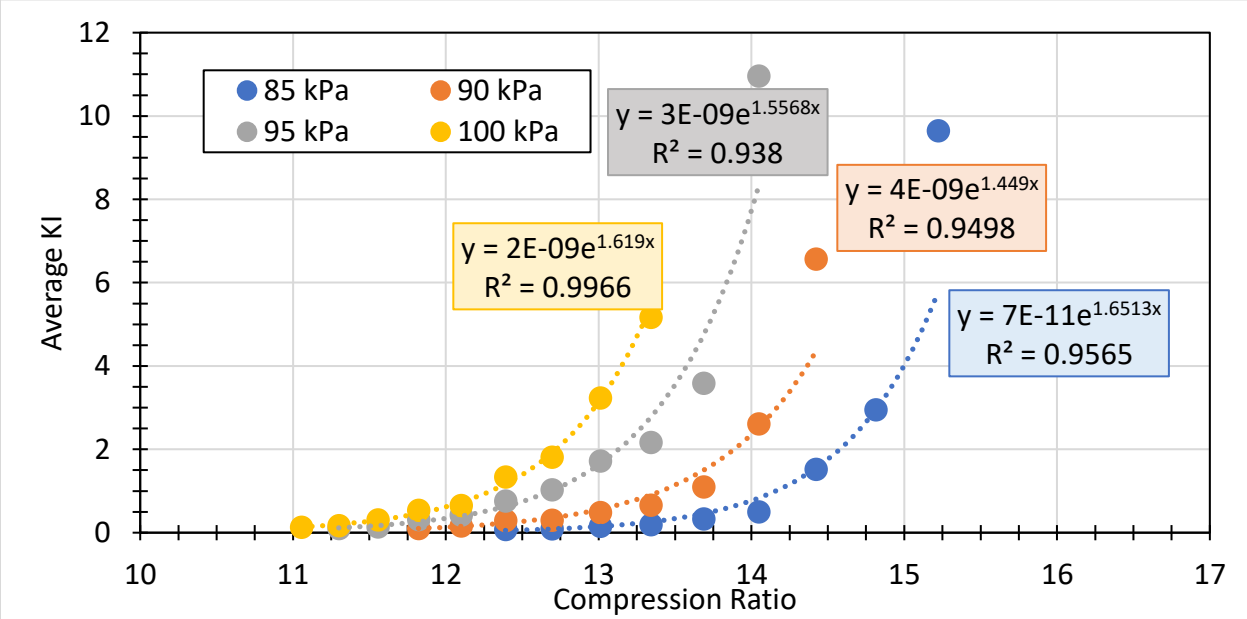

Figure 20: KI Variability: CR vs. KI with different IMP values

Analyzing the results in Figure 20, and comparing the trendlines for the different IMP values, they all have very similar slope values indicating there is little difference between the onset of EGAI. The spacing between the pressure cases remains consistent indicating a linear relationship between knock intensity and pressure.

IMP Parameter Sensitivity

This section aims to determine the amount IMP can vary without generating noticeable differences in KI, affecting MN results. The test was conducted with a consistent CR of 12.8, ignition timing of 15° bTDC, and IMT of 74° +/- 0.25°C. Other testing parameters such as coolant and oil temperature remained constant at nominal values. In Figure 21 the results of the IMP Sensitivity sweep are plotted with the x-axis reserved for IMP and the y-axis the knock intensity.

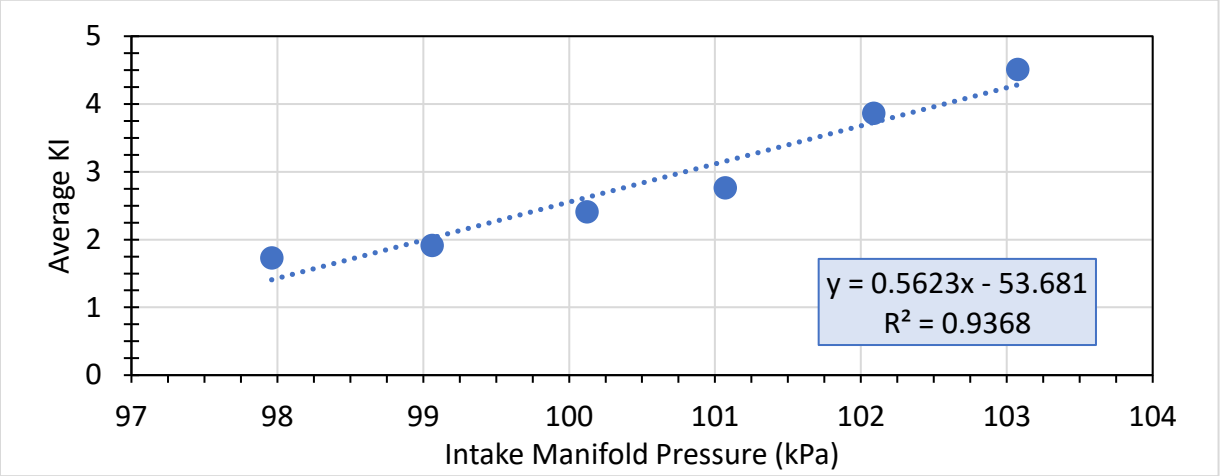

Figure 21: IMP Sensitivity Sweep (98 -103 kPa)

In Figure 21, each data point corresponds to the average KI for a given average IMP over 1000 cycle tests. The plot includes a linear curve fit with a slope of 0.5623 and an R^2 value of

0.9368, indicating a strong correlation. The curve fit slope predicts KI change per kPa change of IAP. Using the same value for KI variation (0.346) as used in the IMT case the allowable variation of IMP is.

$$\frac{0.346\,\frac{kPa^2}{s^2}}{0.562\,\frac{\frac{kPa^2}{s^2}}{kPa}} = 0.615\ kPa$$

In the calculation for allowable variation of IMP, there is an exponential relationship between increasing pressure and knock intensity. For heavy knock conditions, small pressure changes have a larger impact on average knock intensity, but the knock metric has more variability associated with it.

Effect of IMP on MN

The purpose of this study is to investigate the influence of IMP on Methane Number (MN) involves conducting MN tests under varied IMP conditions while maintaining other testing parameters as stable as possible to ensure accuracy. In order to accurately imitate operating at lower elevations, both the IMP and EMP were changed and targeted the same value. Fluctuations in IMP, maintained within +/- 5 kPa, posed challenges in consistency, particularly with λ. The recorded fluctuations remained consistent at +/- 5 kPa and resulted in a larger fluctuation in λ of +/- 0.01. Fortunately, these fluctuations remained consistent across the testing range and were assumed independent of results. To mitigate the impact of varying IMPs on fuel flows, accuracy of flow meters for reference fuels was ensured through calibration procedures (APPENDIX D: GAS FLOW METER C). Gas flow meter calibration was followed at the expected flow rate extrema for the CH_4 and H_2 meters, maintaining the allowable tolerance. Test procedures

included repetition of measurements with the same test gas and operating conditions on different days to minimize transient responses. Results from three days of testing, depicted in Figure 22, illustrate the effect of IMP on MN.

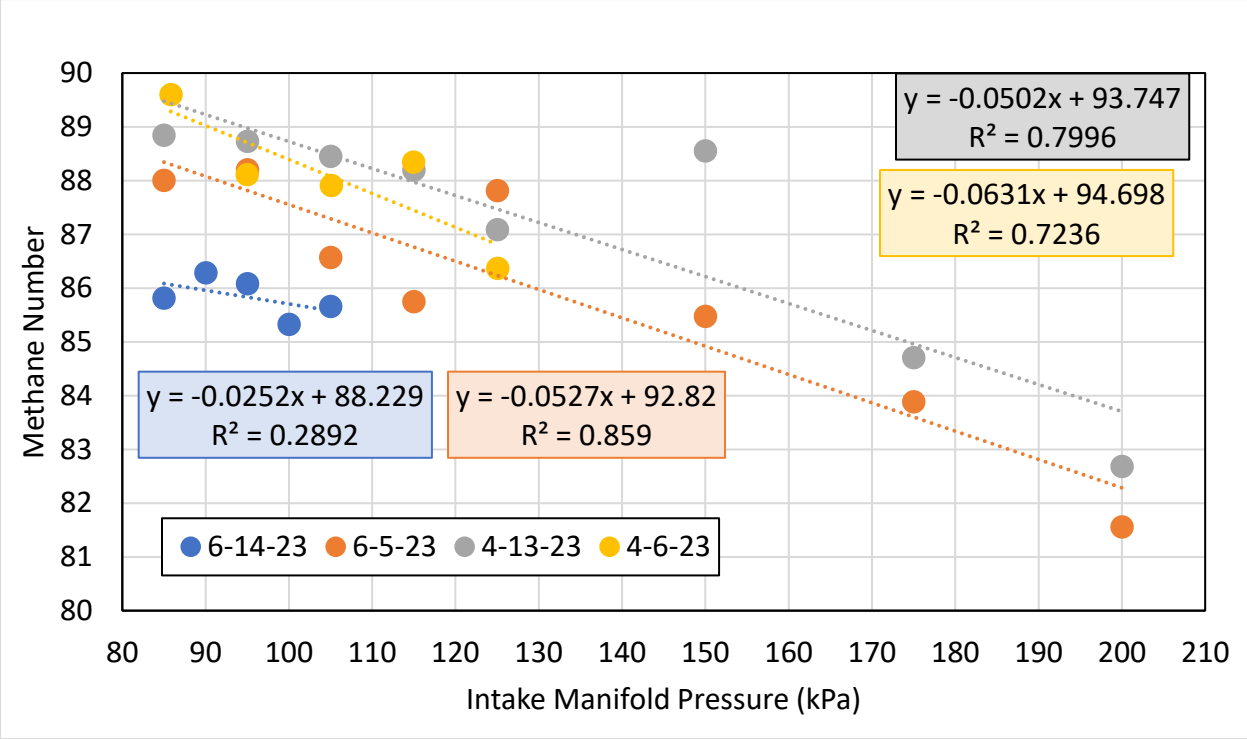

Figure 22: Effect of IMP setpoint on MN results

Variations within the expected ambient pressure range of 85-105 kPa were smaller than the registered variation between test days at identical operating conditions. Exploring elevated pressure conditions (115-200 kPa) revealed a negative relationship between MN and IMP. Results between the days of testing all registered a similar negative correlation with a higher R^2 value achieved with larger pressure variations. Using the average linear regression between the different days of testing, the relationship between MN and IMP is:

$$\frac{dMN}{dIMP} = -0.0487 \frac{MN\ units}{kPa}$$

IMP Discussion

The data shows that engines with elevated IMP demanded significantly more fuel while producing increased power, necessitating higher fuel manifold pressure to meet flow requirements, and overcome IMP. Additionally, higher IAP levels resulted in substantially higher cylinder pressure compared to lower IAP cases, despite similar knock intensity. The impact of hydrogen addition on knock intensity varied with pressure, with higher IMP leading to a reduced effect of hydrogen percentage on knock intensity. Moreover, elevated IAP conditions were found to increase exhaust gas temperatures, indicating higher cylinder temperatures and potential engine wear. To prevent exceeding peak cylinder pressure when increasing CR, tests were conducted in both high-to-low and low-to-high pressure directions, confirming the influence of IMP on measured MN. Additionally, unanswered questions remain regarding the negative relationship between other hydrocarbon percentages and KI reactivity, such as in the case of hydrogen.

3-6 A/F Mixture

The air fuel mixture (λ) ratio is a crucial metric and influences many attributes of operation. Utilizing natural gas presents a challenge in determining the correct mixture of fuel to air with unknown concentrations of different hydrocarbons. In the RON [7] and MON [8] tests, λ is affected by changing the height of the fuel bowl and in the test method, and peak knocking condition is utilized. For gaseous fuels like methane or propane, where accurate chemical compositions are known, fuel flow rates can be calculated to ensure chemically correct operation, adjusting for air pressure. Given the varied fuel composition, the MoTeC PLM to measure λ was implemented. The objective of this section is to investigate the impact of λ on KI

and subsequently on MN. This section is broken into 3 sections with the first, **KI Variablity Study**: plots the relationship between λ and KI. The second, **Parameter Sensitivity** determines the allowable deviation without a registerable difference in KI. The final study **Effect of Mixture Ratio on MN** analyzes the link between MN test results and the mixture ratio value.

KI Variability Study: Mixture Ratio

The test structure for the comparison between CR and KI with different λ values involve incrementally increasing CR and recording operating conditions. The results for this study are include in Figure 23.

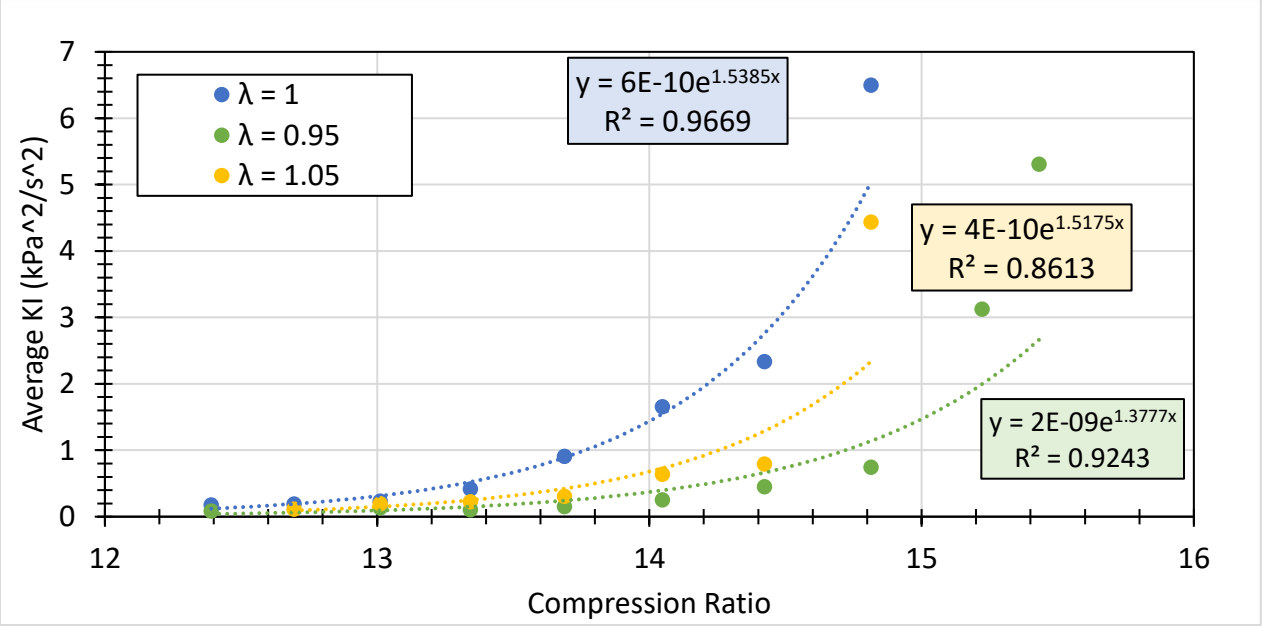

Figure 23: KI Variability: CR vs. KI with varying λ values

In the KI Variability study, the correlation between CR and KI at different λ values was plotted with an exponential trend line drawn, displaying the R^2 value on the chart. Among the λ values, there was a notably stronger correlation coefficient for λ = 1 compared to the others. KI

values were considerably less consistent outside the 0.95-1.05 range, and misfires occurred beyond the 0.8-1.2 range, making an average KI figure impractical. The results from this study indicate a significant connection between stoichiometric operating conditions and predictable knock characteristics.

Parameter Sensitivity: Mixture Ratio

Before conducting this study, it was known the mixture ratio (λ) directly impacts KI, but the extent was unknown, so determining an acceptable range is the objective of this study. Figure 24 details the testing flow chart used for testing fuel reactivity and the impact of λ on KI.

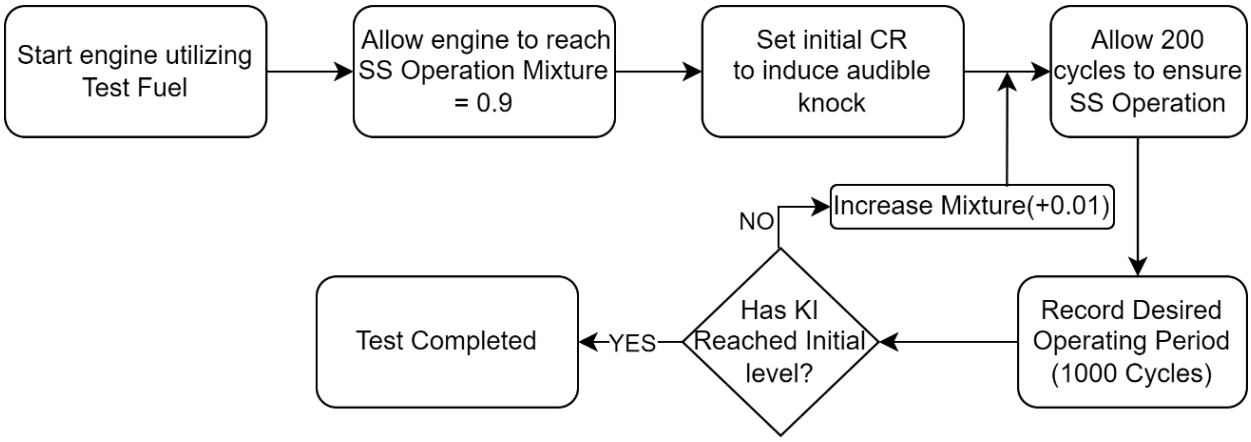

Figure 24: Fuel Reactivity-Mixture Ratio Test Flow Chart

The test was conducted with a consistent CR of 14, ignition timing of 15° bTDC, IMP and EMP are ambient, and IMT of 70° +/- 0.25°C. Other testing parameters such as coolant and oil temperature remained constant at nominal values. In Figure 25 the results of the fuel reactivity sweep are plotted with the x-axis reserved for mixture and the y-axis the knock intensity.

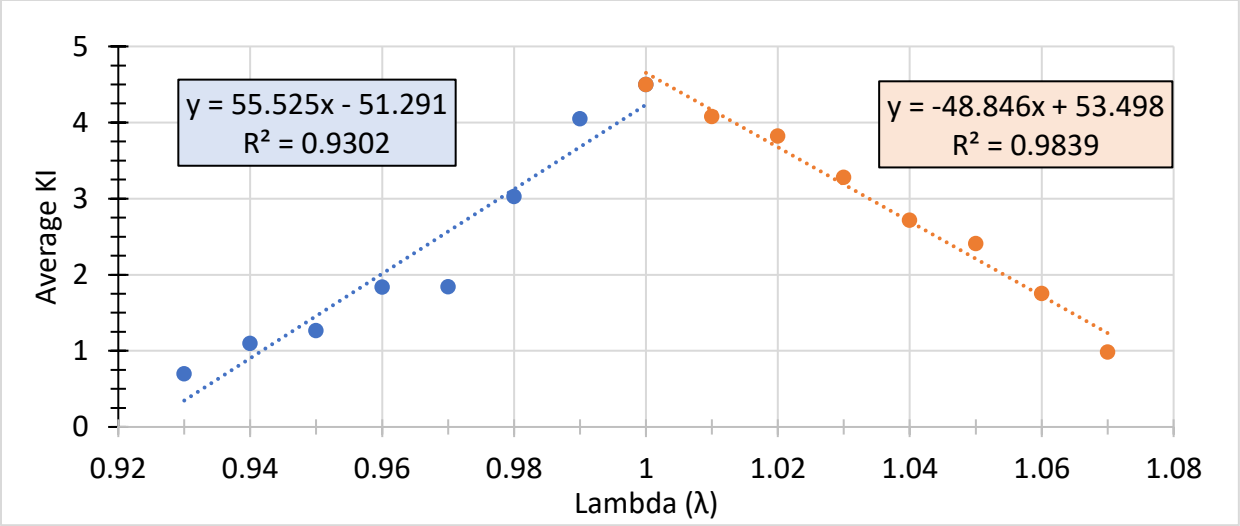

Figure 25: KI Sensitivity Reactivity Results: λ vs. KI with constant CR

Analyzing Figure 25, there appears to be a piecewise linear relationship between λ and average KI. The absolute value of the trendline slopes on either side of the peak value occurring at λ = 1 are about the same. This is a helpful relationship because it allows for a symmetric tolerance band to be applied to λ. To determine an average fluctuation of KI, the 1000 cycle test was split into 5 sections consisting of 200 cycles. The difference between the average of each of these sections and the 1000 cycle dataset determine a typical expected variation amount with consistent operating parameters. The average difference between the 200 cycle and 1000 cycle periods was 0.363, similar to the value used in Figure 15 in IMT (0.346). Using the equation for the line of best fit for the piece-wise function on the rich side, the amount of allowable variation in lambda is:

$$\frac{0.363\frac{kPa^2}{s^2}}{55.525*\frac{\frac{kPa^2}{s^2}}{\lambda}} = 0.0065.$$

Applying the same relationship to the lean condition, the allowable variation is 0.0074. Considering the PLM only registers X.XXX the maximum allowable variation in λ is +/- 0.007.

Effect of Mixture Ratio on MN

The MN measurement requires re-producing knock intensity between a test and reference fuel. Multiple MN tests are performed with different λ values to determine if there is a correlation in the results. The test range was limited to a range of 0.9-1.2 because KI was found to be highly unstable outside this range. Figure 26 shows the results from 2 days of testing. For each day of testing, there was a linear trendline fit to the data to investigate the relationship between λ and MN.

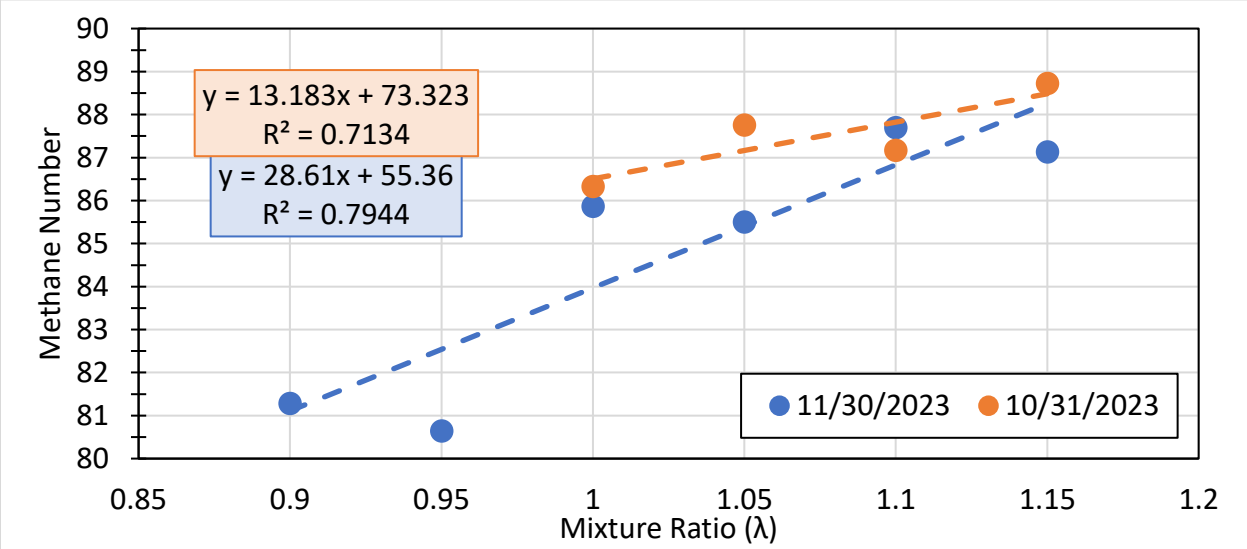

Figure 26: Mixture Ratio vs. MN Results

Considering Figure 26, the results from the 10/31/2023 test, supports the conclusion of a significant relationship between MN and λ. Following this, a second test was conducted spanning a larger range of λ to validate the results from the first test. The second test supported the findings of the first with a larger variation between lean and rich operating conditions. Within the bounds of the test, it was observed that the λ has a significant effect on the MN.

$$\frac{dMN}{d\lambda} = 20.9 \frac{MN\ units}{\lambda}$$

Mixture Ratio Discussion

The data shows a significant impact of λ on KI and MN. Thus, ensuring a consistent method for fuel flow control and real-time λ control is crucial for the MN test method. When exhaust gas composition monitoring for λ is unavailable, peak KI conditions also correspond with λ = 1 and represent the most stable KI values.

3-7 Parameter Sensitivity & Recommended Test Conditions

Parameter Sensitivity

The operating parameters involved in the Methane Number test procedure that were analyzed in this research are summarized in **Table 7**. The methods used to derive the results in **Table 7** are included in previous sections of Chapter 3. For ignition timing and intake manifold temperature, Methane Number outcomes show a weak correlation, allowing operators flexibility in selecting values for stability and ease of operation, while minimizing variation.

Table 7: Parameter Variability and Sensitivity Results

Variable	$\frac{dKI}{d(Variable)}$	**Allowable Variation (+/-)**	$\frac{d(MN)}{d(Variable)}$
Ignition Timing	Non-linear	N/A	0.029
Intake Manifold Temperature	0.286	1.66^{o}C	-0.004
Intake Manifold Pressure	0.562	0.615 kPa	- 0.049
Mixture Ratio (λ)	52.2	0.007 λ Units	20.9

Conversely, intake manifold pressure and mixture ratio exhibit a stronger correlation with Methane Number outcomes, necessitating operators to consider their impact on stability and compare results across testing conditions. Although consistency in each parameter throughout testing is essential, variations within the tolerance provided in **Table 7** are expected and should be maintained.

Recommended Test Conditions

The operation of an ICE is a dynamic environment with the requirement of keeping many variables within a given range and through this research a better understanding of these values was determined. While testing Methane Number of natural gas, and other gaseous fuels, the recommended set points and subsequent allowable variation are provided in Table 8.

Table 8: Research Determined Methane Number Test Parameters

Parameter	**Set Point**	**Allowable Variation (+/-)**
Ignition Timing	12°-21° bTDC	0°
Intake Manifold Temperature	70°C	1.7°C
Intake Manifold Pressure	Atmospheric	0.62 kPa (0.09 psig)
Exhaust Manifold Pressure	Atmospheric	2.5 kPa (0.36 psig)
Mixture Ratio	Stoichiometric (λ=1.000)	0.007 λ

The values presented in Table 8 only account for a small portion of the environment and testing parameters present in the operation of an ICE. These parameters are listed in **Table 9** and were based on the requirements listed by the MON method. In the case of Coolant level, oil

pressure, and oil level, these parameters are unique to the CFR system for continued lubrication and cooling. The connection between the parameters listed in **Table 9** and knock intensity were not investigated in this research.

Table 9: Additional Environment and Testing parameters

Parameter	**Set Point**	**Allowable Variation (+/-)**
Engine RPM	900 RPM	9 RPM
Humidity	0.00534 kg H_2O per kg (37.5 grains of H_2O per lb.) Dry Air	0.0018 kg (12.5 grains)
Coolant Temperature	100°C (212°F)	1.5°C (3°F)
Coolant Level (HOT)	"LEVEL HOT" mark	1 cm (0.4 in.)
Coolant Level (COLD)	Just visible in sight glass	1 cm (0.4 in.)
Oil Temperature	57°C (135°F)	8°C (15°F)
Oil Level (Running & Hot)	Mid-Level in sight glass	0.5 cm (0.2 in.)
Oil Level (Stopped & Cold)	Top of sight glass	0.5 cm (0.2 in.)
Oil Pressure	190 kPa (27.5 psig)	17 kPa (2.5 psig)
Crankcase Internal Pressure	Atmospheric	-2.5 kPa (-0.36 psig)

CHAPTER 4: MN METHOD ADAPTATION: BRACKETING KI METHODS

Stable operation of an engine undergoing EGAI is complex, with many variables that need to be controlled at constant values. Combining the complicated nature of ICE operation and inconsistencies of EGAI, matching knock intensity between a test fuel and a reference fuel blend is challenging. During MN testing the intention is to vary the hydrogen and methane blend ratio to match the KI, but it is difficult to determine how close is close enough, especially with intake temperature, ignition timing, and intake pressure affecting the development of knock. To reduce the time spent matching knock intensity to a higher level of precision and to develop a relationship between MN and KI for given operating parameters, a new method for testing MN was devised. This method eliminates the need to accurately control the reference fuel blend to match specific KI values, which are intrinsically unstable.

4-1 Dynamic Blending KI Bracketing Technique

To establish a direct relationship between KI and MN, an adapted MN method was developed and included in Dynamic Blending KI Bracketing Step-by-step Test Procedure and is also described in a flowchart shown in

Figure **27**. Through testing with the reference fuel blends, an exponential relationship between MN and KI was determined as well as the rationale for using three datasets. Following the Methane Number test, determining the results involves a couple steps which are laid out in steps 1-5 in the MN Bracketing Step-by-Step Post-Processing Procedure. Converting the MN of the three reference fuel blends to that of the test fuel involves linear regression to estimate MN from the average knock intensity. Figure 28 shows an example the relationship between MN and KI for the reference fuel blends, including a linear regression line, and the corresponding MN

results. Linear regression can approximate an exponential relationship within a limited range of MN values, depending on various operating conditions explored in the fuel reactivity studies of Chapter 3. The coefficient of determination (R^2) between the linear regression and reference fuel blends serves as a metric to assess the confidence level in the MN determination during data processing.

Dynamic Blending KI Bracketing Step by Step Test Procedure

1. Select the Compression Ratio (CR), Intake Manifold Temperature, and Ignition timing values.
    a. For fuels with high reactivity start lower, but for NG start CR ~ 10
    b. For bulk of testing, IMT = 70°C
    c. Ignition timing may be altered later but 15° bTDC is a good starting point.
2. Start the CFR engine and allow enough time to reach Steady State Operating Conditions.
3. Switch to the test fuel and set the fuel flow solenoid position to achieve stoichiometric operating conditions ($\lambda = 1.000$).
4. Make gradual increases in compression ratio (+ 0.5) allowing 200 cycles for the engine to reach steady state. Continue gradual increases in compression ratio until the onset of audible knock. Compression ratio will remain constant for the rest of the test.
    a. If audible knock is not achieved before reaching maximum CR, lower the CR and retard the ignition timing and repeat step 4 until audible knock is achieved.

5. Record three (3) 1000-cycle intervals of operating conditions and pressure trace data. Focus on Knock Integral and take note of the average value. This is **Target KI**.
6. Switch the test fuel off and allow the fuel mixing volumes to return to atmospheric pressure while the engine continues motoring to make sure temperature variation is minimized.
7. Switch on the primary reference fuel (methane) and set the fuel flow solenoid valve position to achieve stoichiometric operating conditions ($\lambda = 1.000$). Allow engine to reach steady state and measure **Current KI**.
8. Select the secondary reference fuel (SRF) based on the relation between current KI and Target KI
    a. If Current KI is < Target KI: SRF = Hydrogen (H_2)
    b. If Current KI is > Target KI: SRF = Carbon Dioxide (CO_2)
9. Make gradual increases in SRF until Current KI = ~1.1 x Target KI (TKI-high) while keeping mixture = 1.000 +/- 0.007.
10. Record **TKI-High 1000-cycle** interval of operating conditions and pressure trace data while keeping SRF flow constant.
11. Make gradual increases in SRF until Current KI = ~1.0 x Target KI (TKI-Med) while keeping mixture = 1.000 +/- 0.007.
12. Record **TKI-Med 1000-cycle** interval of operating conditions and pressure trace data while keeping SRF flow constant.
13. Make gradual increases in SRF until Current KI = ~ 0.9 x Target KI (TKI-Low) while keeping mixture = 1.000 +/- 0.007.

14. Record **TKI-Low 1000-cycle** interval of operating conditions and pressure trace data while keeping SRF flow constant.

15. MN test is complete, turn off fuel flow and stop engine.

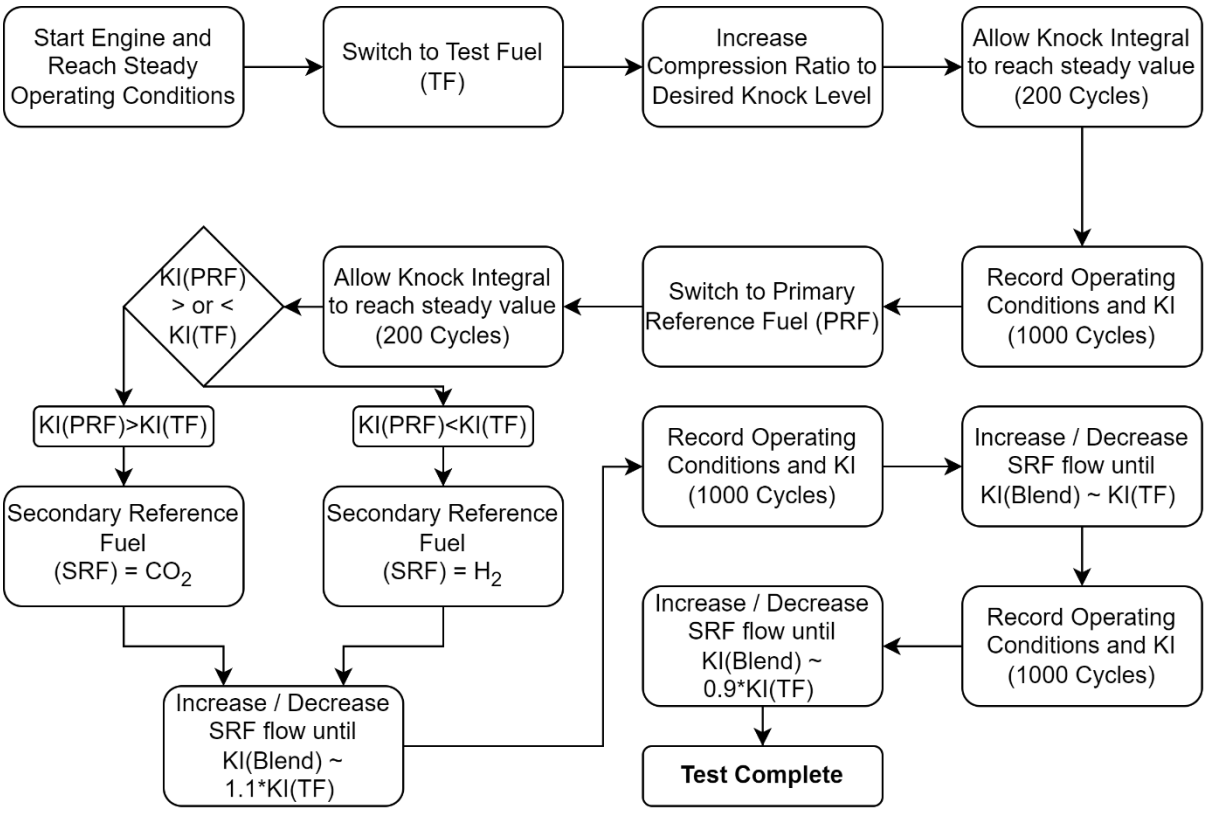

Figure 27: MN Bracketing Test Procedure Flow Chart

Active Blending KI Bracketing Post-Processing Procedure.

1. The Knock Intensity of each power stroke is measured and averaged over each 1000-cycle data collection period.

   1a. TKI-High

   1b. TKI-Med

   1c. TKI-Low

2. Calculate the Methane Number using the Methane and SRF flow rate.

   a. IF SRF = Hydrogen: $MN = \frac{avg.CH_4 mol\ flow}{avg.CH_4 mol\ flow + avg.H_2 mol\ flow} * 100$

   b. IF SRF = CO_2 : $MN = \left(\frac{avg.CO_2\ mol\ flow}{avg.CH_4 mol\ flow + avg.CO_2\ mol\ flow} + 1\right) * 100$

3. Plot MN vs. Avg. KI for blends of CH_4 + SRF
4. Generate a linear regression equation using these 3 points, evaluating the three tests based on the R^2 value achieved.
5. Using the average KI from test fuel blend, calculate the predicted MN.

Active Blending KI Bracketing Examples

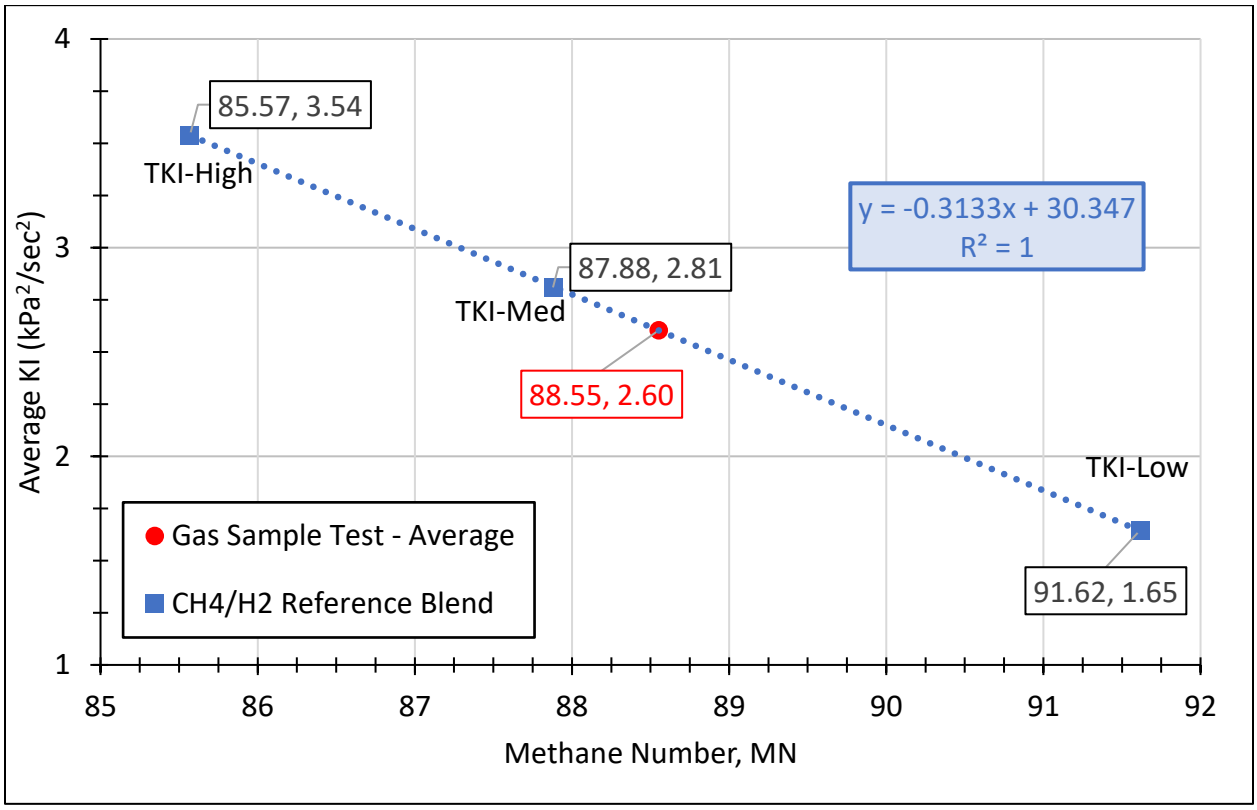

Figure 28: Active Blending Bracketing KI Method Plot (High Confidence)

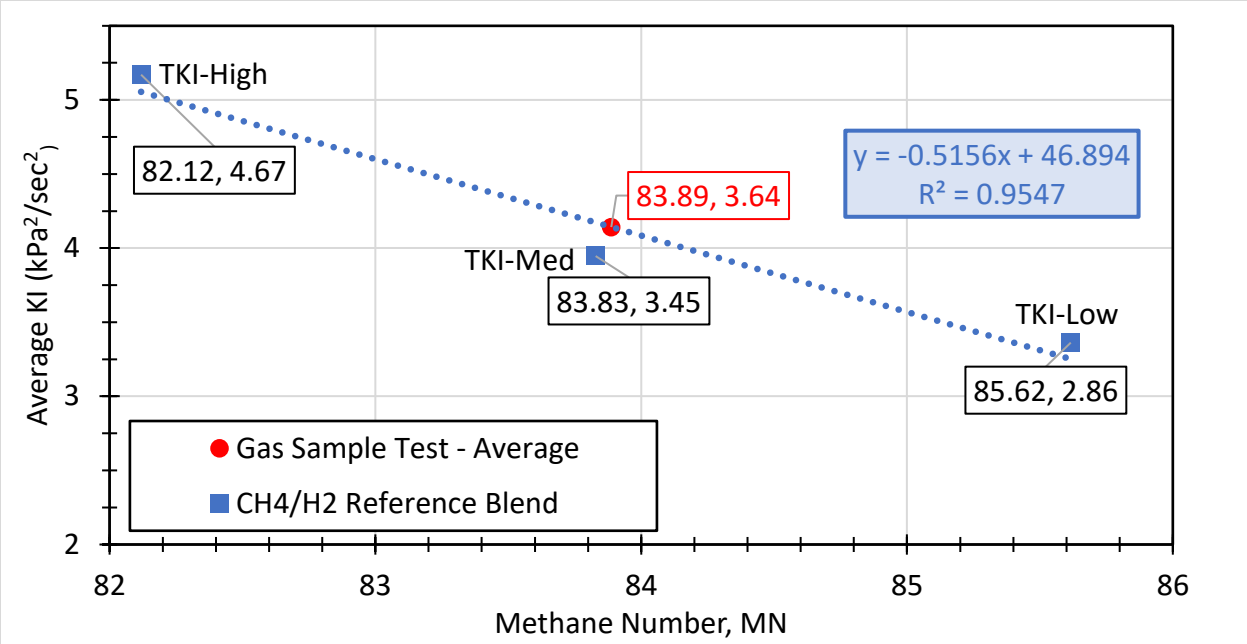

Figure 29: Active Blending Bracketing KI Method (Medium Confidence)

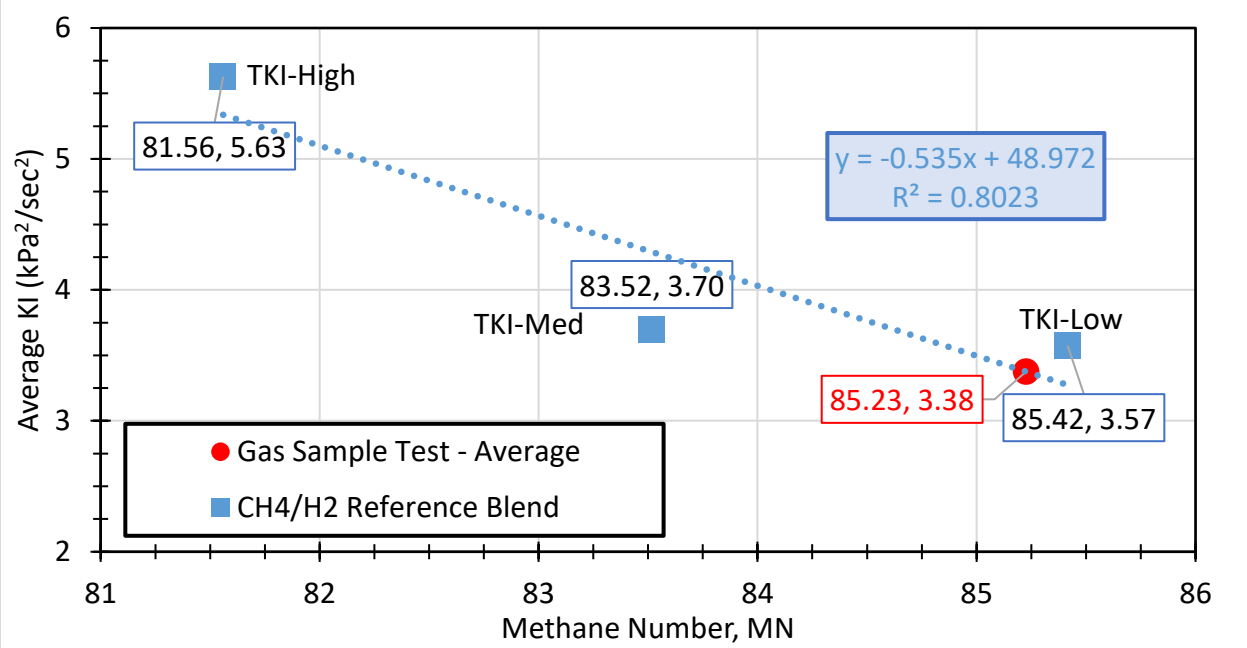

Figure 30: Active Blending Bracketing KI Method (Low Confidence)

Considering the data corresponding to Figure 28, the target KI for the test fuel was 2.60 kPa^2/s^2. The test fuel was replaced with pure methane and SRF flow was increased until the knock intensity surpassed the target KI and a 1000-cycle data set was collected. This blend

deemed “TKI-High” corresponded to an average methane percentage of 85.57 and an average KI of 3.54 kPa^2/s^2. The flow of H_2 decreased until the **Current KI** was near the value of the **Target KI** and a 1000-cycle data set was collected. This blend deemed “TKI-Med” corresponded to an average methane percentage of 87.88 and an average KI of 2.81 kPa^2/s^2. The flow of H_2 was further decreased until the **Current KI** was less than **Target KI** and a 1000-cycle data set was collected. This blend deemed “TKI-Low” corresponded to an average methane percentage of 91.62 and an average KI of 1.65 kPa^2/s^2. Using these (3)-reference fuel blend datapoints, a linear regression trendline is fit with the form:

$$KI(MN) = a(MN) + b$$

Using the coefficients from the linear regression trendline, and the average KI of test fuel 1000 cycle test, the methane number of the fuel blend can be calculated:

$$MN(Test\ Fuel) = \frac{(Average\ KI) - b}{a} = \frac{2.60 - 30.347}{-0.3133} = 88.56$$

Figures 28-30 display different tests with examples of the Bracketing KI Method with varied R^2 values. Determining an acceptable interval for R^2 values involves balancing test accuracy with stability of the KI metric and the MN. According to Leiker et al. [9], MN has a confidence interval of +/- 1 which in this case is a rather large uncertainty. Specifically considering Figure 30 and the central reference fuel data point with an actual MN of 83.5, the methane-hydrogen blend would have corresponded to a MN of 84.5 if it had been the test fuel corresponding to a 1 MN difference. If only 2 reference points had been used in the calculation, the difference would be even larger (1.5 MN). With such an R^2 value, this would indicate the need to re-test the fuel sample. Considering the central reference fuel data point in Figure 29, the 83.8 MN blend would have corresponded to a MN of 84.3 if it had been the test fuel

corresponding to a 0.5 MN difference. Considering the accuracy of MN, the decrease to 0.5 confidence range would be reasonable, indicating the minimum R^2 value be considered is 0.95.

4-2 Dynamic Blending Validation

In evaluating the significance of Methane Number (MN) in characterizing a fuel's propensity for autoignition, it becomes imperative to validate measurement results by comparing them to a fuel with a known MN. To ensure the robustness of the Bracketing KI Method, validation was undertaken using a certified blend of CH4/H2 as the "unknown" sample. The outcomes of this validation test utilizing an 85-15 CH4-H2 blend are depicted in Figure 31.

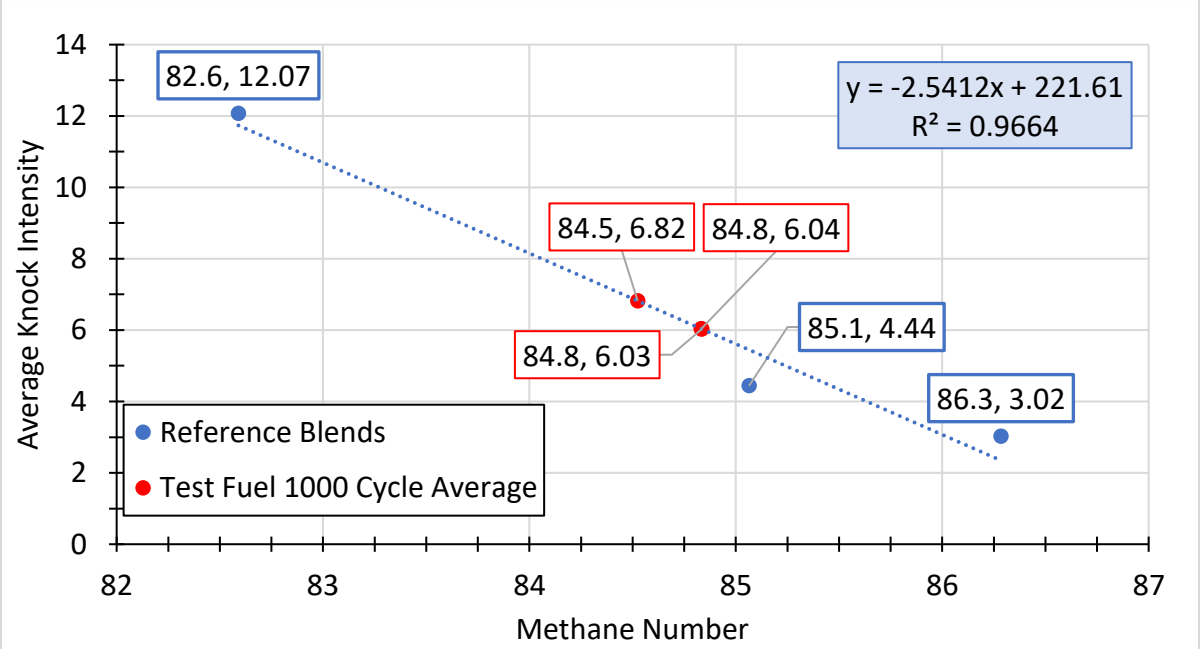

Figure 31: Bracketing KI Method Verification (85-15 CH_4-H_2 Blend)

The results of the verification test had an acceptable R^2 value and therefore indicated a valid MN was determined. The Certificate of Gas Analysis for the 85-15 CH_4-H_2 "unknown" test fuels is provided in Appendix B. and the gas had an actual measured value of methane of 85.09

+/- 2 mol %. According to the definition of MN, this mixture should have resulted in a MN of exactly 85.09 but achieving an average MN of 84.7 is well within the range of expected error. This verifies the Active Blending Bracketing KI technique is a method which produces an accurate MN value for a known blend of methane and hydrogen.

4-3 Certified Premixed Reference Blends MN Technique

When calculating the MN, the measurement of flow rate is crucial for the accuracy of the method. Inherently, the flow meters are a source of error and a possible reason to discredit results. The flowmeters require frequent calibrations and calibration checks. In the liquid fuel methods, isooctane and n-heptane are blended in exact quantities before introducing them to the carburetor, eliminating the need for real time blending. To resemble the RON [7] and MON [8] test methods more closely, Certified Pre-mixed Reference Fuel (CPRF) blends of methane and hydrogen were purchased in 4 concentrations ranging from 75-90% corresponding to the expected range of MN for natural gas. In the section, **Pre-Mixed Blends KI Bracketing Step by Step Test Procedure**, the steps used for testing the MN of a test fuel with Pre-mixed reference blends are listed and in Figure 32, there is a flowchart detailing the adapted MN method.

Pre-Mixed Blends Bracketing KI Step-by-Step Test Procedure

1. Select desired, Compression Ratio (CR), Intake Manifold Temperature, and Ignition timing values.
    a. For fuels with high reactivity start lower, but for NG start CR ~ 10
    b. For bulk of testing, IMT = 70^{o}C
    c. Ignition timing may be altered later but 15^{o} is a good start point.

2. Start the CFR engine and allow enough time to reach Steady State Operating Conditions. Start a timer and allow 2 minutes without a > 0.1°C change in IMT.
3. Switch to test fuel and set fuel flow solenoid position to achieve stoichiometric operating conditions (λ = 1.000).
4. Make gradual increases in compression ratio (+0.5) allowing 200 cycles for the engine to reach steady state. Continue gradual increases in compression ratio until the onset of audible knock. Compression Ratio will remain constant for the rest of the test.
    a. If audible knock is not achieved before reaching maximum CR, lower CR retard ignition time repeat step 4 until audible knock achieved.
5. Record (3)1000-cycle intervals of operating conditions and pressure trace data.
6. Select 3 Premixed Reference Blends (PRF) that bracket the test fuel,
    a. If GC data is unavailable begin with PRF 1 = 85-15 and select PRF 2 and 3 based on KI.
7. Switch test fuel off and allow fuel mixing volumes to return to atmospheric pressure.
8. Switch on Pre-Mixed Blend 1 and set fuel flow solenoid position to achieve stoichiometric operating conditions (λ = 1.000).
9. Record 1000 cycle interval of operating conditions and pressure trace data while keeping flow constant.
10. If PRF 2 and 3 have not been selected determine the closer two blends that will bracket the fuel. Examples provided below:
    a. Test KI = 500, PRF 1(85MN) = 700, PRF 2:(80-20), and PRF 3:(90-10)

b. Test KI = 500, PRF 1(85-15) = 100, PRF 2:(80-20), PRF 3(75-25)

11. Switch on Pre-Mixed Blend 2 and set fuel flow solenoid position to achieve stoichiometric operating conditions (λ = 1.000).

12. Repeat steps 9 & 10 with PRF 3

13. MN test is complete, turn off fuel flow and stop engine.

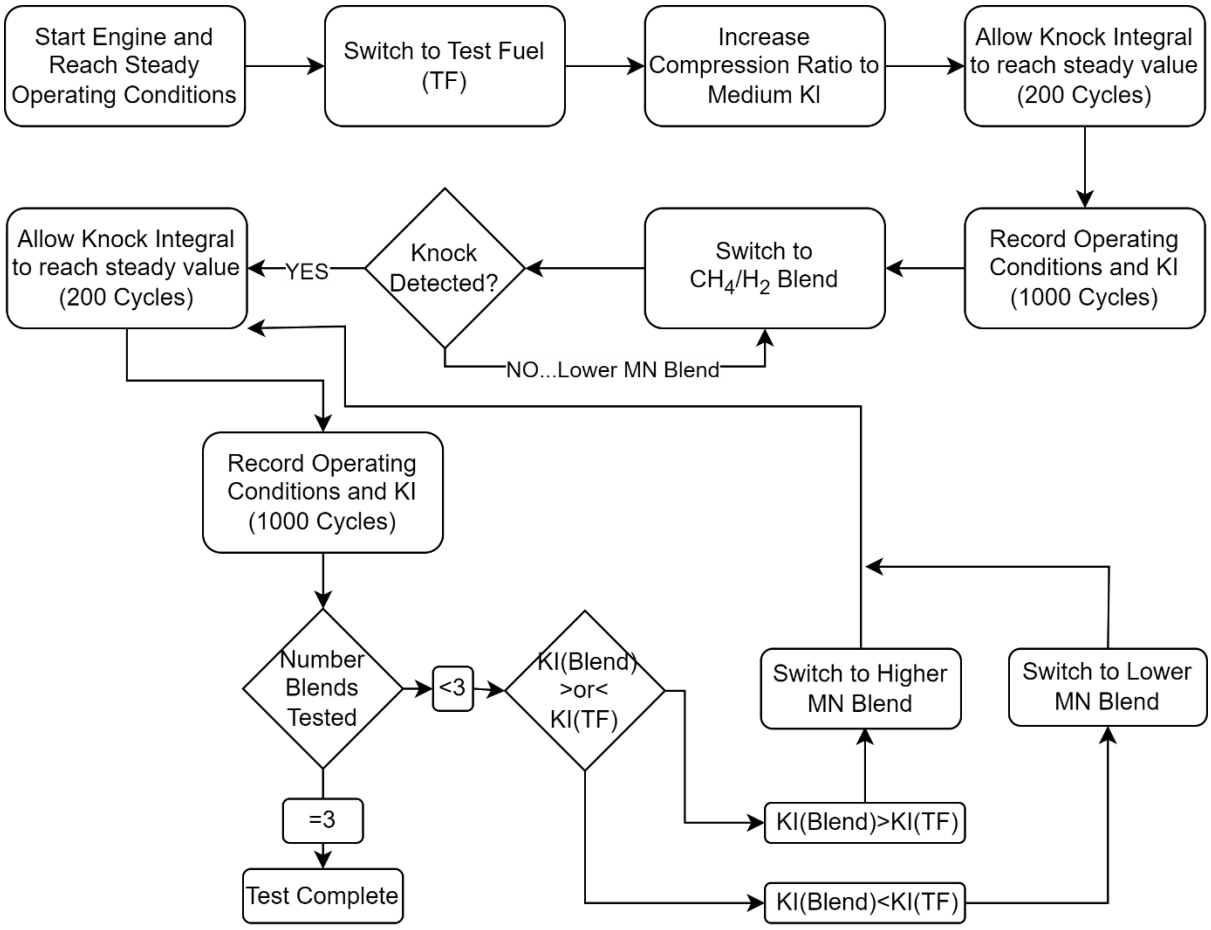

Figure 32: Premixed Blends Method Flowchart (Exponential Regression)

Pre-Mixed Blends Bracketing KI Post-Processing Procedure

1. The Knock Intensity of each power stroke is averaged over 1000 cycles.

1a. TKI-High: Blend with Higher KI than Target KI

1b. TKI-Med: Blend with Similar KI to Target KI

1c. TKI-Low: Blend with Lower KI than Target KI

2. The Methane Number of each blend is included on the Blend Certifications.
3. Plot MN vs. Avg. KI for TKI-High, TKI-Med, and TKI-Low Blends.
4. Generate an exponential regression equation using these 3 points.
5. Using the average KI from test fuel blend, calculate the predicted MN.

Pre-Mixed Blends Bracketing KI Bracketing Examples

Using the Pre-mixed Blends Bracketing KI technique, the MN of a natural gas sample is included in Figure 33. Considering the data corresponding to Figure 33, the **target KI** for the test fuel was 3.61 kPa^2/s^2. The test fuel was replaced with an 80-20 CPRF, the engine was allowed to reach steady knocking conditions, and a 1000-cycle data set was collected. This CPRF resulted in an average KI of 16.9 kPa^2/s^2 and designated **CPRF-High**. This process was repeated with two other CPRFs with higher concentrations of methane bracketing the **target KI**. The 85-15 CPRF resulted in an average KI of 5.45 kPa^2/s^2 being designated **CPRF-Med** and the 90-10 CPRF resulted in an average KI of 0.84 kPa^2/s^2 earning the designation **CPRF-Low**. Using these (3)-reference fuel blend datapoints, an exponential regression trendline is fit with the form:

$$f(MN) = a * \exp(b * MN)$$

Using the coefficients from the linear regression trendline, and the average KI of test fuel 1000 cycle test, the methane number of the fuel blend can be calculated:

$$MN(Test\ Fuel) = \frac{\ln\left(\frac{(Average\ KI)}{a}\right)}{b} = \frac{\ln\left(\frac{3.61}{4.181 * 10^9}\right)}{-0.2414} = 86.45$$

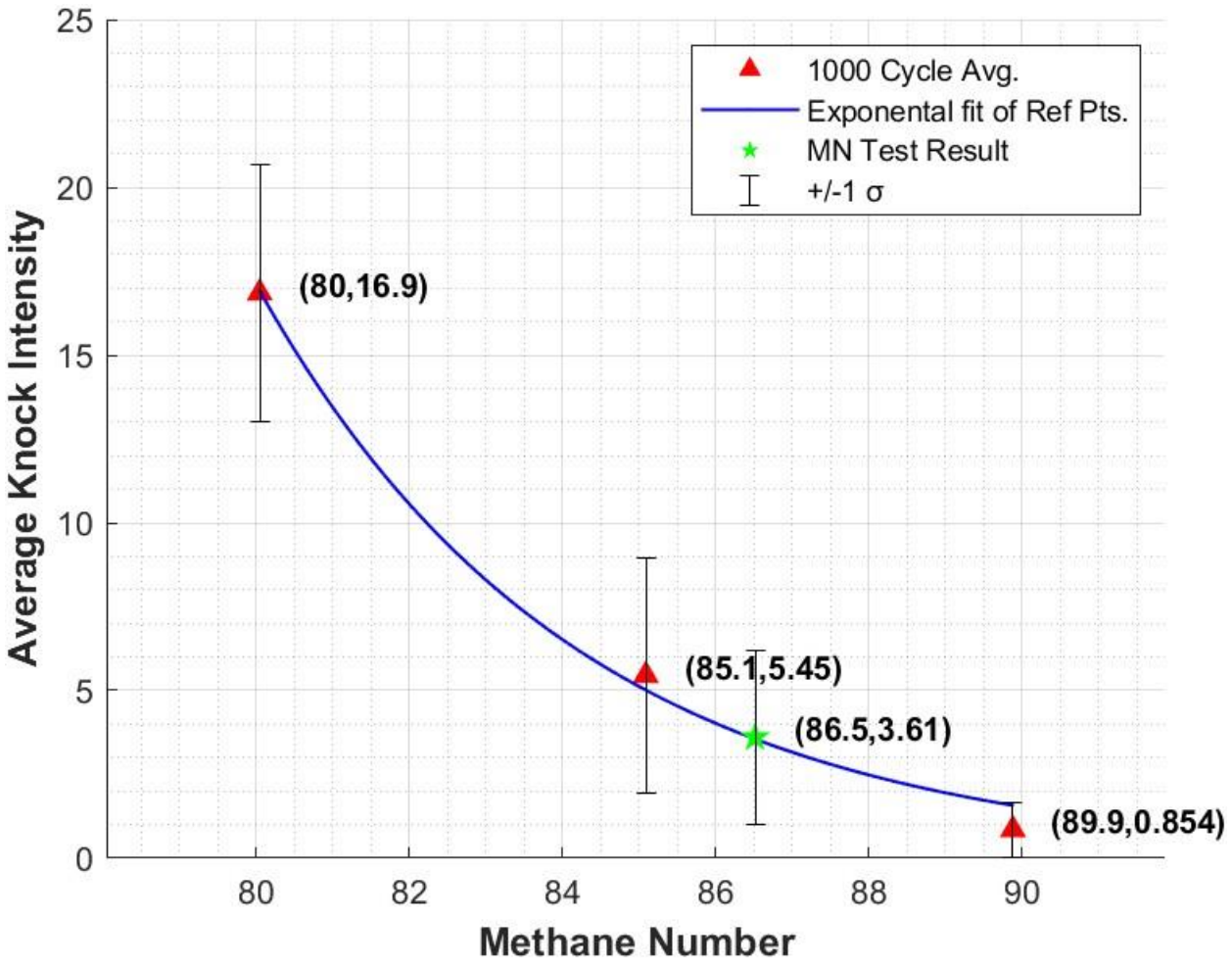

Figure 33: Certified Premixed Reference Blends Method Results

Removing the uncertainty associated with measuring flow rates simplifies the plot allowing for a more streamlined measurement of MN. From the perspective of the operator, this method reduces the overall complexity and makes it much easier to have generate an approximation for MN when operating the engine. Also utilizing pre-mixed fuel blends enables the testing of a wider range of fuel samples with one calibration procedure.

Comparing exponential to linear regression techniques for determining MN, for large differences in MN (> 10) of the pre-mixed reference blends, the exponential has a much higher degree of accuracy while the linear regression techniques tend to over predict. When using two

values smaller increments between PRF more accurately predict MN but a meaningful R^2 value cannot be determined.

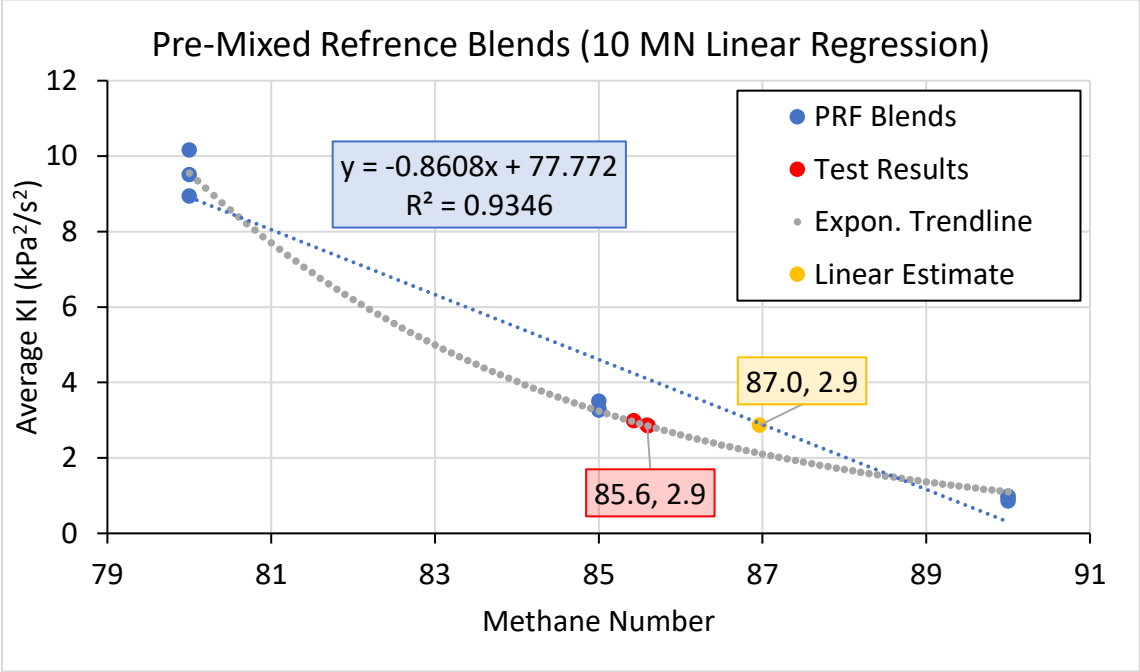

Figure 34: PRF MN Exponential vs. Linear Regression (10MN)

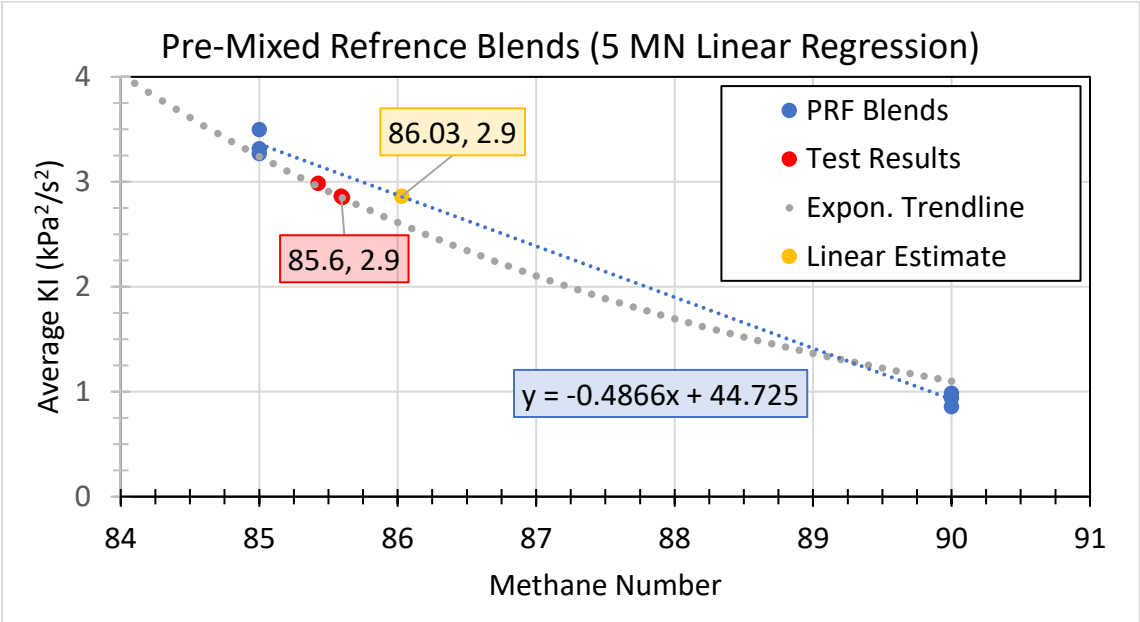

Figure 35: PRF MN Exponential vs. Linear Regression (5MN)

Chapter 3 explores the exponential relationship between Knock Intensity (KI) and Methane Number, evident in the plotted 1000 cycle average KI values presented in Figure 33. Notably, the deviation between the 1000 cycle averages of the (3)1000 sets, particularly within the 80-20 blend, amounts to 0.911. Application of this deviation to the exponential function yields a Methane Number variation of 0.6 which is below the expected variation in the Methane Number unit established by Leiker et al. [9].

Figure 34 and Figure 35 displays the differences between MN quantification techniques. When three reference blends (80, 85, 90) are used to generate a linear regression with R^2 = 0.9346, the result is a 1.4 MN over-prediction compared to the exponential fit. When considering using two reference blends (85, 90) to bracket the fuel which generates a linear regression, the resulting MN is 0.43 greater than the exponential fit value. However, an R^2 value of 1.00 is always the result of a 2-point linear regression.

Active Blending vs. Pre-Mixed Blends

With two different techniques for relating knock intensity of test fuels to reference blends and determining MN, a comparison between these two methods must be made. Figure 33 presents the plots for the certified pre-mixed blends under identical operating conditions, while Figure 36 depicts the active blending technique. Under identical operating conditions aside from compression ratio used, the active blending technique yielded an MN outcome of 86.15, whereas the premixed blends produced an MN of 86.5. This outcome confirms the viability of both techniques to replicate results and provides additional validation for the calibration of the flow meters used in active blending.

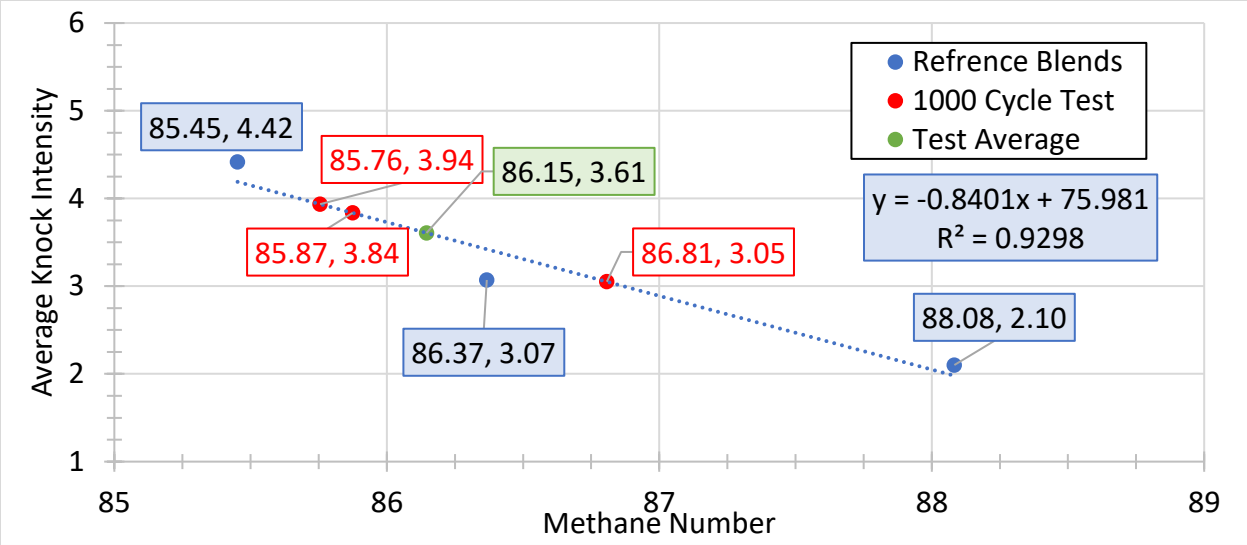

Figure 36: Active Blending Results

Methane Number Measurement Uncertainty

Directly calculating the total uncertainty associated with the Methane Number test procedure is a challenging ordeal with many different variables adding variation to the measurement. To estimate the total uncertainty associated with the Methane Number, multiple tests were conducted over a 6-month period and plotted in **Figure 37**. For tests investigating the uncertainty the following testing parameters were followed, ambient air pressure, stoichiometric mixture, 70°C intake manifold pressure, and 15° bTDC ignition timing. All results included in the uncertainty analysis had an $R^2 > 0.95$, with an average value of 85.6, and a standard deviation of 0.608.

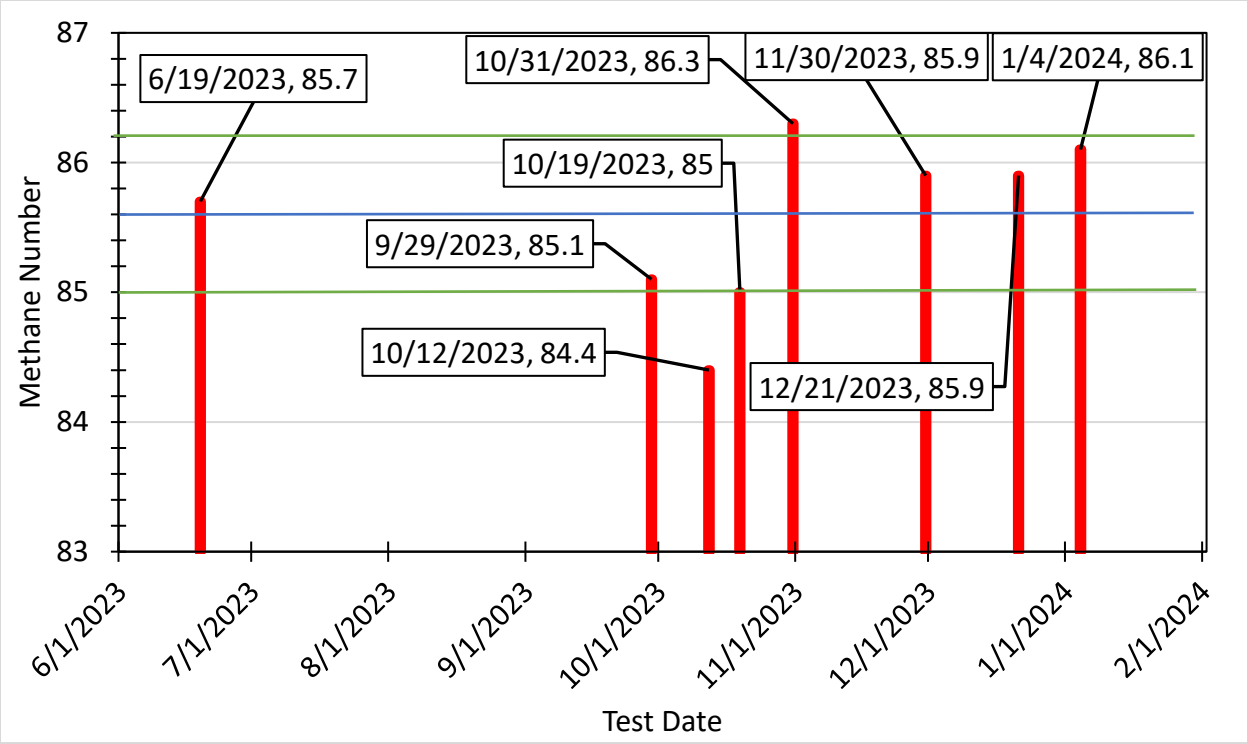

Figure 37: Methane Number 6-month Uncertainty Test Results

Discussion:

The development of a new technique of determining MN through bracketing allows much more flexibility from an operator perspective reducing the requirement to match identically the KI between two different fuels. The bracketing of a fuel allows for deeper understanding of the relationship between KI and MN quantification and allowing results to be validated. Before, without matching the KI exactly between test samples, it was very difficult to quantify what a difference of 0.25 average-KI meant for a MN value. The validation of the bracketing method compared the measured results between dynamic blending and certified methane-hydrogen blends.

Comparing the test results, the anticipated value of MN_C using the ASTM 8221 calculator was 79.9 so an expected result would have been a MN of 80 +/- 1. The natural gas sample that was tested using the dynamic blend KI bracketing technique yielded a MN of 85.6. Compared with the Pre-mixed blends KI bracketing technique results of 85.5. With the validation of the bracketing KI method resulting in a very close result, the accuracy of the Leiker et al. [9] results may be questioned. Leiker may have had sparse experimental data available for his analysis and may have relied on extrapolation & interpolation for low blends of higher hydrocarbon (C_4-C_6) resulting in an over accounting for these components.

CHAPTER 5: COMPARISON OF FFT AND DETONATION METER KI METRICS

This chapter compares the Original Detonation Meter Measurement System on the CFR engine with the CSU FFT Bandpass system. The information outlined in 2-2 Knock Quantification Methods, discusses the different means of adjusting the Knock Intensity of the CFR system under given operating conditions. The purpose of this section is to analyze the CSU FFT and CFR systems to determine if they can reach comparable results under similar knocking conditions.

5-1 EXPERIMENT SETUP

There are many adjustments available on the original CFR knock measurement system for precise tuning of knock quantification. A drawback of these adjustments is they rely on the operator for determining the onset of knock and only provide relative relationships between operating conditions. The spread and meter reading adjustments allow for the system to set a KI for one day and yet it could be much different on another day with the exact same CFR engine operating conditions and settings. The setup and use of the Model 501C-Detonation meter, knock meter face, and D-1 Detonation pickup are outlined in the ASTM D2699 [7] and ASTM 2700 [8]. The first check for the system is to determine the linearity of the Detonation meter which is outlined in APPENDIX A: ASTM D-2699 & ASTM D-2700 CFR KNOCK MEASUREMENT S. After following the steps outlined for the linearity check, the test for comparing the readings between the two systems are outlined in the section: **Setup for CFR Detonation Meter**.

Setup for CFR Detonation Meter

1. With the CFR engine off, adjust the screw on the meter face on the threshold of movement.
2. Bring the engine to steady Operating Conditions using building natural gas.
3. Change fuel to known Reference Blend (90-10).
4. Increase CR until audible knock is detected.
5. Adjust METER READING dials to achieve 50 KI.
6. Increase METER READING coarse dial 1 division.
7. Record ΔKI
8. Change SPREAD and repeat steps 4-6 until ΔKI = 10 divisions.

Comparison of the CFR Detonation meter and CSU's FFT of Bandpass Signal Method

Analyzing the engine and the ability for comparing the two methods of knock measurement, there is one port in the cylinder head for the pressure transducer or detonation meter. This means only one knock measurement system can be tested at a time and makes it such that changes in knock intensity must be recreated at two different times. Below is the testing plan for re-creating engine operating conditions and knock intensity between the two knock measurement systems.

1. Begin testing with the CSU cylinder pressure measurement system.
2. Bring the engine into steady state operating conditions and switch to a consistent source of fuel to prevent fluctuations.
3. Gradually increase engine CR until the onset of audible knock.
4. Perform an Ignition timing sweep (15-25° bTDC) in one degree timing intervals while allowing 1 minute for stabilization prior to collecting a 1000-cycle period for each

ignition timing interval. Pay attention to engine pressure conditions so as not to surpass the rated capacity of the engine.

5. Reduce compression ratio, terminate fuel flow, and stop engine.
6. Remove liquid cooled pressure transducer from cylinder head and install CFR Detonation Pickup. Note: Pay extra attention as to not cross thread pickup in installation.
7. Re-start engine with same fuel source and allow enough time for engine to return to steady state operation.
8. Increase CR to the same dial setting and ensure consistent engine operating parameters to those used with CSU knock measurement system.
9. Perform ignition timing sweep (15-25° bTDC) in one degree timing intervals while allowing 1 minute for stabilization prior to recording Knock Intensity from knock meter for each ignition timing value.

The tests comparing the two knock measurement systems were conducted with 2 different compression ratios and fuels to ensure results are not dependent on fuel composition or knock intensity. The fuels used were the 90-10 and 85-15 certified premixed reference blends of methane and hydrogen.

5-2 RESULTS

Comparisons between the FFT Bandpass and the CFR Detonation meter are limited by the subjective nature of the CFR system. Therefore, the objective of this study is to determine a method for adjusting the settings of the CFR Detonation Meter to output similar readings to the CSU FFT method. **Figure 38** and **Figure 39** show the results from tests investigating the relationship between each method with similar operating conditions (KI). The results for the

comparison between the two methods were not scaled in any way, but rather the initial CFR KI value was set to a low value using the SPREAD dial. When referencing the CFR system, the unit used is the Knock Meter Reading (KMR) and the CSU system used the average KI.

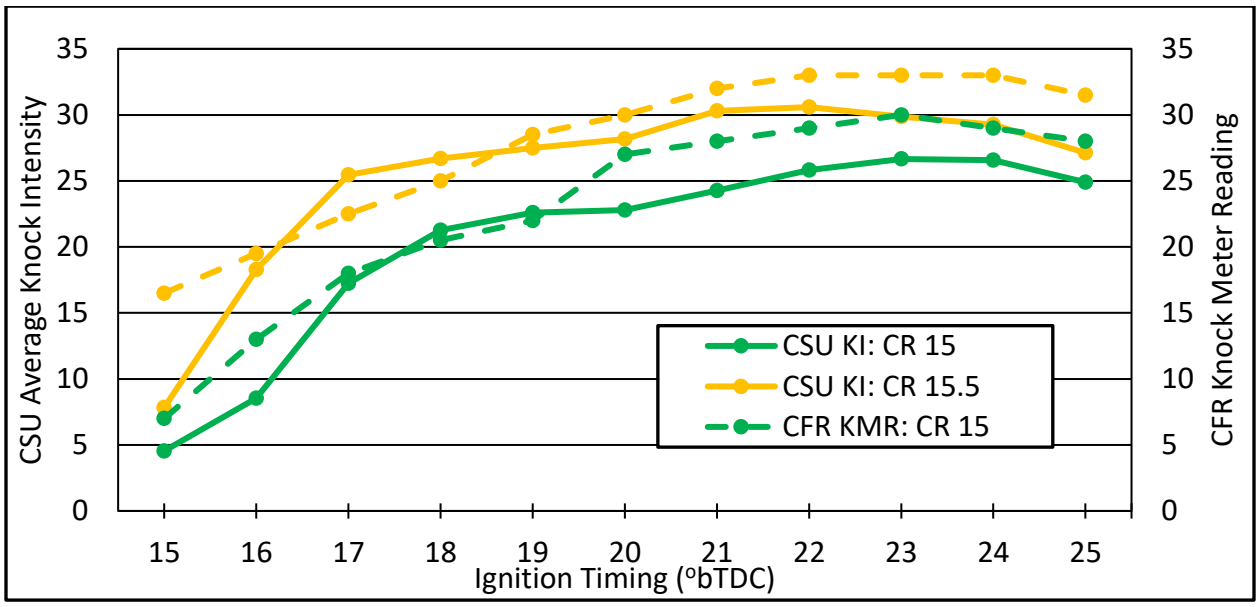

Figure 38: 90-10 Knock Metric Comparison effect of CR

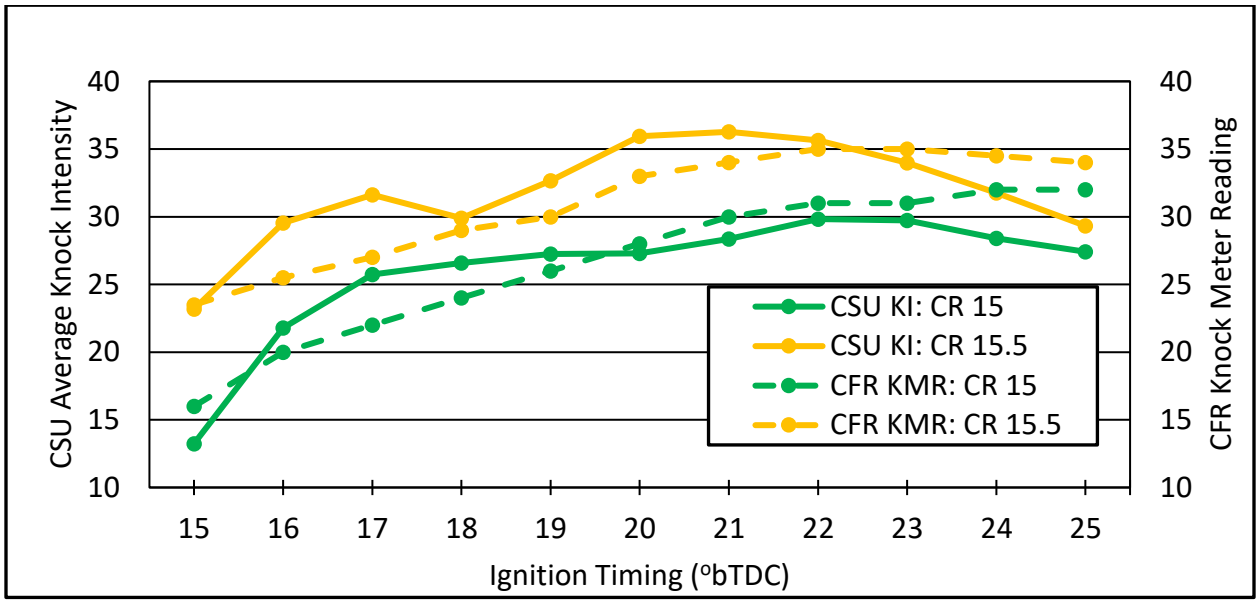

Figure 39: 85-15 Knock Metric Comparison effect of CR

5-3 DISCUSSION

The data shows that the CFR knock system produces similar changes in KI compared to the CSU FFT Bandpass method. The results verify the method used to select the Meter Reading and Spread settings on the Detonation Meter. There is an interesting relation between the two Knock detection systems addressing the linearity between KI with similar changes in knocking characteristics. The CFR KI system has a more linear response over the course of ignition timing values used compared to the FFT Bandpass method. Comparing the two results specifically in **Figure 39**, in the two CRs tested, there is a nonlinear response in the FFT Bandpass method between 15-18 degrees bTDC ignition timing. Comparing these results to the CFR Knock Intensity system, the FFT Bandpass over predicts Knock intensity by as much as 5 units when at other ignition timings the two lines cross. Additionally at higher ignition timing values the FFT Bandpass KI value decays more as compared to the CFR KI value. Even with these discrepancies between methods, they produce a KI metric that can be used to accurately determine MN.

Comparing the two metrics, they each provide a benefit and inherit drawback depending on the application. The FFT Bandpass system provides consistent KI values without intervention from the operator and operational parameters. The system also provides much more insight into cylinder pressures and detailed analysis into the engine operation. In a research environment, such insight is beneficial, but in a regulatory environment, such information would not be necessary. The drawback to the FFT Bandpass method is its real benefit with the sensitivity of the method not being able to be adjusted to gain finer resolution between knocking conditions. The CFR KI method provides such adjustment in resolution and allows a definitive KI metric without the use of post-processing.

CHAPTER 6: CONCLUSIONS AND FUTURE WORK

6-1 CONCLUSIONS

The purpose of this work was to evaluate the current method for determining MN and evaluate the effect environment and test parameters have on end gas auto-ignition on a spark ignited, natural gas engine. This evaluation was completed using a Cooperative Fuel Research engine with modifications implemented to operate using gaseous fuels and control environment parameters. The noteworthy impacts of environment parameters and testing methods have on KI and MN are as follows:

1. The ignition timing used for MN has a substantial impact on the Knock Intensity for a given compression ratio, but this remains constant between the test fuel and reference fuels. Allowing the operator to utilize ignition timing values ranging from 12º–25º bTDC.
2. The intake manifold temperature has minimal influence on MN results but does increase the intensity of EGAI. It was maintained at 70°C (158°F) ± 1.66°C (2.98°F) to facilitate EGAI while mitigating the risk of backfire.
3. Intake manifold pressure significantly affects MN results and knock intensity. It was concluded that MN tests should occur at ambient atmospheric pressure, with fluctuations restricted to ± 0.615 kPa. A 10 kPa increase in pressure yields a 0.5 MN variation, which is within the anticipated metric fluctuation.
4. The Air/Fuel ratio can vary significantly over the course of a test and has a significant impact on the KI. It was determined that a λ of 1.000 corresponded to the peak KI value and was the least variable condition. To minimize the effects of λ variations, the unit should be kept within a range of +/- 0.007.

5. This study compared KI metrics between the CSU FFT Bandpass and CFR Knock Detection methods, each offering advantages and disadvantages based on the testing situation. Both systems are considered viable for determining MN, with steps for matching sensitivity outlined in this report.
6. MN test uncertainty was approximated through testing a consistent fuel sample multiple times over a 6-month period with consistent test parameters and different environment conditions. These results of these tests concluded the MN test results have a standard deviation of 0.61 MN units.

6-2 FUTURE WORK

To answer the question of why $MN_C \neq MN$, additional testing should be done with different fuels offering a range of MN values. The testing with additional fuels should focus on high CH_4 and modest C_2H_6 compositions with detailed testing every 1% volume fraction for C_3H_8 and C_4H_{10}. As hydrogen blending begins to appear in commercially available fuels, understanding the role hydrogen plays in EGAI for these fuels will be crucial, therefore detailed testing with hydrogen volume fractions up to 20% will provide a benchmark for engine manufacturers and consumers.

Humidity is an environmental condition that has the possibility of changing significantly over the course of a testing day and its relationship with KI and MN needs to be better understood. Current research has concluded a significant relationship between KI and humidity within the bounds established by ASTM for liquid fuels. Thus, the CFR engine at CSU needs a method of measuring and controlling humidity supplied to the engine while testing.

REFERENCES

[1] Heywood, "Internal Combustion Engine Fundamentals," New York(New York): McGraw-Hil, 1988.

[2] *ASTM Standard Terminology Relating to Gaseous Fuels,* ASTM: D4150-21b, 2021.

[3] Enviornmental Protection Agency. (2023, August, 3). *Renewable Natural Gas* [Online]. Available: https://www.epa.gov/lmop/renewable-natural-gas.

[4] S. M. Bayliff, "Evaluation of Controlled End Gas Auto Ignition With Exhaust Gas Recirculation in a Stoichiometric, Spark Ignited, Natural Gas Engine," M.S. thesis, Dept. Mech. Eng., Colorado State Univ., CO, 2019.

[5] K. Kumano and S. Yamaoka, "Analysis of Knocking Suppression Effect of Cooled EGR in Turbo-Charged Gasoline Engine," *SAE,* vol. 01, no. 1217, 2014.

[6] D. M. Wise, "Investigation into Producer Gas Utilization in High Performance Natural Gas Engines," Ph.D. dissertation, Dept. Mech. Eng., Colorado State Univ., CO, 2013.

[7] *ASTM Standard Test Method for Research Octane Number of Spark-Ignition Engine Fuel,* ASTM:D-2699, 2004.

[8] *ASTM Standard Test Method for Motor Octane Number of Spark-Ignition Engine Fuel,* ASTM:D-2700, 2019.

[9] M. Leiker, K. Christoph, M. Rankl, W. Cantellieri and U. Pfeifer, "Evaluation of Antiknocking Property of Gaseous Fuels by Means of Methane Number and its Practical Application to Gas Engines," in *ASME*, New York, American Society of Mechanical Engineers, 1972.

[10] *ASTM Standard for Determining the Calculated Methane Number (MN_C) of Gaseous Fuels Used in Internal Combustion Engines,* ASTM:D8221, 2018.

[11] *Gas infrastructure - Quality of gas - Group H,* EN 16726:2015+A1:2018, 2018.

[12] Waukesha Engine Division, (2003) Waukesha CFR F-1 & F-2 Research Method (F-1) Motor Method (F-2) Octane Rating Units Operation and Maintenance (2nd ed.) *Dresser Industries*

[13] Motorsports Technologies. (2005, Jun. 23). *MoTeC PLM User's Manual* [Online]. Available: https://www.motec.com.au/hessian/uploads/PLM_User_Manual_b76e597aaa.pdf

[14] Brunt, M., Pond, C., and Biundo, J. (1998 Feb.) Gasoline Engine Knock Analysis Using Cylinder Pressure Data. *SAE International* [Technical Paper] 98096, Available: https://doi.org/10.4271/980896

[15] Elmqvist, C., et al., (2003, Oct.) Optimizing Engine Concepts by Using a Simple Model for Knock Prediction. *SAE International* [Technical Paper] 2003-01-3123, Available: https://doi.org/10.4271/2003-01-3123

[16] C. Michaelis, (2019, Dec. 5) Detonation Pickup Basics. *Engine Buzz* [Online]. Available: https://enginebuzz.com/2019/12/05/detonation-pickup-basics/.

[17] U.S. Department of Commerce (2023) Thermophysical Properties of Fluid Systems. *National Institute of Standards and Technology* [Online]. Available: https://webbook.nist.gov/chemistry/fluid/

[18] P. Fleming. (2024, Jan. 10) The Joule-Thomson Effect. *LibreTexts Chemistry* [Online]. Available: https://chem.libretexts.org/Bookshelves/Physical_and_Theoretical_Chemistry_Textbook.

[19] M. Essen, S. Gersen, G. Dijk and T. Mundt, et al. (2016, Oct. 24) The Effect of Humidity on the Knock Behavior in a Medium BMEP Lean-Burn High-Speed Gas Engine. *SAE Int. J. Fuels Lubr.,* vol. 9, no. 3, pp. 695-702, 2016.

[20] Colorado State University ATMOS, (2023, Dec. 12) Fort Collins Weather Station Custom Data Plots [Online]. Available: https://ccc.atmos.colostate.edu/~autowx/fclwx_plotsearch_form.php.

APPENDIX A: ASTM D-2699 & ASTM D-2700 CFR KNOCK MEASUREMENT SETUP

CFR Knock Measurement Linearity Check

- Described by ASTM D2699:
- NOTE: Mentions Nonlinearity 20 > KI > 80
- System Linearity Check Procedure: Pg 27-28
    1. Disconnect Detonation Pickup & Connect 1.5 V DC Battery
    2. Set SPREAD = 5.0 & TIME CONSTANT = 1
    3. Adjust METER READING such that Knock Meter = 50
    4. Change SPREAD = 8.0
    5. Adjust METER READING such that Knock Meter = 80
    6. Record METER READING
    7. Repeat Steps 4-6 with SPREAD = 2, 3, 4, 5, 6, 7, 8
    8. NOTE: A Perfect System should produce METER READINGS that are exactly 10x SPREAD Setting

Described by ASTM D2700 pg 28-30:

1. Prepare PRF Blend
2. Adjust A/F Ratio for maximum KI
3. Adjust Meter Reading Setting so Knock Meter ~50 +/- 2
4. Use Spread set to 12-14 for 90 ON
    - This number will decrease when testing fuels < 80 ON
    - This number will decrease when testing fuels > 100 ON

5. Mentions how to Increase/Decrease but not a procedure for how to set SPREAD and METER READING

APPENDIX B: REFRENCE BLEND CERTIFICATES OF GAS ANALYSIS

Commercial Purity CH_4 Certification

Airgas
an Air Liquide company

Airgas Specialty Gases
Airgas USA LLC
24075 US Hwy 6
Stryker, OH 43557
Airgas.com

CERTIFICATE OF BATCH ANALYSIS

Grade of Product: CP

Part Number:	ME CP300	Reference Number:	141-402850128-1
Cylinder Analyzed:	7398111Y	Cylinder Volume:	360.0 CF
Laboratory:	124 - Stryker (SAP) - OH	Cylinder Pressure:	2400 PSIG
Analysis Date:	Sep 15, 2023	Valve Outlet:	350
Lot Number:	141-402850128-1		

ANALYTICAL RESULTS

Component	Requested Purity	Certified Concentration
METHANE	99.5 %	99.5 %
Moisture	10.0 PPM	< 10.0 PPM
ETHANE	1000.0 PPM	< 1000.0 PPM
Nitrogen	4000.0 PPM	< 4000.0 PPM
Oxygen	50.0 PPM	< 50.0 PPM

Cylinders in Batch:

1513108, 22521, 3166576Y, 4147470Y, 4322039Y, 5594231Y, 5594336Y, 55949, 5799536Y, 6537708Y, 6537736Y, 6537765Y, 6738106Y, 6789753Y, 6854858Y, 6856975Y, 6996921Y, 7398111Y, 7398113Y, 7398118, 7398124, 7398129, A-000795, AGAC110645, C567607, H0484256, HY259, SG-869104, SG30472A, SRLK008674, T-689828, T367230, T834062Y, TW04-777395, TW07-475314, VT745, W25465, W362264, W440645, W481783

Impurities verified against analytical standards traceable to NIST by weight and/or analysis.

90-10 CH_4-H_2 Certification

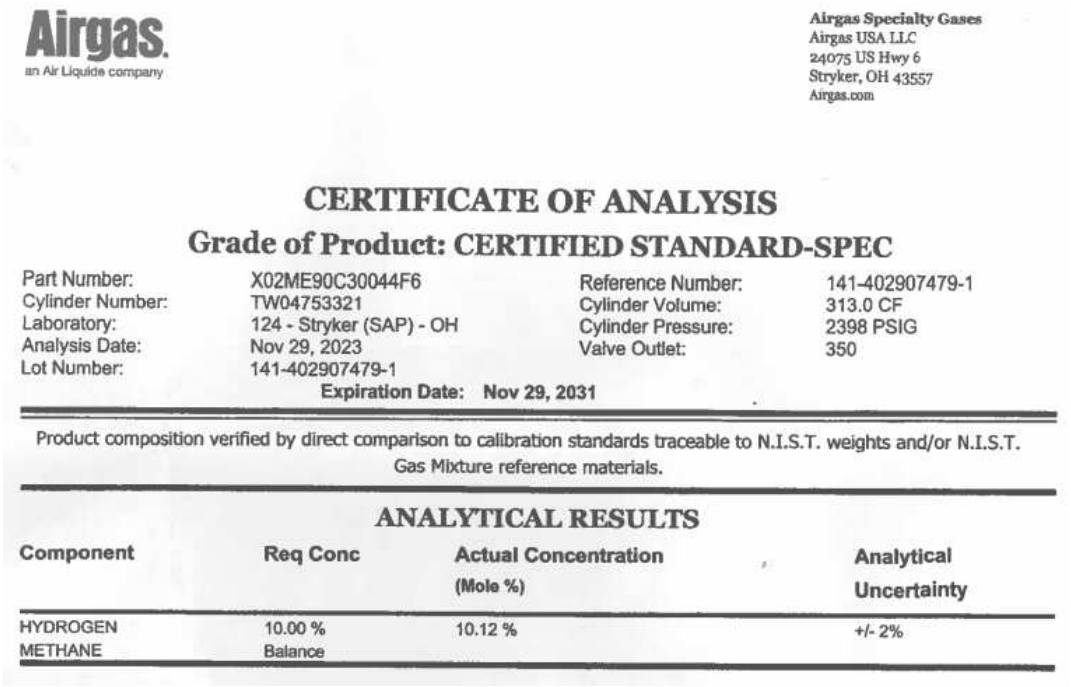

Airgas
an Air Liquide company

Airgas Specialty Gases
Airgas USA LLC
24075 US Hwy 6
Stryker, OH 43557
Airgas.com

CERTIFICATE OF ANALYSIS

Grade of Product: CERTIFIED STANDARD-SPEC

Part Number:	X02ME90C30044F6	Reference Number:	141-402907479-1
Cylinder Number:	TW04753321	Cylinder Volume:	313.0 CF
Laboratory:	124 - Stryker (SAP) - OH	Cylinder Pressure:	2398 PSIG
Analysis Date:	Nov 29, 2023	Valve Outlet:	350
Lot Number:	141-402907479-1		

Expiration Date: Nov 29, 2031

Product composition verified by direct comparison to calibration standards traceable to N.I.S.T. weights and/or N.I.S.T. Gas Mixture reference materials.

ANALYTICAL RESULTS

Component	Req Conc	Actual Concentration (Mole %)	Analytical Uncertainty
HYDROGEN	10.00 %	10.12 %	+/- 2%
METHANE	Balance		

85-15 CH_4-H_2 Certification

Airgas
an Air Liquide company

Airgas Specialty Gases
Airgas USA LLC
24075 US Hwy 6
Stryker, OH 43557
Airgas.com

CERTIFICATE OF ANALYSIS

Grade of Product: CERTIFIED HYDROCARBON

Part Number:	X02ME85C3000002	Reference Number:	141-402908060-1
Cylinder Number:	4147474Y	Cylinder Volume:	321.0 CF
Laboratory:	124 - Stryker (SAP) - OH	Cylinder Pressure:	2398 PSIG
Analysis Date:	Nov 29, 2023	Valve Outlet:	350
Lot Number:	141-402908060-1	Expiration Date:	Nov 28, 2031

Traceability Statement: Hydrocarbon Process standards are NIST traceable either directly by weight or by comparison to Airgas laboratory standards that are directly NIST traceable by weight.

CERTIFIED CONCENTRATIONS

Component	Requested Concentration	Reported Mole %	Accuracy
HYDROGEN	15.00 %	14.91 %	+/- 2%
METHANE	85 %	85.09 %	+/- 2%

80-20 CH_4-H_2 Certification

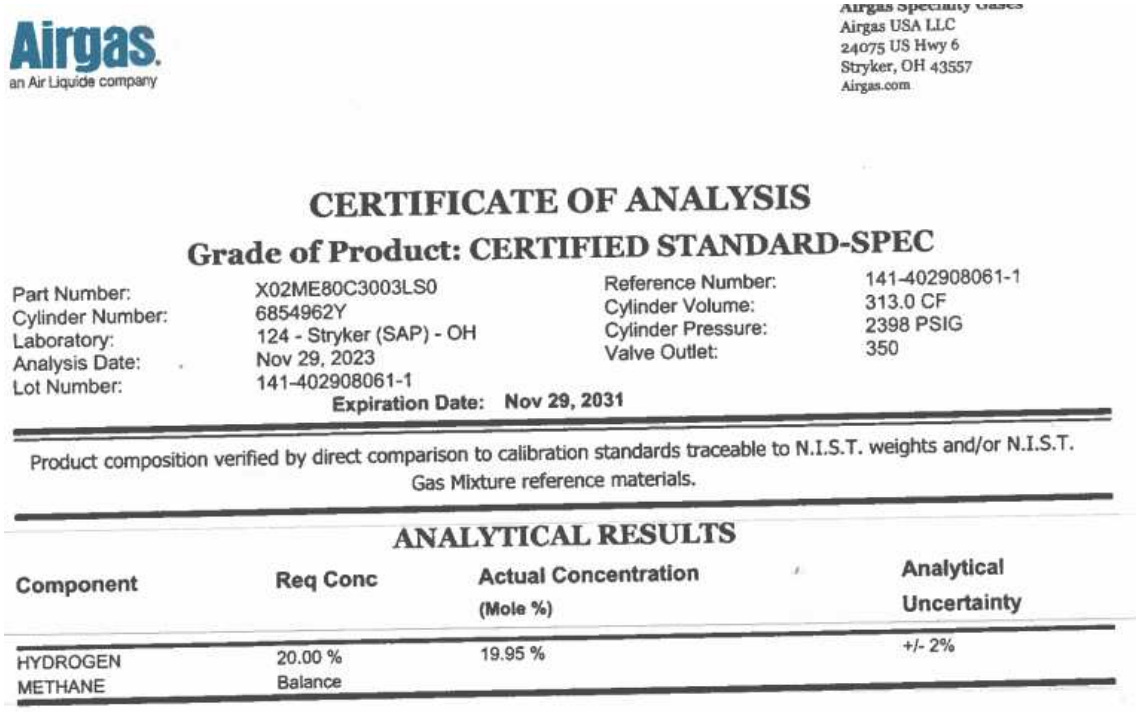

Airgas
an Air Liquide company

Airgas Specialty Gases
Airgas USA LLC
24075 US Hwy 6
Stryker, OH 43557
Airgas.com

CERTIFICATE OF ANALYSIS

Grade of Product: CERTIFIED STANDARD-SPEC

Part Number:	X02ME80C3003LS0	Reference Number:	141-402908061-1
Cylinder Number:	6854962Y	Cylinder Volume:	313.0 CF
Laboratory:	124 - Stryker (SAP) - OH	Cylinder Pressure:	2398 PSIG
Analysis Date:	Nov 29, 2023	Valve Outlet:	350
Lot Number:	141-402908061-1		

Expiration Date: Nov 29, 2031

Product composition verified by direct comparison to calibration standards traceable to N.I.S.T. weights and/or N.I.S.T. Gas Mixture reference materials.

ANALYTICAL RESULTS

Component	Req Conc	Actual Concentration (Mole %)	Analytical Uncertainty
HYDROGEN	20.00 %	19.95 %	+/- 2%
METHANE	Balance		

75-25 CH_4-H_2 Certification

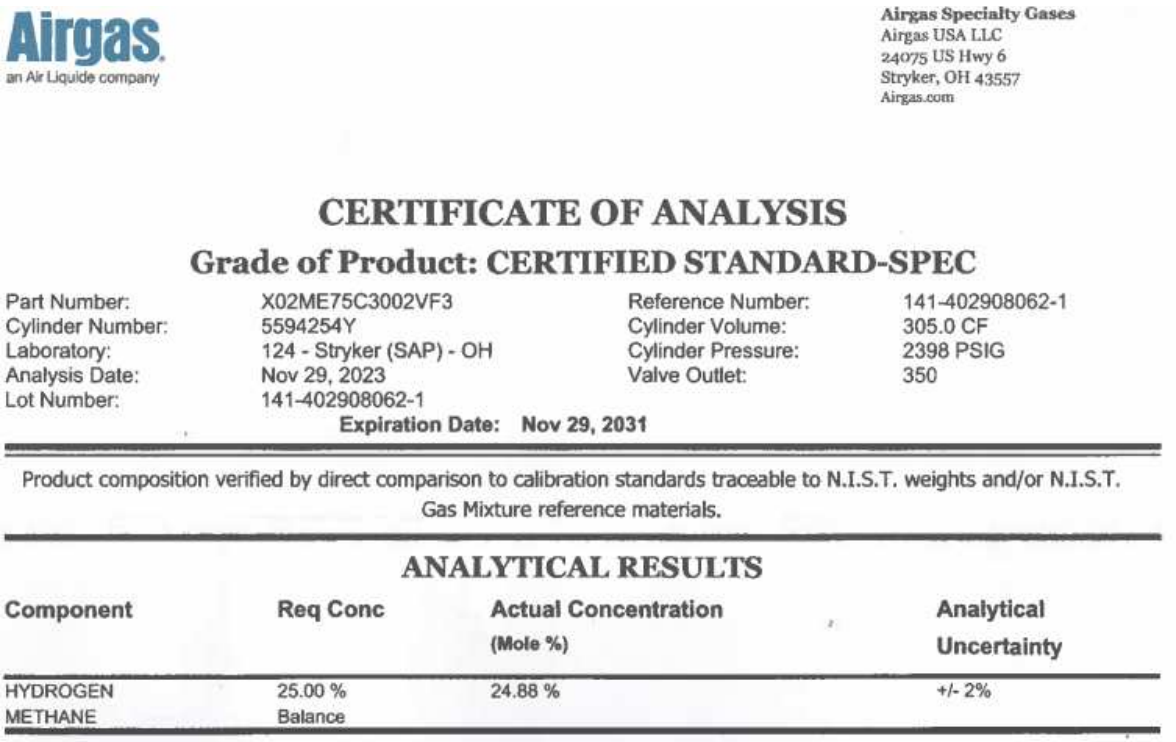

Airgas
an Air Liquide company

Airgas Specialty Gases
Airgas USA LLC
24075 US Hwy 6
Stryker, OH 43557
Airgas.com

CERTIFICATE OF ANALYSIS

Grade of Product: CERTIFIED STANDARD-SPEC

Part Number:	X02ME75C3002VF3	Reference Number:	141-402908062-1
Cylinder Number:	5594254Y	Cylinder Volume:	305.0 CF
Laboratory:	124 - Stryker (SAP) - OH	Cylinder Pressure:	2398 PSIG
Analysis Date:	Nov 29, 2023	Valve Outlet:	350
Lot Number:	141-402908062-1		

Expiration Date: Nov 29, 2031

Product composition verified by direct comparison to calibration standards traceable to N.I.S.T. weights and/or N.I.S.T. Gas Mixture reference materials.

ANALYTICAL RESULTS

Component	Req Conc	Actual Concentration (Mole %)	Analytical Uncertainty
HYDROGEN	25.00 %	24.88 %	+/- 2%
METHANE	Balance		

APPENDIX C: METHANE NUMBER ANALYSIS MATLAB SCRIPT

```
clear; clc; close all;
%This program is intended to take .tdms code from the CFR and calculate the
%Methane number. In order for this code to work there needs to be 6 files
%total. The output of this program is a .xlsx file
% The Perf Labview file should be recorded at 8 Hz for 2.5 min (1200 data
% pts) and the Combustion LV should be 1000 cycles and begin at 15s

% STEP 1: Declare where the files are saved:
% Note: This will change
datafilepath = 'C:\Users\dbaucke\Desktop\Methane Number Overflow\3-10-24\MN Control
Test\';


% STEP 2: Declare the names of the files that are going to be used:
file_ending ='_CR030_NA_Lam1.000_15BTDC_3-10-24';

% STEP 3: Declare the desired values for testing:
Perf_PlottingFlag = 1;     % Turns on the scatter plotting section: takes about a min
DesiredValues = zeros(2,4);% Creates a matrix 1 row long with 6 columns
DesiredValues(1,1) = 73;   % Intake Air Temperature (C)
DesiredValues(2,1) = 1;    % Intake Air Temperature (C) Variation
DesiredValues(1,2) = 85;  % Intake Air Pressure (kPa)
DesiredValues(2,2) = 5;    % Intake Air Pressure (kPa) Variation
DesiredValues(1,3) = 1.00;    % Mixture (Lambda)
DesiredValues(2,3) = 0.05; % Mixture (Lambda) Variation
DesiredValues(1,4) = 900;  % Engine RPM
DesiredValues(2,4) = 1;    % Engine RPM

diaryname = [datafilepath 'Comb Stats.xlsx']; % Declares a name of file that will be
created
if exist(diaryname, 'file') % If the file exists
    delete(diaryname);  % Delete the old file
end
% Jump to data saving section

if exist('Results\', 'dir') % If the Folder "Results\" exists
     rmdir("Results\","s") % Deletes Previous run results silently.
     mkdir Results\ % Make Directory
else
     mkdir 'Results\' % Make Directory
end

knockvalues = zeros(1000,6);
combustion_stats = zeros(6,20);
EngineRPM = zeros(1000,6); % RPM
Int_Manifold_Temp = zeros(1000,6); % Degrees C
Int_Manifold_Pres = zeros(1000,6); % kPa
Exh_Manifold_Pres = zeros(1000,6); % kPa
Fuel_Pres = zeros(1000,6); % kPa
```

```
CH4_Flow_G = zeros(1000,6); % g/min
H2_Flow_G = zeros(1000,6); % g/min
CH4_Flow_L = zeros(1000,6); % L/min
H2_Flow_L = zeros(1000,6); % L/min
Lambda = zeros(1000,6);
e_power = zeros(1000,6); % kW


%% Import Test fuel data (Takes about min)
for ii = 1:3 % Test PR Loop
    datafilename = ['PR_ControlTest_', num2str(ii), file_ending, '.tdms'];
    fullpath = [datafilepath, 'Test\', datafilename];
    PR_Data = tdmsread(fullpath);

    %Open Tables
    STATS = PR_Data{1,1};
    CycleStats = PR_Data{1,3};
    Pressuretraces = PR_Data{1,4}; %Saves data in the (1,4) position into Pressure
traces

    %Save Table values as Array
    knockvalues(:,ii) = table2array(CycleStats(:,4)); % Saves each knock value into
array that is indexed so all are saved
    combustion_stats(ii,:) = table2array(STATS(1,1:20)); % Saves all combustion data
into a usable form
end

for ii = 1:3 %PerfLoop
    datafilename = ['Perf_ControlTest_', num2str(ii), file_ending, '.tdms'];
    fullpath = [datafilepath, 'Test\', datafilename];
    PR_Data = tdmsread(fullpath);% Reads data into a 1x1 table
    STATS = PR_Data{1,1};% Opens the table so we can see the data inside
    EngineRPM(:,ii) = table2array(STATS(202:1201,2));
    Int_Manifold_Temp(:,ii) = table2array(STATS(202:1201,7));
    Int_Manifold_Pres(:,ii) = table2array(STATS(202:1201,9));
    Exh_Manifold_Pres(:,ii) = table2array(STATS(202:1201,10));
    Fuel_Pres(:,ii) = table2array(STATS(202:1201,11));
    CH4_Flow_L(:,ii) = table2array(STATS(202:1201,12)); % L/min
    H2_Flow_L(:,ii) = table2array(STATS(202:1201,13)); % L/min
    CH4_Flow_G(:,ii) = table2array(STATS(202:1201,14)); % g/min
    H2_Flow_G(:,ii) = table2array(STATS(202:1201,15)); % g/min
    Lambda(:,ii) = table2array(STATS(202:1201,51));
    e_power(:,ii) = table2array(STATS(202:1201,52));
end


%% Import Ref fuel data
for ii = 1:3 % Ref PR Loop
    datafilename = ['PR_ControlRef_', num2str(ii), file_ending, '.tdms']; % This is
done so we can look at multiple files at one time
    fullpath = [datafilepath, 'Ref\', datafilename];
    PR_Data = tdmsread(fullpath); % Reads data into a 1x4 table
    STATS = PR_Data{1,1}; %Saves data in the (1,1) position into STATS
    CycleStats = PR_Data{1,3}; %Saves data in the (1,3) position into CycleStats
```

```
    Pressuretraces = PR_Data{1,4}; %Saves data in the (1,4) position into Pressure
traces
    knockvalues(:,ii+3) = table2array(CycleStats(:,4)); % Saves each knock value into
array that is indexed so all are saved
    combustion_stats(ii+3,:) = table2array(STATS(1,1:20)); % Saves all combustion
data into a usable form
end

for ii = 1:3 %Perf Loop
    datafilename = ['Perf_ControlRef_', num2str(ii), file_ending, '.tdms'];
    fullpath = [datafilepath, 'Ref\', datafilename];
    PR_Data = tdmsread(fullpath);
    STATS = PR_Data{1,1};
    EngineRPM(:,ii+3) = table2array(STATS(202:1201,2));
    Int_Manifold_Temp(:,ii+3) = table2array(STATS(202:1201,7));
    Int_Manifold_Pres(:,ii+3) = table2array(STATS(202:1201,9));
    Exh_Manifold_Pres(:,ii+3) = table2array(STATS(202:1201,10));
    Fuel_Pres(:,ii+3) = table2array(STATS(202:1201,11));
    CH4_Flow_L(:,ii+3) = table2array(STATS(202:1201,12)); % L/min
    H2_Flow_L(:,ii+3) = table2array(STATS(202:1201,13)); % L/min
    CH4_Flow_G(:,ii+3) = table2array(STATS(202:1201,14)); % g/min
    H2_Flow_G(:,ii+3) = table2array(STATS(202:1201,15)); % g/min
    Lambda(:,ii+3) = table2array(STATS(202:1201,51));
    e_power(:,ii+3) = table2array(STATS(202:1201,52));
end

%% Data Analysis
% This section will be used for saving data to an .xls file

% Declaring/initializing Arrays for mean and Standard deviation calcs
Meanknockvalues = zeros(1,6);
MeanEngineRPM = zeros(1,6);
MeanInt_Manifold_Temp = zeros(1,6);
MeanInt_Manifold_Pres = zeros(1,6);
MeanExh_Manifold_Pres = zeros(1,6);
MeanFuel_Pres = zeros(1,6);
MeanCH4_Flow_G = zeros(1,6); % g/min
MeanH2_Flow_G = zeros(1,6); % g/min
MeanCH4_Flow_L = zeros(1,6); % L/min
MeanH2_Flow_L = zeros(1,6); % L/min
MeanLambda = zeros(1,6);
MeanE_power = zeros(1,6);

STDevknockvalues = zeros(1,6);
STDDevEngineRPM = zeros(1,6);
STDDevInt_Manifold_Temp = zeros(1,6);
STDDevInt_Manifold_Pres = zeros(1,6);
STDDevExh_Manifold_Pres = zeros(1,6);
STDDevFuel_Pres = zeros(1,6);
STDDevCH4_Flow_G = zeros(1,6); % g/min
STDDevH2_Flow_G = zeros(1,6); % g/min
STDDevCH4_Flow_L = zeros(1,6); % L/min
STDDevH2_Flow_L = zeros(1,6); % L/min
STDDevLambda = zeros(1,6);
STDDevE_power = zeros(1,6);
```

```
for ii = 1:6
    % Entire Dataset MEAN
    Meanknockvalues(1,ii) = mean(knockvalues(:,ii));
    MeanEngineRPM(1,ii) = mean(EngineRPM(:,ii));
    MeanInt_Manifold_Temp(1,ii) = mean(Int_Manifold_Temp(:,ii));
    MeanInt_Manifold_Pres(1,ii) = mean(Int_Manifold_Pres(:,ii));
    MeanExh_Manifold_Pres(1,ii) = mean(Exh_Manifold_Pres(:,ii));
    MeanFuel_Pres(1,ii) = mean(Fuel_Pres(:,ii));
    MeanCH4_Flow_G(1,ii) = mean(CH4_Flow_G(:,ii)); % g/min
    MeanH2_Flow_G(1,ii) = mean(H2_Flow_G(:,ii)); % g/min
    MeanCH4_Flow_L(1,ii) = mean(CH4_Flow_L(:,ii)); % L/min
    MeanH2_Flow_L(1,ii) = mean(H2_Flow_L(:,ii)); % L/min
    MeanLambda(1,ii) = mean(Lambda(:,ii));
    MeanE_power(1,ii) = mean(e_power(:,ii));

    % Standard Deviation
    STDevknockvalues(1,ii) = std(knockvalues(:,ii));
    STDDevEngineRPM(1,ii) = std(EngineRPM(:,ii));
    STDDevInt_Manifold_Temp(1,ii) = std(Int_Manifold_Temp(:,ii));
    STDDevInt_Manifold_Pres(1,ii) = std(Int_Manifold_Pres(:,ii));
    STDDevExh_Manifold_Pres(1,ii) = std(Exh_Manifold_Pres(:,ii));
    STDDevFuel_Pres(1,ii) = std(Fuel_Pres(:,ii));
    STDDevCH4_Flow_G(1,ii) = std(CH4_Flow_G(:,ii)); % g/min
    STDDevH2_Flow_G(1,ii) = mean(H2_Flow_G(:,ii)); % g/min
    STDDevCH4_Flow_L(1,ii) = mean(CH4_Flow_L(:,ii)); % L/min
    STDDevH2_Flow_L(1,ii) = mean(H2_Flow_L(:,ii)); % L/min
    STDDevLambda(1,ii) = mean(Lambda(:,ii));
    STDDevE_power(1,ii) = mean(e_power(:,ii));
end

% Knock Analysis: Break each run into a certain number of segments and
% average them to determine an average running condition:
% Also Decided to add a Methane number Average because it is easy now


% 100 Cycle average section
cycleIAT100avg = zeros(10,6);   % Declaring an empty array 10x6 so we can to fill
with the IAT
cycleKI100avg = zeros(10,6);    % Declaring an empty array 10x6 so we can to fill
with the KI
cycleMN100avgVol = zeros(10,6); % Declaring an empty array 10x6 so we can to fill
with the MN Vol
cycleMN100avgMass = zeros(10,6);% Declaring an empty array 10x6 so we can to fill
with the MN Mass

for ii = 1:6 % For each Collumn in the knock intensity chart
    for j = 0:9 % Breaking the dataset into 10 incriments:
        tempSUM = 0; %initalizing the tempSum Variable
        cycleSUM = 0; %Initalizing the cycleSUM Variable
        cycleMNVolSum = 0; %Initalizing the cycleMNVolSUM Variable
        cycleMNMassSum = 0; %Initalizing the cycleMNMassSUM Variable
        for jj = 1:100 % Could have done a counter but decided to do indexing
            tempSUM = Int_Manifold_Temp(j*10+jj,ii) + tempSUM; % Grabs temperature
data and sums it every cycle and adds it to the total
```

```
            cycleSUM = knockvalues(j*100+jj,ii) + cycleSUM; % grabbing and summing
the data we need
            cycleMNVolSum = 100 *
CH4_Flow_L(j*10+jj,ii)/(CH4_Flow_L(j*10+jj,ii)+H2_Flow_L(j*10+jj,ii)) +
cycleMNVolSum; % Calculating the Volume based MN
            cycleMNMassSum = 100 *
(CH4_Flow_G(j*10+jj,ii)/16.043)/((CH4_Flow_G(j*10+jj,ii)/16.043)+(H2_Flow_G(j*10+jj,i
i)/2.016)) + cycleMNMassSum; % Calculating the Mass based MN
        end
        cycleIAT100avg(j+1,ii) = tempSUM/100;
        cycleKI100avg(j+1,ii) = cycleSUM/100; % Save the data to the array
        cycleMN100avgVol(j+1,ii) = cycleMNVolSum/100; % Save the data to the array
        cycleMN100avgMass(j+1,ii) = cycleMNMassSum/100; % Save the data to the array
    end
end

% Create an Average MN for each 1000 cycle used for linear fiting data
meanMNmass = zeros(1,6);
meanMNvol = zeros(1,6);
for i = 1:6
    meanMNmass(i) = mean(cycleMN100avgMass(:,i));
    meanMNvol(i) = mean(cycleMN100avgVol(:,i));
end

%% Save Data for Sweep trends
% We are going to use the write table function and then this will write to
% a file name that was already specified:
% Sheet 1: Combustion Stats;
CombStatsNames = ["Test #", "Avg. Peak", "Peak Std. Dev.", "Peak COV", "Max Peak",
"Min Peak",...
    "Avg. Peak Loc.", "Peak Loc. Std. Dev", "Peak Loc. COV", "Avg. IMEP", "IMEP STD
DEV",...
    "IMEP COV", "Avg. NMEP", "NMEP STD DEV", "NMEP COV", "Avg. PMEP", "PMEP STD
DEV",...
    "PMEP COV", "MFB 10%",  "MFB 50%", "MFB 90%", "Avg. IMT", "IMT STD DEV", "Avg.
IMP",...
    "IMP STD DEV", "Mean Lambda", "Lambda STD DEV", "Avg. RPM", "RPM STD DEV",...
    "Avg. Fuel Pres.", "Fuel Pres. STD DEV", "Avg. ePower", "ePower STD Dev"];
RowNames = ["Test 1:"; "Test 2:"; "Test 3:"; "Ref 1:"; "Ref 2:"; "Ref 3:"];
writematrix(CombStatsNames,diaryname,'Sheet',1); % Writes in the column headers
writematrix(RowNames,diaryname,'Sheet',1,'Range','A2:A7'); % Writes in the row names
so I can keep them separated in the Excel program
writematrix(combustion_stats,diaryname,'Sheet',1,'Range','B2:U7'); % Writes in the
Combustion Stats data in

writematrix(MeanInt_Manifold_Temp',diaryname,'Sheet',1,'Range','V2:V7'); % Writes in
the intake Manifold Temp Average
writematrix(STDDevInt_Manifold_Temp',diaryname,'Sheet',1,'Range','W2:W7'); % Writes
in the intake Manifold Temp Std Dev
writematrix(MeanInt_Manifold_Pres',diaryname,'Sheet',1,'Range','X2:X7'); % Writes in
the Intake Manifold Pressure Average
writematrix(STDDevInt_Manifold_Pres',diaryname,'Sheet',1,'Range','Y2:Y7'); % Writes
in the intake Manifold Pressure Std Dev
writematrix(MeanLambda',diaryname,'Sheet',1,'Range','Z2:Z7'); % Writes in the Lambda
Average
```

```
writematrix(STDDevLambda',diaryname,'Sheet',1,'Range','AA2:AA7'); % Writes in the
Lambda Std Dev
writematrix(MeanEngineRPM',diaryname,'Sheet',1,'Range','AB2:AB7'); % Writes in the
RPM Average
writematrix(STDDevEngineRPM',diaryname,'Sheet',1,'Range','AC2:AC7'); % Writes in the
RPM Std Dev
writematrix(MeanFuel_Pres',diaryname,'Sheet',1,'Range','AD2:AD7'); % Writes in the
Fuel Pressure Average
writematrix(STDDevFuel_Pres',diaryname,'Sheet',1,'Range','AE2:AE7'); % Writes in the
Fuel Pressure Std Dev
writematrix(MeanE_power',diaryname,'Sheet',1,'Range','AF2:AF7'); % Writes in the E-
power Average
writematrix(STDDevE_power',diaryname,'Sheet',1,'Range','AG2:AG7'); % Writes in the E-
power Std Dev



% Sheet 2 : Knock Intensity / MN
ColNames = ["", "KI Test 1: ", "KI Test 2: ", "KI Test 3: ",...
                "KI Ref 1: ",  "KI Ref 2: ",  "KI Ref 3: ",...
            "", "MN Test 1: ", "MN Test 2: ", "MN Test 3: ",...
                "MN Ref 1: ",  "MN Ref 2: ",  "MN Ref 3: "];
Row1Names = [""; "Average"; "Std Dev";];
Row2Names = [""; "Mass"; "Volume";];
writematrix(ColNames,diaryname,'Sheet',2); % Writes in the collumn headers
%warning('OFF', 'Added specified worksheet.'); % Turns off the error for creating a
new worksheet
writematrix(Row1Names,diaryname,'Sheet',2,'Range','A1:A4'); % Writes in the row names
so I can keep them separated in the Exel program
writematrix(Row2Names,diaryname,'Sheet',2,'Range','H1:H3'); % Writes in the row names
pt 2
writematrix(meanMNmass(1,4:6),diaryname,'Sheet',2,'Range','L2:N2'); % Writes in MN of
reference fuels
writematrix(meanMNvol(1,4:6),diaryname,'Sheet',2,'Range','L3:N3'); % Writes in MN of
reference fuels
writematrix(knockvalues(:,1:3),diaryname,'Sheet',2,'Range','B5:D1004'); % Writes in
the Test KI data in
writematrix(knockvalues(:,4:6),diaryname,'Sheet',2,'Range','E5:G1004'); % Writes in
the Reference KI data in
writematrix(Meanknockvalues(:,1:6),diaryname,'Sheet',2,'Range','B2:G2'); % Writes in
the Mean KI data in
writematrix(STDevknockvalues(:,1:6),diaryname,'Sheet',2,'Range','B3:G3'); % Writes in
the Test KI data in

% Sheet 3



% Re-Name The sheets:
Excel = actxserver('Excel.Application'); % Open Excel Automation server
Excel.Visible=1; % Make Excel visible
Workbook = Excel.Workbooks.Open(diaryname); % Open Excel file
Sheets = Excel.ActiveWorkbook.Sheets;% Get the list of sheets in the workbook

Sheets.Item(1).Name = 'Combustion Stats'; % Rename the first sheet
```

```
Sheets.Item(2).Name = 'Knock Intensity'; % Rename the second sheet

Workbook.Save(); % Save the file
Excel.Quit(); % Quit Excel, remove the COM server and delete the related objects
Excel.delete();
clear Excel; % Deletes Variable Excel
clear Workbook; % Deletes Variable Workbook
clear Sheets; % Deletes Variable Workbook

%% Plotting of relationships
% Creating a time array so we can keep track of time and strokes
cycletime = zeros(1000,1); % Creates a matrix 100 rows long with one column
for j = 1:1000 % Goes through all 100 rows
    cycletime(j) = j * 1/8; % Using the frequency we can calculate time
end

cycle10time = zeros(100,1); % Creates a matrix 100 rows long with one column
for j = 1:100 % Goes through all 100 rows
    cycle10time(j) = j * 10/8; % Using the frequency we can calculate time
end

cycle25time = zeros(40,1); % Creates a matrix 100 rows long with one column
for j = 1:40 % Goes through all 100 rows
    cycle25time(j) = j * 25/8; % Using the frequency we can calculate time
end

cycle100time = zeros(10,1); % Creating a time array so we can keep track of time and
strokes
for j = 1:10
    cycle100time(j) = j * 100/8;
end

% MN vs Knock Intensity Mass
figure('Name', 'Mass Flow MN vs. KI','NumberTitle','on');
for ii = 4:6 % For each Column in the knock intensity chart

scatter(cycleMN100avgMass(:,ii),cycleKI100avg(:,ii),30,'filled','o','MarkerFaceAlpha'
,.3 ,'DisplayName', join([RowNames(ii) "100 cycle Avg."])) % The 100 Cycle data for
variability
    hold on
    text(mean(cycleMN100avgMass(:,ii))-0.8,mean(cycleKI100avg(:,ii)),['('
num2str(mean(cycleMN100avgMass(:,ii)),3) ',' num2str(mean(cycleKI100avg(:,ii)),3)
')'])% Plots the X,Y value of the Average point
end

% Create a line of Best fit
linearCoefficients = polyfit(meanMNmass(4:6), Meanknockvalues(4:6), 1);
xfit = zeros(6);
for i = 1:6
    xfit(i) = (Meanknockvalues(i)-linearCoefficients(2))/linearCoefficients(1); %
Creates the fitted x values that correspond to the knock Intensity
end
scatter(meanMNmass(1,4:6), Meanknockvalues(1,4:6), 50, 'filled', '^',
'MarkerFaceColor', 'red', 'DisplayName', '1000 Cycle Avg.') % The entire 1000 Cycle
average
```

```
plot(xfit(4:6), Meanknockvalues(4:6), 'b.-', 'MarkerSize', 15, 'LineWidth', 1,
'DisplayName', 'Linear fit of Ref Pts.'); % Plots the reference Line
scatter(mean(xfit(1:3)), mean(Meanknockvalues(1:3)), 100,
'filled','pentagram','MarkerFaceColor','red', 'DisplayName','Calculated MN'); %
Average Value from the test points
%ORIGIONAL: errorbar(mean(xfit(1:3)), mean(Meanknockvalues(1:3)), max(xfit(1:3))-
mean(xfit(1:3)), mean(xfit(1:3))-min(xfit(1:3)),...
    %max(Meanknockvalues(1:3))-mean(Meanknockvalues(1:3)),
mean(Meanknockvalues(1:3))-min(Meanknockvalues(1:3)),'DisplayName','Uncertainty',
'Color','red'); % x-Loc, y-Loc , yneg, ypos, xneg, xpos
errorbar(mean(xfit(1:3)), mean(Meanknockvalues(1:3)), 0, 0,...
    max(Meanknockvalues(1:3))-mean(Meanknockvalues(1:3)), mean(Meanknockvalues(1:3))-
min(Meanknockvalues(1:3)),'DisplayName','Uncertainty', 'Color','red'); % x-Loc, y-Loc
, yneg, ypos, xneg, xpos
text(mean(xfit(1:3))+0.3, mean(Meanknockvalues(1:3)), ['(' num2str(mean(xfit(1:3)),3)
',' num2str(mean(Meanknockvalues(1:3)),3) ')'],"FontWeight","bold")% Plots the X,Y
value of the Average point

% Addons that make the plot pretty and readable
legend % Turns on the legend
title('Methane Number vs 100 Cycle KI','FontSize',13,'FontWeight','bold')
grid on % Turns on the box around the plot
grid minor % Turns on the smaller grid lines
xlim([(min(cycleMN100avgMass(:,4))-2) (max(cycleMN100avgMass(:,6))+1)]) % Establishes
the x boundaries based on the max and min MN
ylabel('Average Knock Intensity','FontSize',12,'FontWeight','bold')
xlabel('Mass Based Methane Number','FontSize',12,'FontWeight','bold')
hold off
ax = gca;
exportgraphics(ax,"MassBasedMN.jpg")

% This Line writes the Calculated Methane Number to the Exel sheet
writematrix(xfit(1:3,1)', diaryname, 'Sheet', 2, 'Range', 'I2:K2'); % Writes in the
Calculated Mass MN

% Operating Conditions Vs Time Subplot matrix
if Perf_PlottingFlag == 1
    colors = ["#9FFF33","#28B12A","#3EF4CE","#493EF4","#783EF4","#F43ED8"];
            % LghtGreen,DarkGreen,  Teal,      Blue,    Purple,  Pink

    f = figure('Name','Engine Operating Condition vs
Time','NumberTitle','on','Position',[1000,40,700,950]); % Naming the entire figure
with this step

    subplot(4,1,1) % Intake Air Temperature
    title('Intake Air Temperature','FontSize',13,'FontWeight','bold')
    Filt_Int_Manifold_Temp = zeros(100,6);
    for i = 1:6 % For each Collumn in engine data chart
        for j = 1:100
            Filt_Int_Manifold_Temp(j,i)= mean(Int_Manifold_Temp(j*10-9:j*10,i));
        end

scatter(cycle10time(:),Filt_Int_Manifold_Temp(:,i),5,'filled','o','MarkerFaceColor',c
olors(1,i)) % The 100 Cycle data for variability, Size, Filled datapoints, Circles,
        y1 = yline(mean(Int_Manifold_Temp(:,i)),'LineStyle','--');
```

```
        y1.Color= colors(1,i);
        hold on
    end
    grid on
    box on
    % x and y coordinates start at bottom left corner and go CCW
    Ymax= DesiredValues(1,1)+DesiredValues(2,1);
    Ymin= DesiredValues(1,1)-DesiredValues(2,1);
    xlim([0 125]) % Establishes the x boundaries based on the max and min MN
    ylim([Ymin-DesiredValues(2,1) Ymax+DesiredValues(2,1)])
    patch([0 125 125 0],[Ymin Ymin Ymax Ymax],'green','FaceAlpha', 0.05) %
Establishes a light box with an opacity of 0.1%
    ylabel('Intake Manifold Temp(C)','FontSize',12,'FontWeight','bold')
    xlabel('Time (s)','FontSize',12,'FontWeight','bold')

    subplot(4,1,2) % Mixture
    title('Intake Manifold Pressure (kPa)','FontSize',13,'FontWeight','bold')
    Filt_Int_Manifold_Pres = zeros(10,6);
    for i = 1:6 % For each Collumn in engine data chart
        for j = 1:40
            Filt_Int_Manifold_Pres(j,i)= mean(Int_Manifold_Pres(j*25-24:j*25,i));
        end

scatter(cycle25time(:),Filt_Int_Manifold_Pres(:,i),7,'filled','o','MarkerFaceColor',c
olors(1,i))
        y2 = yline(mean(Int_Manifold_Pres(:,i)),'LineStyle','--');
        y2.Color= colors(1,i);
        hold on
    end
    grid on
    box on
    Ymax = DesiredValues(1,2)+DesiredValues(2,2);
    Ymin = DesiredValues(1,2)-DesiredValues(2,2);
    xlim([0 125]) % Establishes the x boundaries based on the max and min MN
    ylim([Ymin-DesiredValues(2,2) Ymax+DesiredValues(2,2)])
    patch([0 125 125 0],[Ymin Ymin Ymax Ymax],'green','FaceAlpha', 0.05) %
Establishes a light box with an opacity of 5%
    ylabel('Intake Manifold Pres (kPa)','FontSize',12,'FontWeight','bold')
    xlabel('Time (s)','FontSize',12,'FontWeight','bold')

    subplot(4,1,3) % Mixture
    title('Intake Mixture (Lambda)','FontSize',13,'FontWeight','bold')
    Filt_Lambda = zeros(10,6);
    for i = 1:6 % For each Collumn in engine data chart
        for j = 1:40
            Filt_Lambda(j,i)= mean(Lambda(j*25-24:j*25,i));
        end

scatter(cycle25time(:),Filt_Lambda(:,i),7,'filled','o','MarkerFaceColor',colors(1,i))
% Cycle data, Size, Filled datapoints, Circles, Color
        yline(mean(Lambda(:,i)),'LineStyle','--', 'Color',colors(1,i));
        hold on
    end
    grid on
    box on
```

```
    Ymax = DesiredValues(1,3)+DesiredValues(2,3);
    Ymin = DesiredValues(1,3)-DesiredValues(2,3);
    xlim([0 125]) % Establishes the x boundaries based on the max and min MN
    ylim([Ymin-DesiredValues(2,3) Ymax+DesiredValues(2,3)])
    patch([0 125 125 0],[Ymin Ymin Ymax Ymax],'green','FaceAlpha', 0.05) %
Establishes a light box with an opacity of 5%
    ylabel('Lambda','FontSize',12,'FontWeight','bold')
    xlabel('Time (s)','FontSize',12,'FontWeight','bold')

    subplot(4,1,4) % RPM
    title('Engine RPM','FontSize',13,'FontWeight','bold')
    for i = 1:6 % For each Collumn in engine data chart

scatter(cycletime(:),EngineRPM(:,i),5,'filled','o','MarkerFaceColor',colors(1,i),'Dis
playName',RowNames(i)); % The 100 Cycle data for variability, Size, Filled
datapoints, Circles,
        hold on
    end
    grid on
    box on
    Ymax =DesiredValues(1,4)+DesiredValues(2,4);
    Ymin =DesiredValues(1,4)-DesiredValues(2,4);
    xlim([0 125]) % Establishes the x boundaries based on the max and min MN
    ylim([Ymin-DesiredValues(2,4) Ymax+DesiredValues(2,4)]) % Establishes the desired
Y bounds of the image
    ylabel('Engine RPM','FontSize',12,'FontWeight','bold')
    xlabel('Time (s)','FontSize',12,'FontWeight','bold')
    patch([0 125 125 0],[Ymin Ymin Ymax Ymax],'green','FaceAlpha',
0.05,'DisplayName','Go Zone') % Establishes a light box with an opacity of 1%
    legend('Location','southoutside','NumColumns',7) %Adds a Legend below the 4th
Subplot
    hold off % Display the plot

    % Saving Plot:
    exportgraphics(f,"OperationParameters.jpg") % Exports the whole subplot figure to
a file specified in the ()
    movefile('OperationParameters.jpg', 'Results') % Moves the File to the Results
folder
else
    % Do NOTHING
end

movefile('MassBasedMN.jpg', 'Results') % Moves the Mass image to the results folder
movefile('Results', datafilepath) % Moves the Results folder to the desired location
```

APPENDIX D: GAS FLOW METER CALIBRATION

In this section, I want to talk about the steps used for flow meter calibration and how it was conducted. The following are images of the positive displacement flow device and a diagram depicting how the device was plumbed in-line for calibration measurements.

Figure 40: 1ft^3-Positive Displacement Gas Flow Meter

Figure 41: Positive Displacement Gas Flow Meter identification tag.

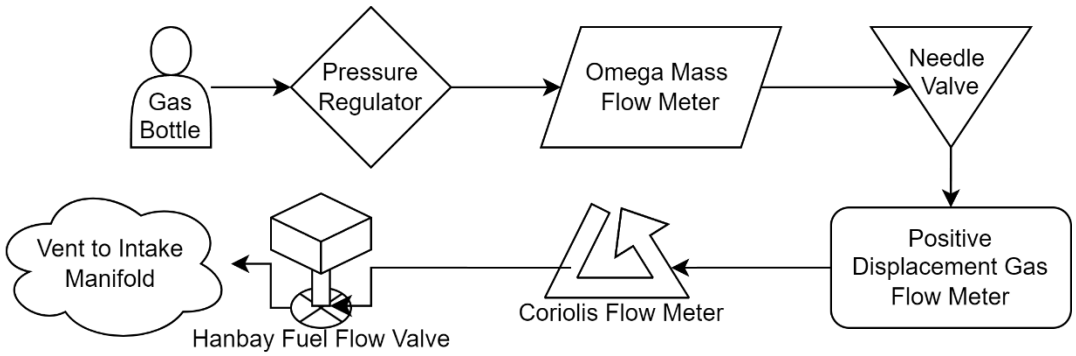

Figure 42: Gas flow meter calibration using PDGFM.

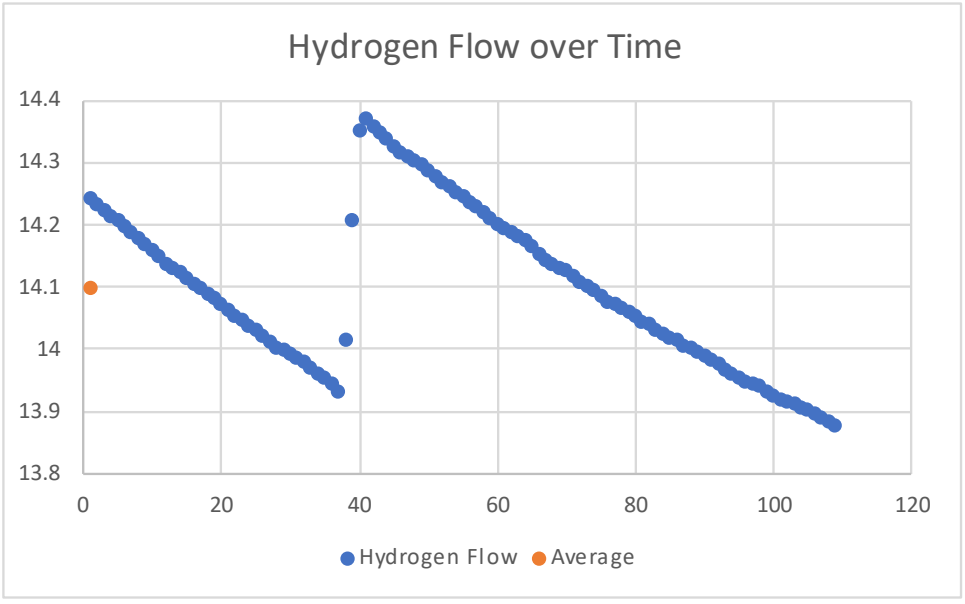

Figure 43: Recorded flow rate for hydrogen.

Coriolis Flow total (g)	Actual Flow Volume (L)	MW CH4 (g/mol)	R (kPa*L/ mol*kelvin)	Pressure (kPa)	Temp (K)	Mass Flowed(g)
71.45	28.3168	16.04	8.314	388	288	73.6247

Methane Flow Table Comparing Coriolis Flow meter and PDGFM.

ABREVIATIONS, ACRONYMS AND SYMBOLS

Abbreviation	Term
aH	Absolute Humidity
A/F	Air Fuel Ratio
ASTM	American Society of Testing and Materials
AVL	Anstalt für Verbrennungs Motoren (Institute for Internal Combustion Engines)
aTDC	After Top Dead Center
bmep	Brake Mean Effective Pressure
bTDC	Before Top Dead Center
CA50	Crank Angle of 50% Heat Release
c-EGAI	Controlled End Gas Autoignition
CIM	Combustion Intensity Metric
CFR	Cooperative Fuel Research (Engine)
CFD	Computational Fluid Dynamics
CH_4	Methane (Chemical Formula)
CNG	Compressed Natural Gas
CO	Carbon Monoxide
CO_2	Carbon Dioxide
COV	Coefficient of Variance
CPRF	Certified Premixed Reference Blends
CR	Compression Ratio
EGAI	End Gas Auto Ignition
EMP	Exhaust Manifold Pressure

FFT	Fast Fourier Transform
f-EGAI	Fractional End Gas Auto Ignition
H_2	Hydrogen (Chemical Formula)
IAP	Intake Air Pressure
IAT	Intake Air Temperature
ICE	Internal Combustion Engine
IMP	Intake Manifold Pressure
IMT	Intake Mixture Temperature
IMEP	Indicated Mean Effective Pressure
KI	Knock Intensity
LabVIEW	Laboratory Virtual Instrument Engineering Workbench
LECM	Large Engine Control Module
LNG	Liquified Natural Gas
LPG	Liquified Petroleum Gas
MN	Methane Number
MN_c	Calculated Methane Number
MON	Motor Octane Number
MWM	Motoren-Werke Mannheim A.G.
NA	Naturally Aspirated
NMEP	Net Mean Effective Pressure
ON	Octane Number
PDGFM	Positive Displacement Gas Flow Meter
PID	Proportional – Integral - Derivative

PMEP	Pumping Mean Effective Pressure
PRF	Primary Reference Fuel
rH	Relative Humidity
RON	Research Octane Number
RPM	Revolutions Per Minute
RSM	Response Surface Method
SI	Spark Ignited
SRF	Secondary Reference Fuel
TDC	Top Dead Center
TEL	Tetraethyl Lead
VFD	Variable Frequency Drive
VI	Virtual Instrumentation
%	Mol-Fraction
λ	Lambda (Actual A/F)/(Stoichiometric A/F) … also called the mixture ratio
ϕ	Equivalence Ratio
η	Efficiency
η_v	Volumetric Efficiency
θ	Crank Angle
Ψ	Phase Angle
ω	Rotation Frequency